



**PRODUCTION OF ETHERS FROM GLYCEROL AND TERTIARY BUTYL
ALCOHOL USING REACTIVE DISTILLATION**

**By
Parinya Intaracharoen**

**A Thesis Submitted in Partial Fulfillment of the Requirements for the Degree
MASTER OF ENGINEERING
Department of Chemical Engineering
Graduate School
SILPAKORN UNIVERSITY
2009**

**PRODUCTION OF ETHERS FROM GLYCEROL AND TERTIARY BUTYL
ALCOHOL USING REACTIVE DISTILLATION**

By

Parinya Intaracharoen

A Thesis Submitted in Partial Fulfillment of the Requirements for the Degree

MASTER OF ENGINEERING

Department of Chemical Engineering

Graduate School

SILPAKORN UNIVERSITY

2009

การผลิตอิเทอร์จากกลีเซอรอลและเทอร์เชียรี บิวทิล แอลกอฮอล์โดยหากลั่นแบบมีปฏิริยา

โดย

นายปริญญา อินทเธริญ

วิทยานิพนธ์นี้เป็นส่วนหนึ่งของการศึกษาตามหลักสูตรปริญญาวิศวกรรมศาสตรมหาบัณฑิต

สาขาวิชาวิศวกรรมเคมี

ภาควิชาวิศวกรรมเคมี

บัณฑิตวิทยาลัย มหาวิทยาลัยศิลปากร

ปีการศึกษา 2552

ลิขสิทธิ์ของบัณฑิตวิทยาลัย มหาวิทยาลัยศิลปากร

50404202 : MAJOR : CHEMICAL ENGINEERING

KEY WORDS : REACTIVE DISTILLATION/ SIMULATION PROGRAM/ BIODIESEL/ GROUP CONTRIBUTION/ CETANE IMPROVER

PARINYA INTARACHAROEN : PRODUCTION OF ETHERS FROM GLYCEROL AND TERTIARY BUTYL ALCOHOL USING REACTIVE DISTILLATION. THESIS ADVISORS : ASST.PROF.WORAPON KIATKITTIPONG, D.Eng., AND PROF.SUTTICHA ASSABUMRUNGRAT, Ph.D.. 106 pp.

The production of ethers from glycerol and tertiary butyl alcohol using reactive distillation was investigated in this study. Firstly, thermodynamic equilibrium was considered. Three group contribution methods i.e. Joback's, Benson's and Gani's were used to predict the thermodynamic properties and subsequently equilibrium compositions using Gibbs free energy minimization method. Gani's group contribution method can predict the equilibrium composition well. Secondly, the kinetic study of the reaction catalyzed by Amberlyst-15 were performed at three temperature levels of 338, 348 and 358 K to obtain the parameters in the Arrhenius' equation and the Van't Hoff equation. Two kinetic models of Langmuir-Hinshelwood (LH) and Power Law (PL) based on activity and concentration were employed to fit with the experimental results to determine the best-fitted kinetic parameters which minimize the relative root mean square deviation (RMSD). It was observed that the LH based on activity model showed the best reaction rate description. Finally, the obtained kinetic parameters were used to investigate the production of tertiary butyl of glycerol in reactive distillation. The effect of design and operating variables on reactive distillation were investigated. The suitable reactive distillation configuration consists of 7 rectifying stage, 6 reaction stages and 1 stripping stage. The simulation results were well validated by the experimental results. The effects of various operating parameters such as reflux ratio, location of feed stage, heat duty of reboiler and feed flow rate on the reactive distillation performance were simulated.

Department of Chemical Engineering Graduate School, Silpakorn University Academic Year 2009

Student's signature

Thesis Advisors' signature 1. 2.

50404202 : สาขาวิชาวิศวกรรมเคมี

คำสำคัญ : การกลั่นแบบมีปฏิริยา/การจำลองระบบ/ กรู๊ปคอนทริบิวชัน/สารเติมแต่งเชื้อเพลิง

ปริญญญา อินทรเจริญ : การผลิตอีเทอร์จากกลีเซอรอลและเทอร์เชียรี บิวทิล แอลกอฮอล์ โดยหอกกลั่นแบบมีปฏิริยา. อาจารย์ที่ปรึกษาวิทยานิพนธ์ : ผศ.ดร.วรพล เกียรติกิตติพงษ์ และ ศ.ดร.สุทธิชัย อัสสะบำรุงรัตน์. 106 หน้า.

งานวิจัยนี้เป็นการผลิตอีเทอร์จากกลีเซอรอลและเทอร์เชียรี บิวทิล แอลกอฮอล์โดยหอกกลั่นแบบมีปฏิริยา ในส่วนแรกเป็นการพิจารณาสมดุลทางอุณหพลศาสตร์ โดยวิธีกรู๊ปคอนทริบิวชัน 3 วิธีได้แก่ วิธีของโจแบค วิธีของกานี และวิธีของเบนสัน ถูกนำมาใช้ในการทำนายค่าสมบัติทางอุณหพลศาสตร์ และองค์ประกอบสารที่ภาวะสมดุลในลำดับถัดมาโดยวิธีการหาค่าพลังงานอิสระของกิบส์ที่ต่ำที่สุด ซึ่งพบว่าวิธีของกานีสามารถทำนายองค์ประกอบสารที่ภาวะสมดุลได้ดี ในส่วนที่สองเป็นการศึกษาจลนพลศาสตร์ของปฏิริยาโดยใช้ตัวเร่งปฏิริยาแอมเบอร์-ลิส 15 ที่อุณหภูมิ 338, 348 และ 358 เคลวิน เพื่อให้ได้พารามิเตอร์ที่แสดงด้วยสมการของอาร์เรเนียสและแวนฮอฟ แบบจำลองทางจลนพลศาสตร์ 2 แบบได้แก่แบบจำลองของแลงเมียร์-ฮินเชลวูดและแบบจำลองตามกฎยกกำลังซึ่งอธิบายในรูปของความเข้มข้นและแอกติวิตีถูกนำมาใช้ในการอธิบายผลการทดลอง โดยพิจารณาจากค่าความเบี่ยงเบนของรากกำลังสองที่น้อยที่สุดเพื่อให้ได้แบบจำลองที่เหมาะสมที่สุด ซึ่งพบว่าแบบจำลองแลงเมียร์-ฮินเชลวูดที่อธิบายในรูปแอกติวิตีสามารถใช้อธิบายอัตราการเกิดปฏิริยาได้ดีที่สุด ในส่วนสุดท้ายจะนำค่าตัวแปรทางจลนพลศาสตร์ที่ได้มาใช้ในการจำลองการผลิตอีเทอร์จากกลีเซอรอลในหอกกลั่นแบบมีปฏิริยา โดยทำการศึกษาผลของการออกแบบและตัวแปรในการดำเนินงาน ซึ่งพบว่ารูปแบบของหอกกลั่นแบบมีปฏิริยาที่เหมาะสมที่สุดประกอบด้วยชั้นเรกติฟายอิงจำนวน 7 ชั้น ชั้นการเกิดปฏิริยาจำนวน 6 ชั้นและชั้นสตรippingจำนวน 1 ชั้น โดยผลจากแบบจำลองสอดคล้องกับการยืนยันด้วยผลการทดลองเป็นอย่างดี และทำการจำลองกระบวนการเพื่อศึกษาผลของตัวแปรในการดำเนินงาน ได้แก่ อัตราการป้อนกลับตำแหน่งของสายป้อน พลังงานความร้อนที่ให้กับหม้อต้มซ้ำ และอัตราการไหลของสารตั้งต้นที่มีต่อสมรรถนะของหอกกลั่นแบบมีปฏิริยา

ภาควิชาวิศวกรรมเคมี

บัณฑิตวิทยาลัย มหาวิทยาลัยศิลปากร

ปีการศึกษา 2552

ลายมือชื่อนักศึกษา.....

ลายมือชื่ออาจารย์ที่ปรึกษาวิทยานิพนธ์ 1. 2.

ACKNOWLEDGEMENTS

The author wishes to express his sincere gratitude and appreciation to his advisor, Assistant Professor Worapon Kiatkittipong, and co advisor, Professor Suttichai Assabumrungrat for their valuable suggestions, stimulating, useful discussions throughout this research and devotion to revise this thesis otherwise it cannot be completed in a short time. In addition, the author would also be grateful to Assistant Professor Choowong Chaisuk, as the chairman, Assistant Professor Chanchai Thongpin, and Associate Professor Navadol Laosiripojana as the members of the thesis committee. The author would like to thank the financial supports from Silpakorn University Research and Development Institute (SURDI) and the Thailand Research Fund (TRF).

Most of all, the author would like to express his highest gratitude to his parents who always pay attention to through these years for suggestions and their wills. The most success of graduation is devoted to my parents.

Finally, Many thanks for kind suggestions and useful help to Mr. Kittipong Koomsup, Mr. Khamron Yoothongkham, the members of the Center of Excellence on Catalysis and Catalytic Reaction Engineering, Department of Chemical Engineering, Faculty of Engineering, Chulalongkorn University, the members of Department of Materials science and Engineering and the members of Department of Chemical Engineering, Faculty of Engineering and Industrial Technology, Silpakorn University for their assistances.

Table of Contents

	Page
English Abstract	d
Thai Abstract	e
Acknowledgments	f
List of Tables	j
List of figure	k
Chapter	
1 Introduction	1
2 Theory	3
Biodiesel	3
Etherification of glycerol	6
Group contribution method	7
Joback group contribution method	7
Gani group contribution method	8
Benson group contribution method	9
Conventional reactor versus reactive distillation	11
Reactive distillation configurations	12
Advantages of reactive distillation	13
Aspen Plus program	13
Features of Aspen Plus program	14
Benefits of Aspen Plus program	14
3 Literature reviews	15
Production of <i>tert</i> -butyl ether of glycerol	15
Kinetic mechanism models of esters and ethers production	18
Group contribution method	21
Ethers production in reactive distillation	23
4 Research procedure	25
Thermodynamic study	26
Kinetic study	26

Chapter	Page
Chemical and catalysts	26
Batch reactor apparatus and experimental procedure.....	27
Sample analysis.....	28
Reactive Distillation study.....	29
Experiment procedure of reactive distillation.....	29
Reactive distillation experiment in laboratory	29
Reactive distillation simulation by Aspen Plus program.....	30
5 Result and Discussion	32
Equilibrium thermodynamic analysis.....	32
Estimation of normal boiling point	33
Estimation of critical properties.....	33
Estimation of heat of formation	36
Estimation of Gibbs free energy	37
Equilibrium constant parameters determination	37
Kinetic study.....	41
The effect of external mass transfer	41
Development of mathematical models	42
Kinetic parameter determination.....	44
Reactive distillation: Experiment and simulation.....	52
Performance of Reactive Distillation at standard condition.....	52
Effect of design variables	55
Number of stripping stages	55
Number of rectifying stage	55
Effect of operating parameters.....	59
Effect of reflux ratio	59
Effect of heat duty	60
Effect of feed stage location.....	60
Effect of feed flow rate.....	61
6 Conclusions and recommendations.....	64

Chapter	Page
Thermodynamic study.....	64
Kinetic study.....	64
Reactive distillation study	65
Recommendations.....	65
Bibliography.....	67
Appendix.....	73
Appexdix A: Nomenclature.....	74
Appexdix B: Joback group contribution method.....	77
Appexdix C: Gani group contribution method.....	80
Appexdix D: Benson group contribution method.....	83
Appexdix E: Aspen Plus program.....	87
Appexdix F: UNIFAC method	97
Appexdix G: Proceeding	103
Biography.....	106

List of Tables

Table		Page
1	Details of chemicals use in the study.	27
2	Physical properties of Amberlyst-15 catalyst.	27
3	Operating conditions of gas chromatography.	28
4	Percent error of critical temperature, critical pressure and normal boiling temperature for Joback's and Gani's method comparison with database.	35
5	Percent error of heat of formation estimated by Joback's, Benson's and Gani's method.	36
6	Gibbs free energy estimation for Joback's, Benson's and Gani's method compare with database.	37
7	Equilibrium constant of etherification between glycerol and <i>tert</i> -butyl alcohol.	41
8	Reaction rate constants and activation energy.	50
9	Sorption equilibrium constant and values of the adsorption enthalpies and adsorption entropies of H ₂ O for LH-A kinetic model.	51
10	Feed conditions and specification of Reactive Distillation column under the standard condition for Aspen Plus simulator.	53
11	Joback's subgroup.	78
12	Joback constant for any subgroup.	79
13	Gani's 1st order subgroup.	81
14	Gani's 2nd order subgroup.	82
15	Benson's subgroup.	85
16	ΔH_{fk}^0 and S_k^0 constant for Benson's method calculation.	86
17	N_e, S_e, N_{oi} and N_{ts} constant for Benson's method calculation.	86
18	UNIFAC-VLE group interaction parameters, a_{mk} , in Kelvins [†]	102

List of Figures

Figures	Page
1	Transesterification of triglycerides with alcohol. 4
2	Biodiesel production flowchart 5
3	Etherification of glycerol with isobutene and <i>tert</i> -butyl alcohol. 6
4	(a) Carbon bond with Hydrogen, Fluorine, Chlorine and Iodine..... 10
	(b) 2, 2', 6, 6'-tetramethylbiphenyl structure..... 10
5	Conventional process involving reaction followed by separation. 11
6	Concept of reactive distillation. 12
7	Reaction scheme for the etherification of glycerol with <i>tert</i> -butyl alcohol. 16
8	Eley-Rideal and Langmuir-Hinshelwood mechanism. 19
9	Schematic diagram for all steps in this study. 25
10	Schematic diagram of the autoclave reactor. 28
11	Reactive distillation setup. 31
12	Normal boiling temperature the components in the system and related reaction..... 34
13	Critical temperature for all components in the system. 34
14	Critical pressure for all components in the system..... 35
15	Heat of formation of the components in the system and related reaction. 36
16	The effect of reaction temperature on equilibrium conversion of glycerol from simulation and experiment..... 38
17	Equilibrium composition from simulation and experiment (5 bar, glycerol:TBA=1:4)..... 39
18	Arrhenius's plots for K_{1c} , K_{2c} and K_{3c} estimated by minimize Gibbs free energy..... 40
19	The effect of speed level on the glycerol conversion (Catalyst = A-15, catalyst weight = 1.025 g, TBA:G = 4:1, T = 338 K, P = 5 bar and reaction time = 8 h)..... 42

Figures	Page
20 Mole change with time at 338 K(catalyst weight = 1.025 g, G:TBA = 1:4, 5 bar). (solid lines: PL-A model, dashed lines: PL-C model)	45
21 Mole changes with time at 348 K(catalyst weight = 1.025 g, G:TBA = 1:4, 5 bar). (solid lines: PL-A model, dashed lines: PL-C model)	45
22 Mole changes with time at 358 K(catalyst weight = 1.025 g, G:TBA = 1:4, 5 bar). (solid lines: PL-A model, dashed lines: PL-C model)	46
23 Mole change with time at 338 K(catalyst weight = 1.025 g, G:TBA = 1:4, 5 bar and $T = 338$ C), (symbols: experiment results, solid lines: LH-A model).....	47
24 Mole change with time at 348 K(catalyst weight = 1.025 g, G:TBA = 1:4, 5 bar and $T = 338$ C), (symbols: experiment results, solid lines: LH-A model).....	47
25 Mole change with time at 358 K(catalyst weight = 1.025 g, G:TBA = 1:4, 5 bar and $T = 338$ C), (symbols: experiment results, solid lines: LH-A model).....	48
26 average RMSD values of PL and LH kinetic model for both activity and concentration in each temperature	48
27 Arrhenius's plots for PL-A (dashed lines) and PL-C (solid lines)	49
28 Arrhenius's (solid line) and Van't Hoff plots (dashed line) of LH-A model	50
29 The configuration of standard model Reactive distillation column	53
30 Mole fraction and temperature profile inside the column at standard operating condition.....	54
31 Effect of the number of stripping stages on the conversion and selectivity for various reaction stages (rectifying stages = 6)	56
32 Effect of the number of rectifying stages on the conversion and selectivity for various reaction stages (stripping stages = 1)	56

Figures	Page
33	Concentration profiles of bottom at standard operating condition..... 58
34	Mole fraction and temperature profiles at standard operating condition change with stages..... 58
35	Effect of reflux ratio on reactive distillation performance..... 59
36	Effect of heat duty on reactive distillation performance..... 60
37	Effect of glycerol feed stage location on glycerol conversion for various TBA feed stage location 61
38	Effect of glycerol feed stage location on glycerol conversion for various TBA feed stage location 62
39	Effect of TBA feed flow rate on glycerol conversion for various glycerol feed flow rate 62
40	Effect of TBA feed flow rate on selectivity for various glycerol feed flow rate 63
41	Aspen startup..... 88
42	Aspen Plus program..... 89
43	Rgibbs flowsheet in Aspen Plus program..... 89
44	Component data browser..... 90
45	Find components in Aspen Plus program 90
46	Property method and model 91
47	Estimation field in Aspen Plus program 92
48	Selection parameter to estimate..... 92
49	Select method to estimate properties 93
50	Import molecular structure..... 93
51	Calculate bonds of the component..... 94
52	Stream detail..... 94
53	Block setup..... 95
54	Define reactions in the reactor..... 95
55	The result form Aspen Plus program..... 96

CHAPTER 1

INTRODUCTION

Global warming is a major problem in the world. The ways to solve this problem of each country are different based on their resources and geography. One of the ways to solve the problem is of using clean sources or renewable sources that are interesting. This ways can decrease carbon dioxide (CO₂) in the air and carbon life cycle more than using source from fossil.

Biodiesel is an alternative fuel for diesel engines. Biodiesel represents a mixture of alkyl (usually methyl or ethyl) esters of long-chain aliphatic acids. Because its primary feedstock is a vegetable oil or animal fat, biodiesel is generally considered to be renewable. Biodiesel have lower emissions of carbon monoxide, unburned hydrocarbons, particulate matter, and air toxics than petroleum-based diesel fuel (Zheng *et al.* 2008). Triglycerides in vegetable oil or animal oil hold promise as alternative diesel engine fuels (Gerpen 2005). However, the direct use of vegetable oils or oil blends is generally considered to be unsatisfactory and impractical for both direct-injection and indirect type diesel engines (Ramadhas *et al.* 2005). Methyl esters or ethyl esters obtained can be (Fukuda *et al.* 2001) produced by chemically reacting a vegetable oil or animal fat with an alcohol such as methanol or ethanol used strong acids or bases as catalysts (Lotero *et al.* 2005). Since the demand of biodiesel increase rapidly, glycerol which is obtained as a by-product became to oversupply. The oversupply of glycerol feed stock will create a glut on the market in many countries. Therefore many research attempts to utilize glycerol in several approaches.

Etherification of glycerol is one of a promising process for oxygenate fuel production. The product form etherification of glycerol with *tert*-butyl alcohol consists of mono-, di- and tri- *tert*-ether of glycerol.

Di- and tri-*tert*-butyl ethers of glycerol are usable as potential decrease carbon monoxide and particulate matter emission from incomplete combustion. Mono-*tert*-butyl ether of glycerol has a low solubility in diesel fuel and therefore the etherification of glycerol must be directed to the maximum formation of di- and tri-ethers (Klepacova *et al.* 2005). However the kinetic parameters of these reactions have not be determined yet.

Since the synthesis of ethers is a typical example of equilibrium-limited reaction that produces by-product H₂O, the presence of H₂O has a strong inhibition effect on the catalytic activity (Cunill *et al.* 1993) and the conversion is generally low due to limits imposed by thermodynamic equilibrium. A combined process of separation and chemical reaction in a single unit operation which is one type of reactive distillation has attracted much attention for overcoming the equilibrium conversion. Reactive Distillation (RD), a multifunctional process which combines reaction and separation in single unit operation, has received much attention for esterification and etherification. It is suitable for many reactions particularly those limited by chemical equilibrium. The most important benefit of reactive distillation is a reduction in capital investment and energy consumption.

From the above reasons, this research focuses on the application of reactive distillation to produce ethers from glycerol and *tert*-butyl alcohol and the objectives are

1. To estimate the missing properties of ether products from etherification glycerol with *tert*-butyl alcohol using different group contribution methods.
2. To determine the kinetic parameters for the synthesis of ethers from glycerol and *tert*-butyl alcohol in batch reactor.
3. To produce *tert*-butyl ethers of glycerol in reactive distillation and investigate the effect of operating conditions on the performance of a reactive distillation.

CHAPTER 2

THEORY

This chapter provides some background information necessary for understanding biodiesel, synthesis of *tert*-butyl ether of glycerol, group contribution method, reactive distillation process and Aspen Plus simulator program. The details are as follows.

1 Biodiesel

Biodiesel is a nonpetroleum-based fuel that consists of alkyl esters derived from either the trans-esterification of triglycerides (TGs) or the esterification of free fatty acids (FFAs) with alcohols. Biodiesel is called the environmentally friendly biofuel since it provides a means to recycle carbon dioxide. In other words, biodiesel does not contribute to global warming. As a point of comparison, pure biodiesel (B100) releases about 90% of the energy that normal diesel does, and hence, its expected engine performance is nearly the same in terms of engine torque and horsepower. The transesterification reaction is shown in Figure 1. Because the reaction is reversible, excess alcohol is used to shift the equilibrium to the products side (Hoydonckx *et al.* 2004).

Among the alcohols used in the transesterification process are methanol, ethanol, propanol, butanol and amyl alcohol. Methanol and ethanol are used most frequently, especially methanol because of its low cost and its physical and chemical advantages (polar and shortest chain alcohol). It can quickly react with triglycerides and NaOH catalyst is easily dissolved in it. The reaction can be catalyzed by alkalis, acids, or enzymes. If more water and free fatty acids are in the triglycerides, acid catalyzed transesterification can be used (Dorado *et al.* 2004).

Industrially, NaOH and KOH are preferred due to their wide availability and low cost.

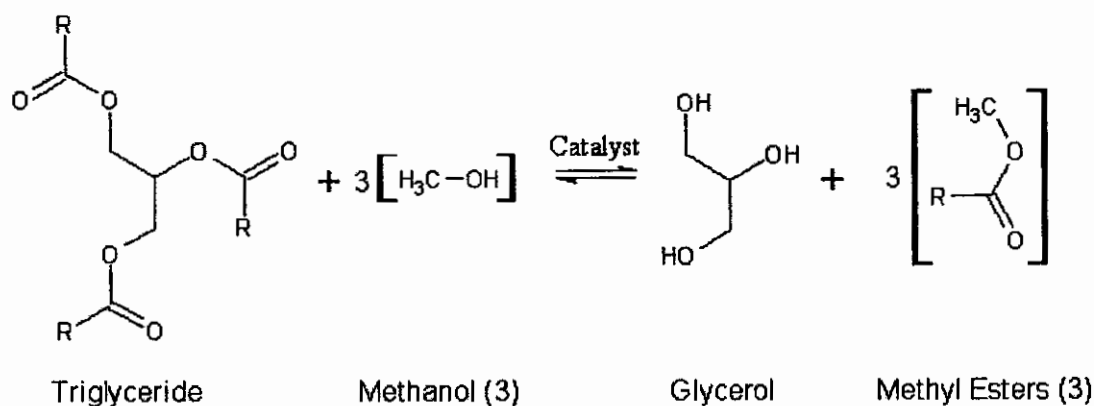


Figure 1 Transesterification of triglycerides with alcohol.

As shown in Figure 2, the base catalyzed production of biodiesel generally occurs using the following steps. Firstly, the catalyst was mixed with alcohol using a standard agitator or mixer. The alcohol/catalyst mix is then charged into a closed reaction vessel and the oil or fat is added. The system from here on is totally closed to the atmosphere to prevent the loss of alcohol. The reaction mix is kept just above the boiling point of the alcohol (around 70 °C) to speed up the reaction and the reaction takes place. Recommended reaction time varies from 1 to 8 hours. Excess alcohol is normally used to ensure total conversion of the fat or oil to its esters. After transesterification of triglycerides, two major products exist: glycerin and biodiesel. Each has a substantial amount of the excess methanol that was used in the reaction. The glycerin phase is much more dense than biodiesel phase and the two can be gravity separated with glycerin simply drawn off the bottom of the settling vessel. The co-product, glycerol, needs to be recovered because of its value as an industrial chemical. Glycerol could be separated because it is insoluble in the esters. The glycerin by-product contains unused catalyst and soaps that are neutralized with an acid and sent to storage as crude glycerin. In some cases the salt formed during this phase is recovered for use as fertilizer. In most cases the salt is left in the glycerin. Water and alcohol are removed to produce 80-88% pure glycerin that is ready to be sold as crude glycerin. In more sophisticated operations, the glycerin is distilled to 99% or higher purity and sold into the cosmetic and pharmaceutical markets.

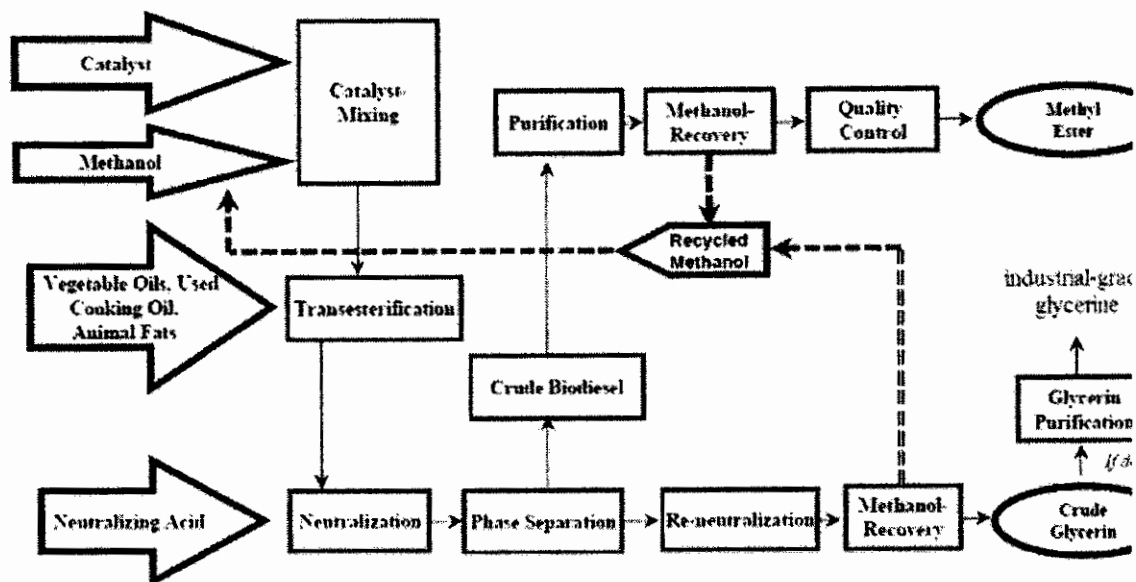


Figure 2 Biodiesel production flowchart.

Cetane number (CN) is widely used as diesel fuel quality parameter. The number relates to the ignition delay (the period that occurs between the start of fuel injection and the start of combustion). Since there are hundreds of components in diesel fuel, with each having a different cetane quality, the overall cetane number of the diesel is the average cetane quality of all the components. Generally, diesel engines run well with a cetane number from 40 to 51. Biodiesel from vegetable oil sources have been recorded as having a cetane number range of 48 to 61 (Romas *et al.* 2009). Biodiesel cetane number depends on the feedstock used for its production. The longer the fatty acid carbon chains and the more saturated molecules has higher the cetane number (Dermibas 2005; Knothe *et al.* 1998). Fuels with higher cetane number which have shorter ignition delays provide more time for the fuel combustion process to be completed. Hence, higher speed diesels operate more effectively with higher cetane number fuels. Premium diesel may have additives to improve cetane number and lubricity, detergents to clean the fuel injectors and minimize carbon deposits, water dispersants, and other additives depending on geographical and seasonal needs. Dimethyl ether may prove advantageous as a future diesel fuel as it has a high cetane number (Jang and Bae 2009). The 2-Ethyhexyl nitrate (2-EHN) (Bornemann *et al.*

2002) or di-*tert*-butyl peroxide (Clothier *et al.* 2000) to diesel oil to improve ignition and boost cetane number.

2 Etherification of glycerol

Glycerol has numerous applications in different industrial processes. One of the interesting processes is glycerol ethers synthesis. A number of studies on the preparation of glycerol ethers from glycerol with isobutylene or *tert*-butyl alcohol by using different catalytic systems have been reported (Noureddini *et al.* 1998; Klepacova *et al.* 2005; Klepacova *et al.* 2006; Karinen *et al.* 2006). The reactions are shown in Figure 3. However, an isobutylene source is limited to catalytic cracking or steam cracking fractions therefore ether products still partly base on fossil. Isobutylene is also a valuable reagent as use as a starting material in other chemical industries. Since *tert*-butyl alcohol is a major by-product in the ARCO process for the manufacture of propylene oxide (Matouq *et al.* 1993), it can provide an alternative route for the ethers synthesis (Matouq *et al.* 1996).

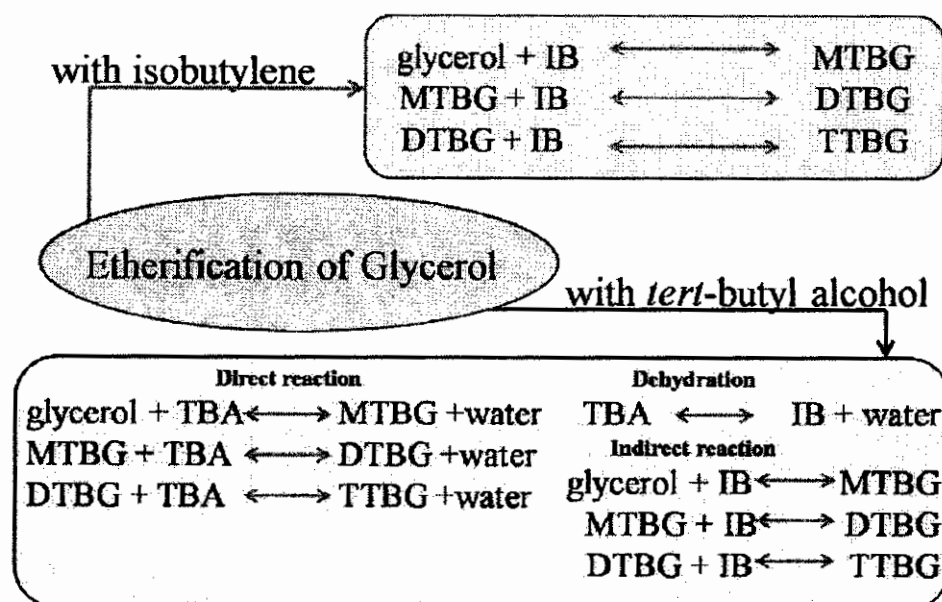


Figure 3 Etherification of glycerol with isobutene and *tert*-butyl alcohol

Tert-butyl alcohol had been proved as an alternative reagent instead of isobutylene to react with ethanol for ETBE production (Goto *et al.* 1999). TBA can directly react with glycerol, or indirectly dehydrated to isobutylene and then react

with glycerol. However, in the case of etherification with glycerol, using *tert*-butyl alcohol as an etherification agent, the reaction was gave lower di- and tri-ethers yield than that of using isobutylene. This might be influenced from water formation from TBA dehydration which inhibit the catalytic activity of ion-exchange resin catalysts (Klepakova *et al.* 2006).

3 Group contribution method

Physical and thermodynamic properties of gases and liquids are of vital concern to the chemical engineer, who is involved in research, in development, in plant design, or in production. But for many compounds of interest to the chemical engineer, the only data available such as the molecular weight and the boiling point and for some of newer, more exotic compounds, even the boiling point may not have been reported. Even for well-known compounds, the data available will often not cover the region of interest to the chemical engineer. It is thus not surprising that in recent years literally thousands of investigated which present methods of estimating a variety of properties. Many of the method are based on theoretical considerations and allow the user to calculate one set of properties from another set already known. Others require only acknowledge of the structure of the compound under consideration and use empirically derived contributions for various atomic or function subgroups within the molecule. Such contributions are then manipulated algebraically to estimate the required output properties. “Structural increment” method are extremely useful if no other property data exist for the compound, since calculated output properties can then be in other methods to estimate a variety of other properties.

3.1 Joback group contribution method

Joback's *et al.* (1984) reevaluated Lydersen's group contribution method scheme, added several new functional groups, and determined new contribution values. The relations for calculations properties are:

$$T_c(K) = T_b[0.5084 + 0.965\{\sum_k N_k (tck)\} - \{\sum_k N_k (tck)\}^2]^{-1} \quad (2.1)$$

$$P_c(\text{bar}) = [0.113 + 0.0032N_{\text{atom}} - \sum_k N_k (pck)]^{-2} \quad (2.2)$$

$$T_b(K) = 198 + \sum_k N_k (tbk) \quad (2.3)$$

$$G_f^0(\text{kJ mol}^{-1}) = 53.88 + \sum_k N_k (gfk) \quad (2.4)$$

where the contributions are indicated as *tck*, *pck* and *vck*. The group identities and Joback's value for contributions to the critical are listed in Appendix B. For calculation of critical temperature (T_c), the value of the normal boiling point (T_b) is needed.

3.2 Gani group contribution method

Constantinou and Gani developed an advance group contribution method on the UNIFAC group but they allow for more sophisticated of the desired properties and also for contributions at a "second order" level. The functions give more flexibility to the correlation while the second order partially overcomes the limitation of UNIFAC which cannot distinguish special configurations such as isomers, multiple group located close together, resonance structures, etc., at the "first order". The general Constantinou and Gani formulation of a function $f[F]$ of a property F is

$$F = f[\sum_k N_k (F_{1k}) + W \sum_j M_j (F_{2j})] \quad (2.5)$$

Where f can be a linear or nonlinear function, N_k is the number of first-order groups of type k in the molecule. F_{1k} is the contribution for the first-order group labeled $1k$ to the specified properties of F . M_j is the number of second-order group of type j in the molecular and F_{2j} is the contribution for the second-order group labeled $2j$ to the specified property of F . The value of W is set to zero for first-order calculations and set to unity for second-order calculations. For the properties, the Constantinou and Gani formulations are

$$T_c(\text{K}) = 181.128 \ln [\sum_k N_k (tc1k) + W \sum_j M_j (tc2j)] \quad (2.6)$$

$$P_c(\text{bar}) = [\sum_k N_k (pc1k) + \sum_j M_j (pc2j) + 0.10022]^{-2} + 1.3705 \quad (2.7)$$

$$T_b(\text{K}) = 204.359 \ln [\sum_k N_k (tb1k) + W \sum_j M_j (tb2j)] \quad (2.8)$$

$$G_f^0(\text{kJ mol}^{-1}) = -14.83 + [\sum_k N_k (gf1k) + W \sum_j M_j (gf2j)] \quad (2.9)$$

The error of this method is large when it is applied with calculations of low carbon atom and second-order is applied. But the Constantinou and Gani method can be quite reliable for the formation properties, especially for species with three or more carbon atoms. The functional groups from Gani's group contribution are listed in Appendix C.

3.3 Benson group contribution method

Benson and coworkers have developed the technique for thermodynamic properties estimation. There are several references to Benson's work such as CHETAH program. Benson's method is detailed of the contribution of bonding arrangements that chosen groups can have with every other type of group or atom except hydrogen. Thus the method involves next-nearest neighbor interactions.

The values from the Benson group can be assumed directly to obtain standard enthalpy of formation ($\Delta H_{f(298.15)}^0$), and heat capacity ($C_p^0(T)$) values. However, obtaining $S_{f(298.15)}^0$ also requires taking molecular symmetry in to account. Finally, obtaining $\Delta G_{f(298.15)}^0$ requires subtracting the entropy of the elements.

The relations are

$$\Delta H_{f(298.15K)}^0 = \sum_k N_k (\Delta H_{fk}^0) \quad (2.10)$$

$$S_{f(298.15K)}^0 = \sum_k N_k (S_k^0 + S_s^0) + S_s^0 \quad (2.11)$$

$$S_{el(298.15K)}^0 = \sum_e v_e (S_e^0) \quad (2.12)$$

$$\Delta G_{f(298.15K)}^0 = \Delta H_{f(298.15K)}^0 - 298.15 [S_{f(298.15K)}^0 - S_{el(298.15K)}^0] \quad (2.13)$$

The Benson's group contribution values are listed in Appendix D. The sample entropy, S_s^0 is independent of T and given by

$$S_s^0 = R \ln(N_{oi}) - R \ln(N_{ts}) \quad (2.14)$$

Where N_{oi} is the number of structural isomers of the molecule and N_{ts} is the total symmetry number. Normally, $N_{oi} = 1$ so it makes no value in equation (2.14). The two cases can be non unit values. The first is when there is a plane of symmetry where the atoms can form mirror image arrangements (optical isomers) so that the atom in the

plane has asymmetric substitutions. For example, the four atoms (H, F, Cl, I) bonded to the carbon shown in Figure 4 (a) can be arranged in two distinct ways, so its $N_{oi} = 2$. The second way for N_{oi} to be different from unity is an otherwise symmetrical molecule is frozen by steric effect onto an asymmetrical conformation. For example, 2, 2', 6, 6'-tetramethylbiphenyl shown in Figure 4 (b) cannot rotate about the bond between the two benzene rings due to its 2, 2' steric effects. Therefore, the plane of the ring have two distinct arrangements ($N_{oi} = 2$) which must be included in the entropy calculation. If the desired species is the racemic mixture (equal amounts of the isomers), each asymmetric center contributes two to N_{oi} , but if the species is a pure isomer, $N_{oi} = 1$.

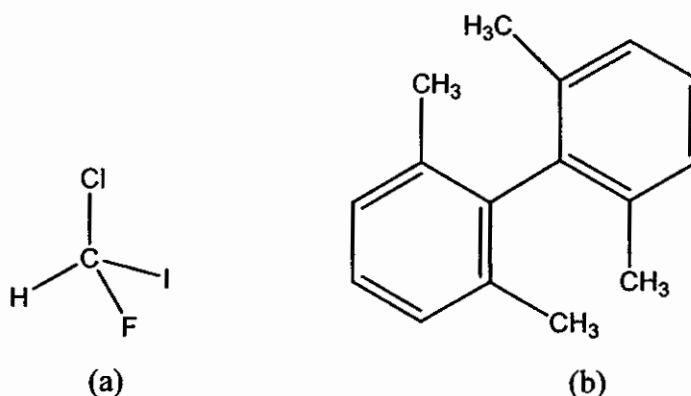


Figure 4 (a) Carbon bond with Hydrogen, Fluorine, Chlorine and Iodine
(b) 2, 2', 6, 6'-tetramethylbiphenyl structure

To obtain N_{ts} , one multiplies the two distinct types of indistinguishability that can occur: “internal” designated N_{is} , and “external” designated N_{es} . The value of N_{is} can be found by rotating terminal groups about their bonds to interior groups. An example is methyl ($-CH_3$) which has three indistinguishable conformations ($N_{is} = 3$) and phenyl which has $N_{is} = 2$. Benzene has $N_{es} = 6$ from rotation about its ring center, etc. Finally N_{ts} is found form;

$$N_{ts} = N_{es} \prod_{k=\text{term}} (N_{is})_k \quad (2.17)$$

4 Conventional reactor versus reactive distillation

A conventional configuration for a chemical process usually involves two steps of chemical reaction and subsequent separation. In the chemical reaction step, reactants are brought into contact with solid catalysts at appropriate process conditions in one or more reactors. The stream leaving the reactor section then goes to one or more separation steps where unconverted reactants are separated from the reaction products and the inerts. The unconverted reactants, in some cases, may be recycled to the reaction section. When a substantial amount of inerts are present in the system, at least two separation units for separation of high purity product and for separation of the unconverted reactants from the inerts are required. The separation process by distillation is typically chosen.

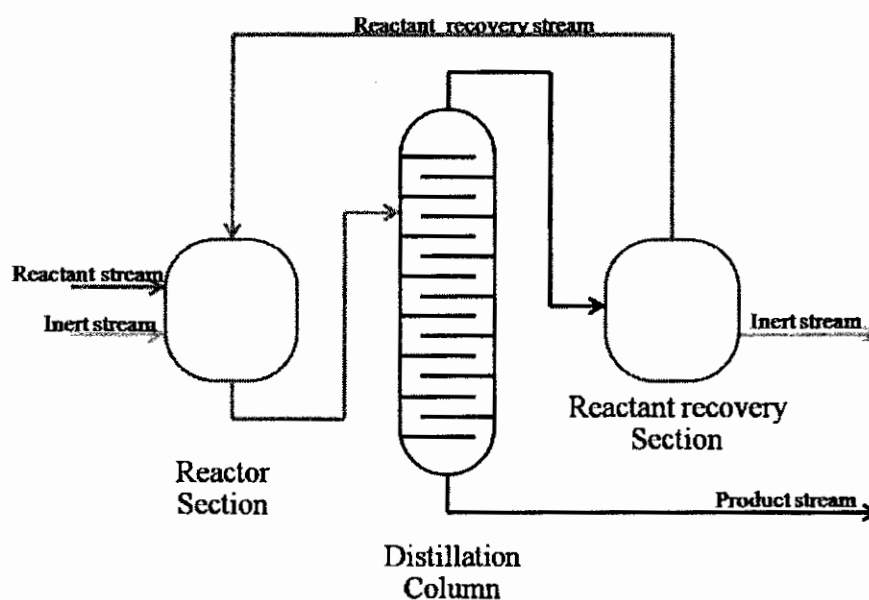


Figure 5 Conventional process involving reaction followed by separation.

Reactive distillation is combination of reaction and separation in one single. Reactive distillation can eliminate conversion limitations of equilibrium control reaction by continuous removal of products from the reaction. Reactive distillation has been applied to many esterification, hydrolysis process and the formation of fuel oxygenates in chemical and petrochemical industries. Reactive distillation was first used by the chemical and petrochemical industry in esterification process to separate

reaction product from reactant to increase product yields (Venkataraman *et al.* 1990). Applications of commercial reactive distillations can be found in many processes as reported in literature methyl acetate process (Fuchigami 1989), ethyl *tert*-butyl ether (Assabumrungrat *et al.* 2004), on pilot scale ethyl acetate process (Lai *et al.* 2007).

4.1 Reactive distillation configurations

The flow diagram of the reactive distillation is shown in Figure 6. The middle section of the column is the reactive section. For a non-azeotropic chemical system, separation of the inerts takes place in the rectifying section and the purification of the product takes place in the stripping section.

The reactive distillation column contains both the catalyst contact device and the distillation device. A reaction occurs in the catalyst contact device and then the reacting phase passes to the distillation device for vapor/liquid contact and separation. For both configurations, a rectification section may be located above the reactive distillation section of the column and a stripping section may be located below it, depending upon purity specifications.

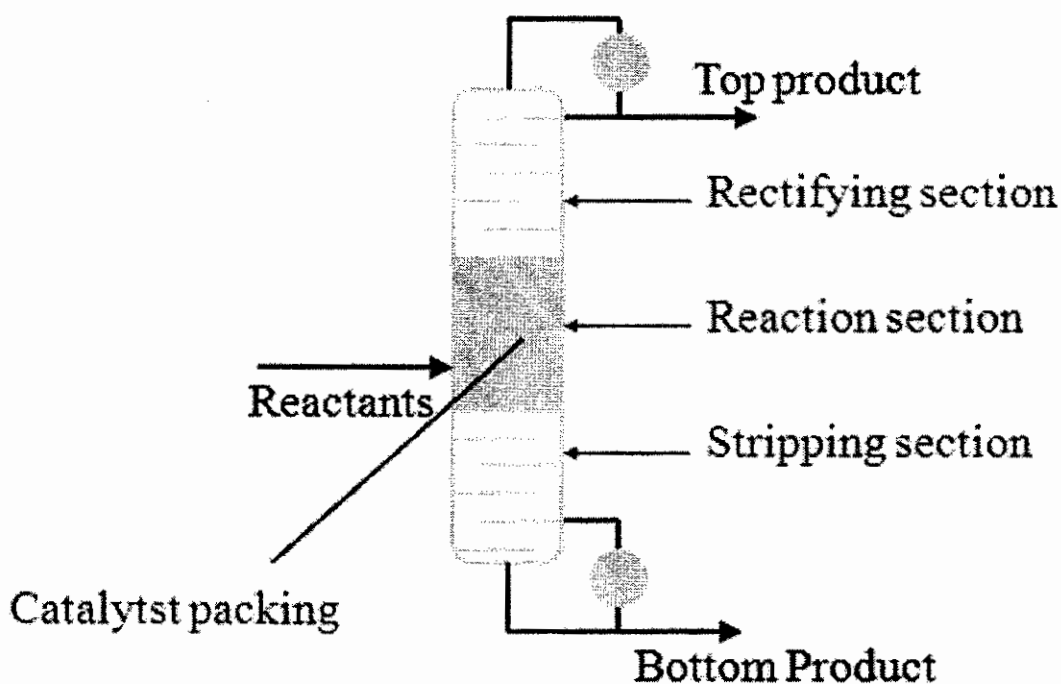


Figure 6 Concept of reactive distillation

4.2 Advantages of reactive distillation

Application of reactive distillation to a catalytic chemical reaction using solid catalysts offers many advantages compared to a conventional process as summarized below:

4.2.1 Two process steps, i.e. separation and reaction, can be carried out in the same device. Such integration leads to lower costs in pumps, piping and instrument.

4.2.2 The heat released from the reaction can be used for vaporization of liquid, leading to savings of energy costs by the reduction of reboiler duties.

4.2.3 Product selectivity can be improved due to a fast removal of reactants or products from the reaction zone. By this, the probability of consecutive reactions, which may occur in the sequential operation mode, is lowered.

4.2.4 If the reaction zone in the reactive distillation column is placed above the feed point, poisoning of the catalyst can be avoided. This leads to longer catalyst lifetime compared to conventional systems.

5 Aspen Plus simulator program

Aspen Plus program is one of the components in the Aspen Engineering Suite. It is an integrated set of products designed specifically to promote best engineering practices and to optimize and automate the entire innovation and engineering workflow process throughout the plant and across the enterprise. It automatically integrates process models with engineering knowledge databases, investment analyses, production optimization and numerous other business processes. Aspen Plus contains data, properties, unit operation models, built-in defaults, reports and other features. Its capabilities develop for specific industrial applications, such as petroleum simulation.

Aspen Plus is process engineering tool for the design and steady-state simulation and optimization of process plants which easy to use, powerful, flexible. Process simulation with Aspen Plus can predict the behavior of a process using basic engineering relationships such as mass and energy balances, phase and chemical equilibrium, and reaction kinetic. Given reliable thermodynamic data, realistic

operating conditions and the rigorous Aspen Plus equipment models, actual plant behavior can be simulated. Aspen Plus can help to design better plants and to increase profitability in existing plants.

5.1 Features of Aspen Plus program

Utilize the latest software and engineering technology to maximize engineering productivity through its Microsoft Windows graphical interface and its interactive client-server simulation architecture.

5.1.1 Contain the engineering power needed to accurately model the wide scope of real-world applications, ranging from petroleum refining to non-ideal chemical systems containing electrolytes and solids.

5.1.2 Support scalable workflow based upon complexity of the model, from a simple, single user, process unit flowsheet to a large, multi-engineer developed, multi-engineer maintained, plant-wide flowsheet.

5.1.3 Contain multiple solution techniques, including sequential modular, equation-oriented or a mixture of both, and allow as quick as possible solution times regardless of the application.

5.2 Benefits of Aspen Plus program

5.2.1 Proven track record of providing substantial economic benefits throughout the manufacturing life cycle of a process, from R&D through engineering and into production.

5.2.2 Allow users to leverage and combine the power of sequential modular and Equation-oriented techniques in a single product, potentially reducing computation times by an order of magnitude while at the same increasing the functionality and suability of the process model.

CHAPTER 3

LITTELATURE REVIEW

This chapter contains the research reviews of etherification of glycerol with *tert*-butyl alcohol, the kinetic models of ethers and esters production, group contribution methods and application of reactive distillation for ethers production.

1 Production of *tert*-butyl ether of glycerol

Tert-Butyl ethers of glycerol with high content of di-ethers and especially tri-ethers are known as potential oxygenates to diesel fuels (diesel, biodiesel and their mixtures). These oxygenate ethers can reduce the emissions and mainly particulate matters (Noureddini *et al.* 1998). When glycerol is etherified with isobutene or *tert*-butyl alcohol, some or all of the hydroxyl groups in the glycerol molecule react. Thus, depending on the extent of etherification, up to five ether isomers may be formed (as show in Figure 7): two monosubstituted monoethers (3-*tert*-butoxy-1,2-propanediol (7a) and 2-*tert*-butoxy-1,3-propanediol (7b)), two disubstituted diethers (1,3-di-*tert*-butoxy-2-propanol (7c) and 2,3-di-*tert*-butoxy-1-propanol (7d)) and one trisubstituted triether (1,2,3-tri-*tert*-butoxy propane(7e)).

Klepacova *et al.* (2005) studied etherification of glycerol with isobutylene or *tert*-butyl alcohol the liquid phase catalyzed by strong acid ion exchange resins of Amberlyst type and by two large-pore zeolites H-Y and H-Beta. In the case of using isobutylene, the highest glycerol conversion of 100% was obtained over both strong acid macroreticular ion-exchange resin A-35 and A-15 at 60°C. However, higher temperature (90°C) causes considerable drop in conversion and yield of desired di-ethers and tri-ethers. The obtained yield is 39.2% in the case of A-35 while 10.8% in the case of A-15. This is become the higher reaction temperature supports some side reactions show below.

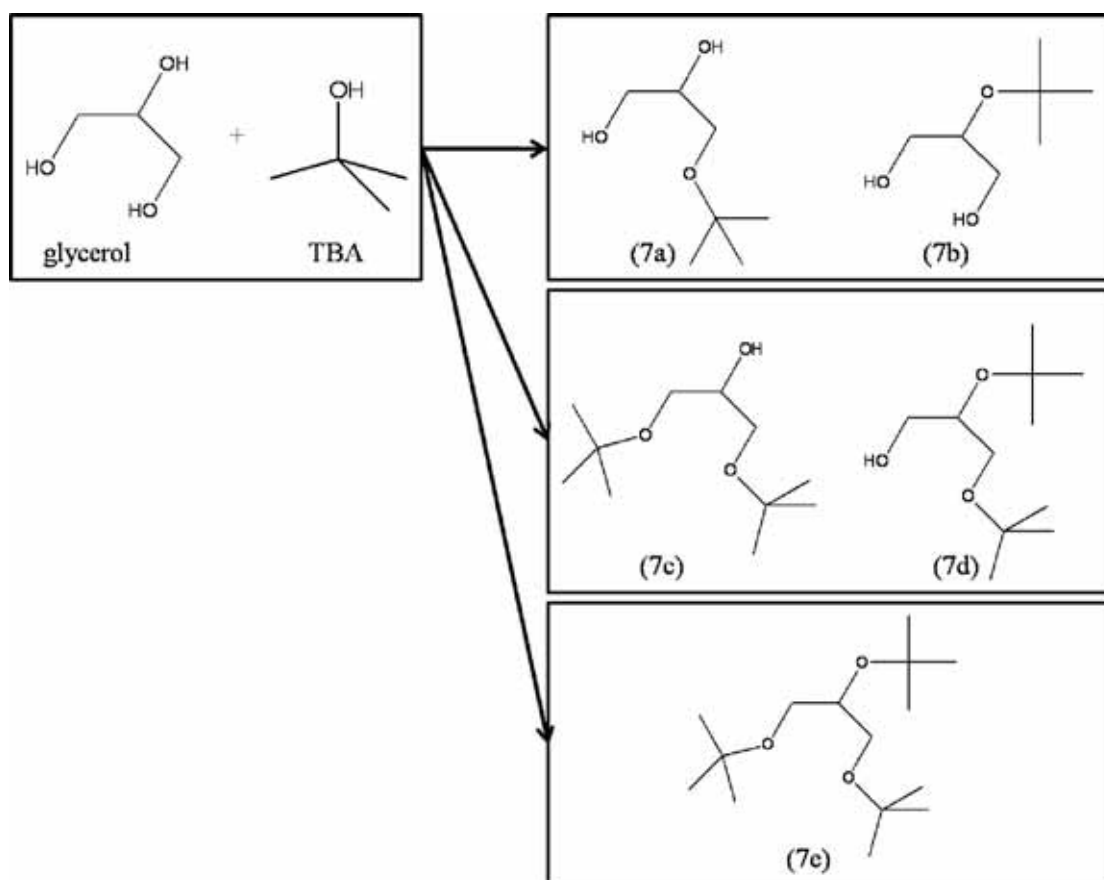


Figure 7 Reaction scheme for the etherification of glycerol with *tert*-butyl alcohol.



The formation of diisobutylenes (DIB) by dimerisation of isobutylene could be occurred when molar ratio of isobutylene to glycerol was over 4:1. Zeolites H-Y and H-Beta provides lower selectivity than ion-exchange resins. Tri-*tert*-butyl ether of glycerol (TTBG) is not formed over H-Beta zeolite because of steric hindrance. The higher amount of lower oligomers of isobutylene (di-isobutylenes) was formed over H-Beta at 90°C. In the case of using *tert*-butyl alcohol, glycerol conversions at 60°C were 86% and 79% while yield of desired di-ethers and tri-ethers were 14.8% and 13.4% in the cases of A-35 and A-15, respectively. The lower in conversion and yield in case of using *tert*-butyl alcohol comparing with isobutylene might because water formation by dehydration of *tert*-butyl alcohol which can deactivate the catalysts.

Klepacova *et al.* (2006) further emphasized on the investigation of Amberlyst type ion exchange resin i.e., Amberlyst 15, Amberlyst 35, Amberlyst 31 and Amberlyst 119. The most suitable catalysts for *tert*-butylation of glycerol are the ion-exchange resins with a high degree of crosslinking i.e., A-15 or A-35. These catalysts have large pores which allow the formation of voluminous molecules of glycerol *tert*-butyl ethers. The optimal reaction temperature is 75°C, the glycerol conversion was 87.8 % on catalyst A-35 (more acid) and 68.4 % on A-15 when *tert*-butyl alcohol was an etherification agent. The conversion of glycerol and the yield of ethers have increased with higher mole ratio $n(\text{TBA})/n(\text{G})$. Water present in the reaction system has an inhibition effect on glycerol *tert*-butylation. The best results were reached when isobutylene was used as etherification agent (XG = 100 %, Yield of di- and tri-ethers is 91.6 % for A-15 and 90.8 % for A-35). No water was formed during this reaction. The higher swelling capacity was shown by ion exchange resins with gel structure A-31 and A-119 because the degree of crosslinking is very low, but their pores are too narrow also after the swelling, so the reaction runs slowly and with difficulty.

Karinen *et al.* (2006) studied the etherification of glycerol with isobutene in liquid phase with acidic ion exchange resin catalyst (A-35). To increase the selectivity of the reaction towards the ethers and to hinder the formation of hydrocarbons it is required that the reaction should be carried out above 70°C with isobutene and glycerol near stoichiometric ratio. Excess of isobutene enhances the oligomerisation reaction whereas and the excess of glycerol increases the viscosity of the reaction mixture. High viscosity affect the mass transfer between liquid solution and catalyst therefore the reaction rate was limited. In a typical 7 h experiment, complete or almost complete conversion of glycerol was achieved at reaction temperatures above 70°C when the initial isobutylene/glycerol ratio was 3 or higher. Addition of *tert*-butyl alcohol to the reaction mixture can hinder the oligomerisation reactions and eliminate the mass transfer limitations therefore improves the selectivity and yield. The formation of tri-ether is favoured when the initial isobutene/glycerol molar ratio is high. The optimal conditions for the formation of the di-ether are stoichiometric initial molar ratio of isobutene/glycerol and 80°C, and at low conversion level as well as with low initial isobutene/glycerol molar ratio the mono-ethers are the main products.

C8 alkenes are the main products in the oligomerisation reaction. The fraction of C12 and C16 hydrocarbons decreases when the reaction is carried out at high temperatures or if the selectivity is controlled by adding *tert*-butyl alcohol to the reaction mixture.

Klepacova *et al.* (2007) investigated the influence of catalyst, and temperature on the etherification of glycerol with isobutylene in the liquid phase catalysed by strong acid ion-exchange resins of Amberlyst type (A-15 and A-35), *p*-toluenesulfonic acid and by two large-pore zeolites H-Y and H-Beta. The highest glycerol conversion 88.7% was achieved over zeolite H-Y after 8 h. Reaction over H-Beta zeolite runs faster with high selectivity to di-ethers, but formation of tri *tert*-butyl ethers of glycerol was sterically hindered. The highest amount of tri-ethers was observed over A-35. In the case of ion-exchange resins A-35 gives about 10% higher initial rate than A-15. From the technological point of view the zeolites are not convenient as catalysts for studied reaction because of their easy deactivation and higher price to that of ion-exchange resins. The homogeneous catalyst (*p*-toluenesulfonic acid) provides better results in di-ethers formation. The most appropriate temperature for etherification of glycerol is 60°C because the reaction rate is sufficient with high conversion and selectivity to ethers. The concentration of glycerol decrease as temperature increases, showing that the side reaction of isobutylene dimerisation became the preferred reaction at higher temperatures and longer reaction times.

2 Kinetic mechanism models of esters and ethers production

The kinetic models of etherification and esterification catalyzed by ion-exchange resins were classified in Langmuir-Hinshelwood model (LH model), Eley-Rideal model (ER model) and Pseudo Homogenous model (PH model or PL model). For high polar reaction media, the PH model has been successful used to estimated kinetic parameter (Sanz *et al.* 2004; Steinigeweg and Gmehling 2004; Jiménez *et al.* 2002) However, the PH model does not considering in sorption effect of the different species (reactants and products) into the catalyst (ion-exchange resin). The LH model and ER model consider the sorption effect in their kinetic model. For LH model, the basic idea mechanism is that all reactants are adsorbed on the catalyst surface before chemical reaction takes place. The ER model is applied when the reaction takes place

between an adsorbed and a non-adsorbed reactant. Figure 8 show the difference between LH model and ER model mechanism. For ER mechanism, firstly an atom adsorbs onto the surface of catalyst (Figure 8a) and another atom passes by which interacts with the one on the surface (Figure 8b). Finally, a molecule is formed and then desorbs (Figure 8c). But for LH mechanism, two atoms adsorb onto the surface of catalyst (Figure 8d). Two atoms diffuse across the surface and interact when they are close (Figure 8e). Finally, a molecule is formed which desorbs from catalyst surface (Figure 8f).

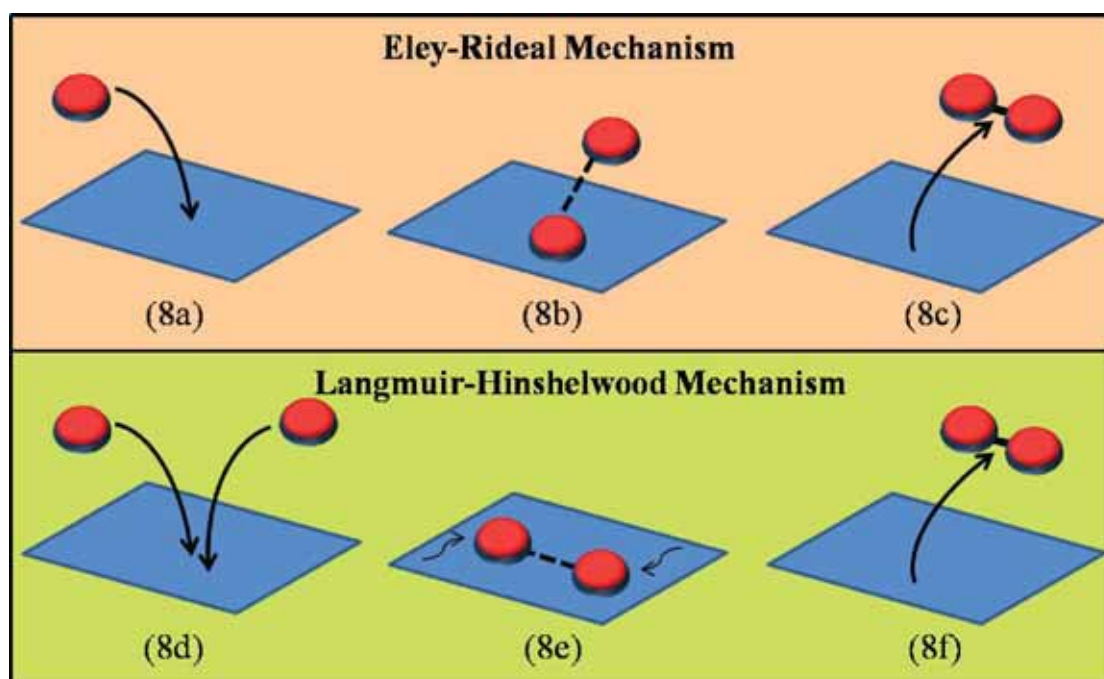


Figure 8 Eley-Rideal and Langmuir-Hinshelwood mechanism.

Delgado *et al.* (2007) was investigated esterification of lactic acid and ethanol in the presence of the commercial ion-exchange resin Amberlyst 15. Experimental kinetic data of the esterification and the hydrolysis reactions were correlated simultaneously with the Langmuir-Hinshelwood (LH) and pseudo-homogeneous (PH) models. The non-ideality of the liquid phase was considered by using activities instead of mole fractions. The activity coefficients of the components in the liquid phase were calculated by using the UNIQUAC equation. The equilibrium constant was calculated from the component composition at equilibrium. The kinetic

parameters of the PH and LH models were obtained by reduction of the experimental kinetic data to minimizing the objective function using the Simplex–Nelder–Mead method. A fourth order Runge-Kutta method was used to solve the differential equation. The quality of the curve fitting was evaluated through the mean relative deviation. The LH model gave the best agreement with the kinetic experimental data. The activation energy of esterification and hydrolysis reactions were found to be 52.29 and 56.05 kJ mol⁻¹.

Zhang *et al.* (2004) studied the esterification of lactic acid with ethanol in the presence of five different ion-exchange resins. Two simplified mechanisms based on LH model were compared by correlating the experimental data. The LH mechanism model were classified in mechanism A and B. Mechanism A assumes that ethanol and water adsorbed much stronger than other components in the esterification solution, so the adsorption of ethyl lactate and lactic acid was neglected. For mechanism B, it was assumed that lactic acid and water had the strongest adsorption than ethyl lactate and ethanol. The rate equation for mechanism A described more accurately the experimental data than mechanism B. Therefore, the former was more reliable for this kind of esterification reaction.

Karinen and Krause (2001) investigated etherification of 2,4,4-trimethyl-1-pentene and 2,4,4-trimethyl-2-pentene with methanol catalyzed by a novel Smopex-101. The LH model which the adsorption of alkenes is assumed to be weak relative to methanol and ether show the activation energies obtained for the etherification of 2,4,4-trimethyl-1-pentene and 2,4,4-trimethyl-2-pentene were 86 and 80 kJ mol⁻¹. An equally good fit was obtained with the ER model, which assumes that the alkenes react without adsorption. In both models the adsorption constants for methanol and ether are of the same order of magnitude. This constitutes a significant difference from the modeling results obtained with conventional ion-exchange resin catalysts and can be explained by the nature of the polymer matrixes.

Mao *et al.* (2007) investigated the etherification of methanol with 2-methyl-1-butene (2M1B) and 2-methyl-2-butene (2M2B) catalyzed by the macroporous cation-exchange resin (D005II). The activity coefficients were estimated by Wilson method. There were three mechanisms adopted for simulating reaction rate equations, containing homogeneous reaction mechanism (PH model), LH mechanism model and

ER mechanism model. The equations based on the LH mechanism model were found to get the best fit with the experimental data. The results showed that the experimental data for thermodynamics agreed with the theoretical predications well, and the activation energy was 88.1 and 102.1 kJ mol⁻¹ for the etherification of 2M1B and 2M2B, respectively, by kinetic calculation.

3 Group contribution method

A group contribution method is a technique to estimate and predict thermodynamic and other properties from molecular structures. Their advantages are that they need no experimental data, and since organic compounds used in chemical industry. Group contribution methods can be applied to really a great number of substances. However, first order group contribution methods cannot distinguish among structural isomers, because the isomers have the same number and kind of groups. The second order groups have been introduced into the group contribution equation.

Benson *et al.* (1976) had proposed additives of molecular properties. It is shown that the zero-order approximation is equivalent to the law of additive of atomic properties, the first-order approximation to the law of additives of bond properties, the second-order approximation to the law of additives of group properties. The results showed agreements for the various rules and certain extensions and limitations. The estimation of bond dissociation energies is possible with the additives rules as are the thermodynamic properties of free radicals. The conclusion showed that for C_p and S° (ideal gases), the additives of atomic properties works to about ± 2 cal mole⁻¹K⁻¹, while the additives of bond properties is usually good to about ± 1 cal mole⁻¹K⁻¹. The latter also estimates H_f^0 to about ± 3 kcal mole⁻¹. The group additives relation is generally obeyed to within ± 0.5 cal mole⁻¹K⁻¹ for C_p and S° and about ± 0.6 kcal mole⁻¹ for H_f^0 .

George *et al.* (1976) used Ambrose, Joback and Chueh-Swanson definitions of group contributions and modified to account for the location of the functional groups in the molecule for predicting the auto ignition temperature (AIT) of pure components. The result proposed that the method can predict the auto ignition

temperature of pure components only from the knowledge of the molecular structure, with an average error of 2.8 % and a correlation coefficient of 0.98.

Iwai *et al.* (1999) introduced the second order of group contribution method for calculate normal boiling point of many substance. This method showed the absolute average error of the normal boiling points of 1.24 K. The proposed method can distinguish the normal boiling points of alkane isomers well. The saturated vapor pressures have been calculated using the present second order groups. The absolute average percent errors are 6.0, 3.6, and 6.0% at T_b-50 , T_b and T_b+50 , respectively.

Constantinou and Gani (2004) had reported the expectation of higher order of group contribution method should be more correct than lower order group contribution method. The methods for prediction of normal boiling point, normal melting point, critical pressure, critical temperature, critical volume, standard enthalpy of vaporization, standard Gibbs energy, and standard enthalpy of formation at 298 K were investigated. This research showed the distinguish among isomers. Compared to the currently-used methods-first order method, this technique (Gani's method) demonstrates significant improvements in accuracy and applicability.

Mavrovouniotis (2004) had presented for the estimation of the standard Gibbs energies of formation of biochemical compounds (and hence the equilibrium constants of biochemical reactions) from the contributions of groups. The method employs a large set of groups and special corrections. The contributions were estimated via multiple linear regressions, using screened and weighted literature data. For most of the data employed, the error is less than 2 kcal mol⁻¹. The method provides a useful first approximation to Gibbs energies and equilibrium constants in biochemical systems.

Rajagopal *et al.* (2005) estimated the standard enthalpy of formation, by Benson's group contribution, and by semi-empirical molecular simulation methods compared with experimental data. Benson's method can estimate hydrocarbon enthalpies satisfactorily. The Benson's estimates of enthalpies of free radicals superior to the molecular simulation parameterization method (PM3) and are less accurate than the specialized computationally intensive PM3-family correlation (PM3-FC) method. The estimation of enthalpies for hydrocarbon radicals is substantially improved by a linear correlation of estimated values from semi-empirical molecular simulation

method PM3 with experimental data. The radical enthalpies are now comparable to molecular simulated PM3-FC estimates. The hydrocarbon cations were divided into classes and estimated enthalpies found by adding Benson's enthalpy of radicals to the average ionization energy for the class. These predictions have an average absolute deviation of $8.6 \text{ kcal mol}^{-1}$. The proposed correlations effectively predict the standard enthalpy of formation of hydrocarbons, free radicals and carbocations. This methodology can be readily implemented in simulation programs to estimate thermochemical properties of hydrocarbons, free radicals and carbocations and to improve the design and optimization of hydroprocessing units reducing costly hydrogen consumption.

Dalmazzone *et al.* (2006) applied Benson's second order groups, for the prediction of critical temperatures and enthalpies of vaporization of covalent compounds. The results were compared to the most common existing first or second order group contribution methods. The overall precision for T_c predictions of 381 compounds is 5.8 K, which is better than Constantinou of 9.2 K and Joback of 23.6 K. It is also precise for prediction of ΔH_{vap} of 319 compounds at 298 K and at the normal boiling point. Furthermore, group contribution may now be used for the computation of gas phase properties, T_c , and ΔH_{vap} at any temperature lower than T_c .

4 Ethers production in reactive distillation

Reactive distillation was proposed in the late 1910s, the first commercial practice started in about 1980s. The integration of separation and reaction process in a one unit can improve the conversion of chemical reactants and the selectivity of the desired products, by shifting the chemical equilibrium boundaries, accelerating reactions, reducing by-products, and overcoming azeotropic limitations. Nowadays, reactive distillation is one of the favored processes for liquid phase synthesis of octane-enhancers for gasoline such as Methyl *tert*-Butyl Ether (MTBE), Tertiary Amyl Methyl Ether (TAME), Ethyl *tert*-Butyl Ether (ETBE), Tertiary Amyl Ethyl Ether (TAEE). Recently, many researches showed the use of MTBE has a tendency to pollute underground water. It is a pending legislation to use of MTBE in many states in US. TAEE or ETBE are the most potential octane enhancers to replace MTBE.

Matouq *et al.* (1996) reported that reactive distillation column was efficient to separate ETBE from an aqueous solution and homogenous catalyst. Catalysts such as NaHSO_4 , H_2SO_4 fail to synthesis ETBE because the dehydration of TBA was dominant. Quitain *et al.* (1999a) studied a continuous synthesis of ETBE from TBA and bio-ethanol (2.5 mol% ethanol in aqueous solution) catalyzed by Amberlyst 15 in reactive distillation column. At standard operating condition, 60 mol% ETBE can be obtained in the distillate and almost pure water was in the residue. The conversion of TBA and ETBE selectivity are 99.9 and 35.9 %, respectively. Aiouache and goto (2004) studied etherification of TAAE in reactive distillation column inserted by a zeolite NaA membrane tube. Assabumrungrat *et al.* (2004) investigated the synthesis of ETBE from a liquid phase reaction between *tert*-butyl alcohol and ethanol in reactive distillation catalyzed by β -zeolite with three compositions (Si/Al ratio=13, 36 and 55). The reactive distillation column packed with β -zeolite shows better performance than that packed with the commercial Amberlyst 15. It is obviously due to the better performance of β -zeolite as reported by previous work (Assabumrungrat *et al.* 2002). The effect of various operating parameters for both types of catalysts follows the same trend.

CHAPTER 4

RESEARCH PROCEDURE

This chapter describes the experimental procedures for the synthesis of *tert*-butyl ethers from glycerol and *tert*-butyl alcohol. Figure 9 show the step of experimental for both autoclave reactor and reactive distillation in this study. For thermodynamic and kinetic study, the etherifications of glycerol and *tert*-butyl alcohol were carryout in autoclave reactor as shown in Figure 10. The results were comparing with the results from simulation program. Reactive distillation study were considering in both experiment (show in Figure 11) and simulation. Details are given for the thermodynamic study, kinetic study and reactive distillation study as follows:

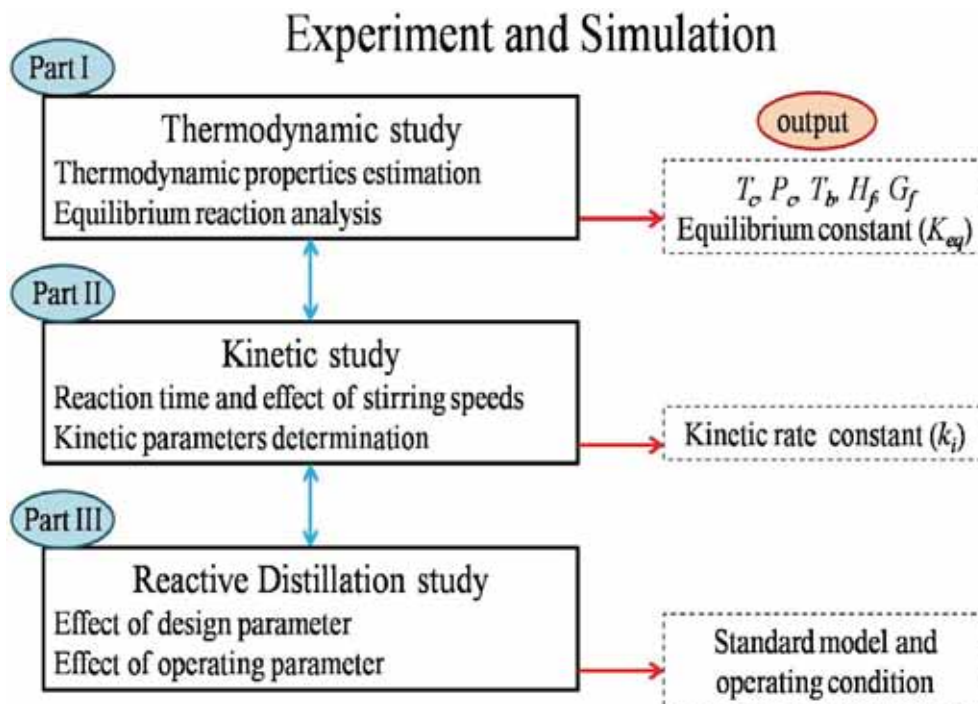


Figure 9 Schematic diagrams for all steps in this study.

1 Thermodynamic study

Due to the component of ether products are not appearing in Aspen Plus data base so the new components must be specified and added to Aspen Plus program. The various group contribution methods that will be applied to estimate the missing properties are Joback's method, Gani's method and Benson's method. The group contribution methods can be classified into first order and second order. All group contribution method was added in Aspen Plus simulator program. Aspen program can be applied to investigate the simulation of several reactions and unit operations. The etherification reaction of glycerol and *tert*-butyl alcohol was added in this simulator program. The Aspen Plus program allow user to add the functional group for each component include the method of group contribution. Firstly, Benson's method, Joback's method and Gani's method were used to estimate critical properties of any component in this study. The details of specification of new components in Aspen Plus Program are showed in Appendix E. The molecular structure should be import from other source because Aspen Plus program define the difference molecular, program define the possible structure are contained in program. In this research will be applied the Chemdraw program to create the new molecular structure. The type of file from Chemdraw program must be mole file (.mol).The functional groups of each component of several methods are listed in Appendix B-D. The properties of all components estimated by Aspen Plus program will be brought to compare with the data from handbook and online data. The equilibrium reactoin of etherification of glycerol with *tert*-butyl alcohol were considering by RGibbs model in Aspen Plus program. All group contribution methd were compare with the result from experinemt to find the best group contribution and determine the equilibrium kinetic constant pararmeter for etherification reaction.

2. Kinetic study

2.1 Chemical and catalysts

The chemicals used in this study consist of standard grade chemicals with purity higher than 99.5% for gas chromatograph calibration and reagent grade chemicals for major experiments. Table 1 provides the details of chemical purity and suppliers. The strong acid ion exchange resin Amberlyst-15, is the strong acid ion

exchange resin that the pore size type is macroreticular pore. The catalysts were dried overnight in an oven at 383 K before use. Table 2 provides the physical properties of Amberlyst-15 catalysts.

Table 1 Details of chemicals use in the study

Chemical materials	Purity (%)	Supplier
Glycerol	99.5	Ajax chemical
<i>tert</i> -butyl alcohol	99.5	Ajax chemical

Table 2 Physical properties of Amberlyst-15 catalyst

Supplier	Chemika Fluka
Ion Exchangr Capacity (meqH ⁺ /kg)	5.0
Surface Area (m ² /g)	900
Pore Dimeter (nm)	1000
Pore Volume (cm ³ /g)	1.82

2.2 Batch reactor apparatus and experimental procedure

Kinetic study of the etherification of glycerol and *tert*-butyl alcohol used Amberlyst-15 as a catalyst was carried out in an autoclave reactor as shown in Figure 9. Autoclave reactor was maintained at a constant temperature by heating jacket with temperature controller around the reactor chambers. For both thermodynamic and kinetic study; 16 ml of glycerol, 83 ml of *tert*-butyl alcohol and 1.025 g of catalysts (A-15) were added into the reactor together at room temperature. The solution was pressurized by N₂ gas to 5 bar to prevent vaporization of liquid solutions and heated to the desired reaction temperature. Liquid samples (0.5 cm³) were taken for analysis at 0, 30, 60, 90, 120, 180, 240, 300, 360, 420, 480 mins. Firstly, the effect of reaction time and stirred speed on equilibrium reaction were investigated to maintain the equilibrium reaction. Finally, the reaction time were set at 480 minute and stirred at about 600 rpm for all reaction to investigate equilibrium reaction and determine the kinetic parameters.

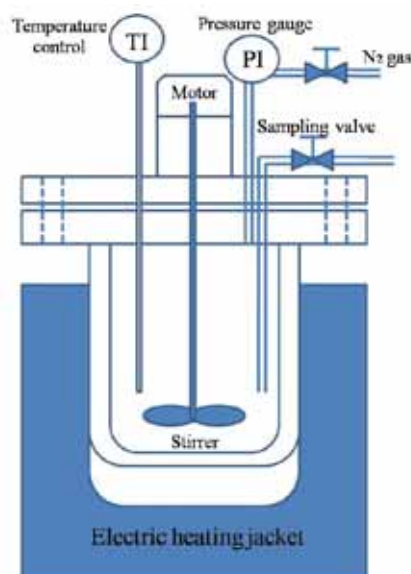


Figure 10 Schematic diagram of the autoclave reactor.

2.3 Sample analysis

The analysis was carried out using gas chromatography (GC). The operating condition of the GC is shown in table 3. A 0.025 microliter of sample was injected into the GC column and the raw data of chromatograms were modified by using calibration curve and were calculated in mole change with time of any components.

Table 3 Operating conditions of gas chromatography

Gas chromatography Shimadzu GC14B	
Operating conditions	
Detector	FID
Carrier gas	Nitrogen (N ₂)
Carrier gas (bar)	30
Capillary column	HP-INNOWAX
Length of column (m)	30
Injection temperature (C)	300
Column temperature (C)	40-240 (hold 5 min)
Heating rate (C/min)	10
Detector temperature (C)	150

3 Reactive distillation study

Reactive distillation study is divided into 2 parts; reactive distillation experiment in laboratory and reactive distillation simulation by Aspen Plus program. The experiments were performed in a packed reactive distillation column as shown in Figure 10. The reactive distillation configuration was consisting of a four-neck round bottom flask with a mantle heater stirrer served as a reboiler. The liquid solution in the reboiler was continuously stirred for homogeneity. The glass vacuum-insulated column consisted of three distinct sections (1) non-reactive rectifying section (2) catalytic reactive section and (3) non-reactive stripping section. The column was connected to the central opening of the four-neck round bottom flask and covered by insulator. Amberlyst 15 ion exchange resin catalysts were packed in the stainless steel mesh. Each pack contained about 1 g of catalyst. The catalyst packings were placed inside the column in the reaction section to allow simultaneous reaction and separation of products. Stainless steel mesh saddles (40 mesh) were used as packing materials in the rectifying and the stripping section of the column. The reactants at room temperature were continuously fed through tubes to reactive distillation column and were controlled flow rate by peristaltic pump. Six thermocouples were connected along the column height to measure the temperature profiles inside the column. Water served coolant was circulated in the condenser located at the top of the column. The reflux ratio was controlled by the solenoid valve with a multi-timer.

1.1 Experiment procedure of reactive distillation

3.1.1. Reactive distillation experiment in laboratory

1. The reactive distillation consist of 4 part; round bottom flask as a reboiler, reactive distillation column, reflux section and condenser section were set up as shown in Figure 11.

2. A mixture solution of *tert*-butyl alcohol 596 ml and glycerol 96 ml (ratio 4:1) was placed inside the round bottom flask. The heater jacket was set as 80 kW to heated liquid solution in side round bottom flask.

3. When first drop of distillate appeared at the top, glycerol was introduced to the highest part of the reaction section and *tert*-butyl alcohol was introduced to the lowest part of the reaction section by using a peristaltic pump.

4. Liquid from the reboiler was withdrawn by another peristaltic pump while the distillate was controlled by the reflux ratio. Then, continuous operation was started.

5. The liquid level in the reboiler was maintained by adjusting the tip of the withdrawing pipe connected to the pump.

6. The experiment was conducted for about 12 hours. The distillate and the residue were collected, weighed and analyzed.

3.1.2. Reactive distillation simulation by Aspen Plus program.

1. Set the data of standard condition into program including the kinetic parameters of reaction and run program.

2. Vary input parameters to study the effect of operating parameters on performance of reactive distillation (e.g. reflux ratio, location of feed stage and reaction section, heat duty, and feed flow rate).



Figure 11 The reactive distillation setup for lab scale.

CHAPTER 5

RESULTS AND DISCUSSION

The results and discussion are divided to three main sections: Equilibrium thermodynamic analysis, kinetic study and reactive distillation study. The result from both experiment and simulation were compare. Details are as follows.

1. Equilibrium thermodynamic analysis

This section was dedicated to equilibrium thermodynamic analysis of etherification between glycerol and *tert*-butyl alcohol. The aim of the study in this part is to analyze the equilibrium limitations by minimize Gibbs free energy method and determine the equilibrium kinetic constant parameter. Firstly, because of the missing thermodynamic properties (critical temperature (T_c), critical pressure (P_c), normal boiling point (T_b), heat of formation (H_f) and Gibbs free energy of formation (G_f)) of ethers product (MTBG, DTBG and TTBG) in Aspen Plus database, the group contribution methods were applied to calculate thermodynamic properties for their ethers. Three types of group contribution methods; Joback's method, Gani's method and Benson's method were investigated. The type of group contribution method can be divided in first order and second order. The basic level uses first order contributions while the higher level uses a small set of second order groups having the first order groups as building blocks. It should be noted that Joback's method is the first order group contribution method while Gani's method is a combination of first order and second order group contribution method. Then the subgroup from different group contribution methods will be added to Aspen plus simulator to create the thermodynamic data of unavailable component in Aspen Plus database. Finally, the Gibbs free energy of their ethers product calculate from the best group contribution were use to determine the equilibrium conversion and equilibrium composition.

1.1 Estimation of normal boiling point

The boiling point of an element or a substance is the temperature at which the vapor pressure of the liquid equals the environmental pressure surrounding the liquid. Almost other thermo chemical properties are predictable from boiling point and critical constants, so the precise forecast of boiling point is much needed. Many research proposed a group contribution method that gives an approximate value of the boiling point of aliphatic and aromatic hydrocarbons. The boiling point is estimated with the sum of contributions of all structural groups found in the molecule. For this study, Gani's method and Joback's method were used to estimate the normal boiling point for all components. The values of normal boiling point of glycerol, *tert*-butyl alcohol, isobutylene, ethanol, methanol, methyl *tert*-butyl ether (MTBE) and ethyl *tert*-butyl ether (ETBE) taken from Aspen Plus database were compared with the calculated normal boiling point from Gani's method and Joback's method as presented in Figure 12. The result showed that the predicted normal boiling points from both Joback's method and Gani's method are in good agreement with the values the aspen data base.

1.2 Estimation of critical properties

Critical temperature (T_c) and critical pressure (P_c) are very important properties in chemical engineering field because almost all other thermo chemical properties are predictable from boiling point and critical constants with using corresponding state theory. There are several methods to predict critical constants. For calculation of critical properties in this study, Joback's and Gani's methods were applied for ether products and other component. Figure 13 and 14 show the critical temperature and critical pressure, respectively, of the components estimated by difference group contribution method. The results were compared with properties from the Aspen Plus database. However, no available data of glycerol ether products are currently present to compare with the estimated value. Therefore, we estimated the critical properties comparing to the available database of ether products i.e. MTBE and ETBE including their reactant i.e. methanol and ethanol, respectively. The deviation between the estimated value from various group contribution methods and the value from the database are summarized in Table 4. The results show that Gani's method is more slightly accurate than Joback's method.

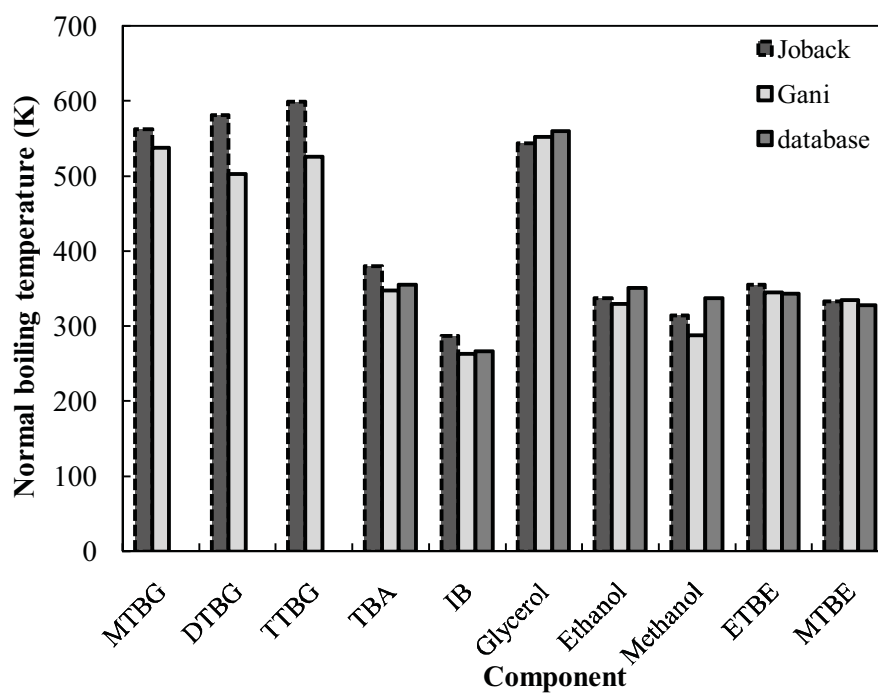


Figure 12 Normal boiling temperatures the components in the system and related reaction.

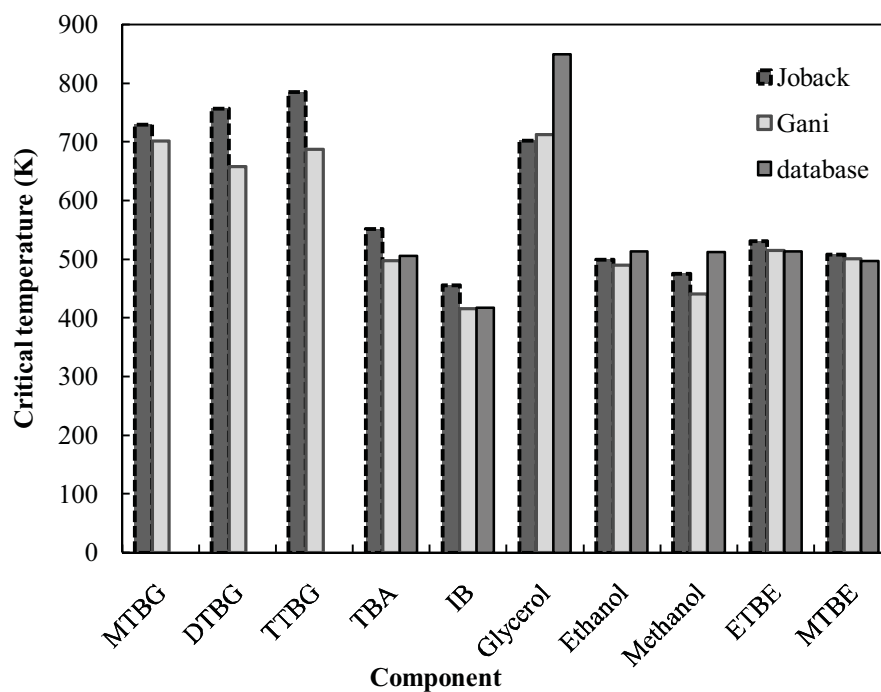


Figure 13 Critical temperatures the components in the system and related reaction.

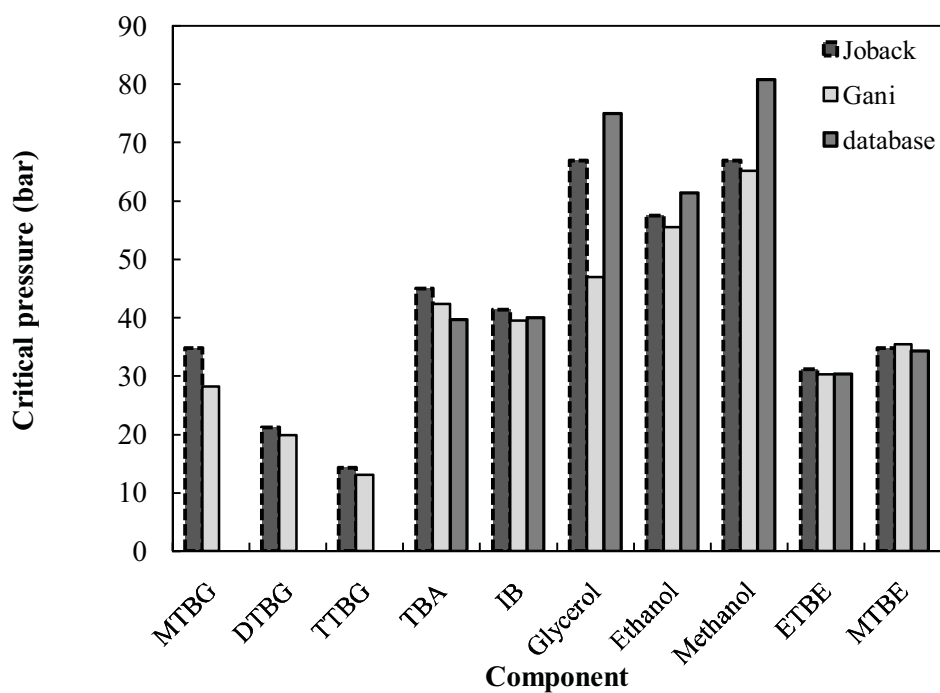


Figure 14 Critical pressure the components in the system and related reaction.

Table 4 Percent error of critical temperature, critical pressure and normal boiling temperature for Joback's and Gani's method comparison with database.

name	% Error					
	T_b (K)		T_c (K)		P_c (bar)	
	Joback	Gani	Joback	Gani	Joback	Gani
MTBG	-	-	-	-	-	-
DTBG	-	-	-	-	-	-
TTBG	-	-	-	-	-	-
TBA	6.42	-2.16	-7.65	-19.54	11.70	6.22
IB	7.23	-1.36	8.28	-0.67	3.28	-1.28
Glycerol	-2.91	-1.40	-8.90	-7.34	35.69	8.27
Ethanol	-4.20	-6.51	-2.98	-5.05	-10.13	-14.07
Methanol	-7.42	-17.09	-7.89	-16.35	-20.96	-24.34
ETBE	3.34	0.42	3.29	0.15	2.38	-0.34
MTBE	1.44	2.14	2.28	0.76	1.34	3.21

1.3 Estimation of heat of formation

Heat of formation is defined as the enthalpy change when one mole of a compound is formed from the elements in their stable states. For calculation of heat of formation in this study, Joback's, Gani's and Benson's method were investigated. The results from their group contribution method compared with properties from Aspen Plus database for TBA, IB, glycerol, ethanol methanol, MTBE and ETBE as show in Figure 15.

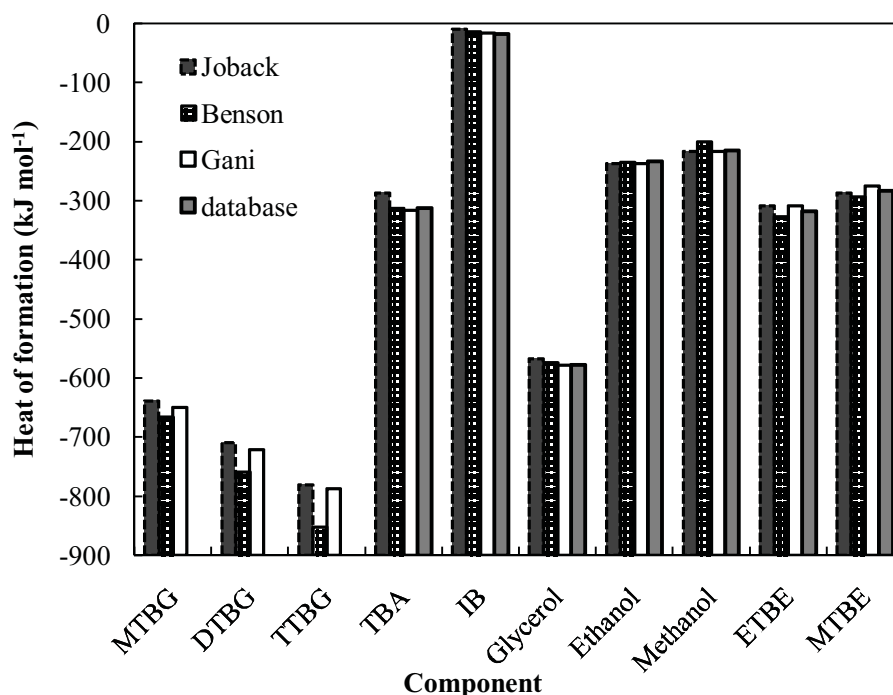


Figure 15 Heat of formation of the components in the system and related reaction.

Table 5 Percent error of heat of formation estimated by Joback's, Benson's and Gani's method

name	%Error		
	Joback	Benson	Gani
TBA	-8.97	0.05	1.32
IB	-74.63	-20.13	-12.11
Glycerol	-1.88	-0.74	0.02
Ethanol	1.20	0.28	1.39
Methanol	0.56	-7.10	0.71
ETBE	-3.13	2.94	-3.08
MTBE	1.50	3.51	-3.06

1.4 Estimation of Gibbs free energy

For calculation of Standard Gibbs free energy of formation, Joback's method, Gani's method and Benson's method were investigated. Standard Gibbs free energy of formation is the most important property for RGibbs reactor which minimizes Gibbs free energy of formation of each component in the studied system. Higher order group contribution methods are expected to give more precise predictions; therefore, the The results of Gibbs free energy of formation using first order (Joback's method), first-second order (Gani's method), and second order (Benson's method) are illustrated in Table 6. Gani's method show the lowest percent error compare with other method.

Table 6 Gibbs free energy estimation for Joback's, Benson's and Gani's method compare with database.

Name	G_f (kJ mol ⁻¹)				%Error		
	Joback	Benson	Gani	database	Joback	Benson	Gani
MTBG	-370.18	-369.64	-388.19	-	-	-	-
DTBG	-301.84	-318.50	-356.33	-	-	-	-
TTBG	-233.50	-269.07	-269.59	-	-	-	-
TBA	-151.18	-157.03	-180.70	-177.60	-14.87	-11.57	1.74
IB	62.09	96.90	59.41	58.08	6.90	66.84	2.29
Glycerol	-438.52	-417.35	-446.67	-447.10	-1.92	-6.65	-0.09
Ethanol	-170.86	-152.85	-173.21	-167.85	1.79	-8.93	3.19
Methanol	-179.28	-191.14	-181.44	-162.32	10.44	17.75	11.78
ETBE	-102.52	-103.43	-110.93	-121.70	-15.76	-15.01	-8.84
MTBE	-110.94	-103.78	-107.10	-117.50	-5.58	-11.67	-8.84

1.5 Equilibrium constant parameters determination

Equilibrium reaction of glycerol with *tert*-butyl alcohol was studied by minimizing the Gibbs free energy using RGibbs reactor model in Aspen Plus program. UNIFAC method was used for mixture property estimation. The effect of temperature on etherification of glycerol with *tert*-butyl alcohol in term of glycerol conversion was illustrated in Figure 16. The simulation results were compared with

the experimental results from this study and from Klepacova *et al.* (2005). TBA was fed in excess with a constant ratio of TBA to glycerol of 4:1. Only Gani's group contribution method showed a good agreement with the experimental results in term of glycerol conversion. Glycerol conversion at equilibrium decreased with increasing reaction temperature since overall reaction is exothermically.

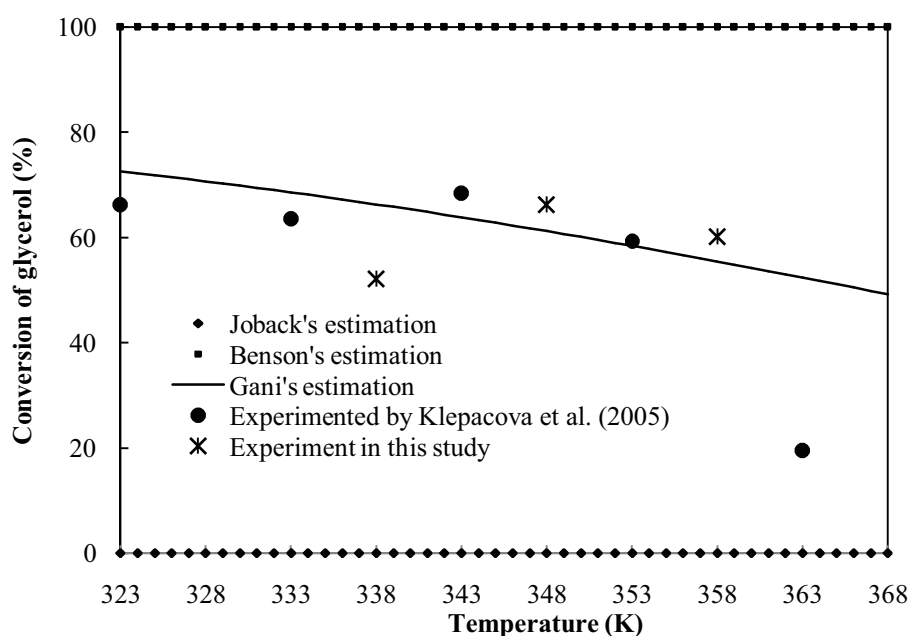


Figure 16 The effect of reaction temperature on equilibrium conversion of glycerol from simulation and experiment.

Furthermore, the Gani group contribution was used to predict product distribution at equilibrium in operating temperature of 323 K to 368K. The product distribution at operating temperature of 323 K from the simulation was compare with the experimental result from Klepacova *et al.* (2005) as shown in Figure 17. The simulation results also showed good agreement in term of product distribution. However MTBG was obtained as a main product rather than DTBG and TTBG which are more desirable products.

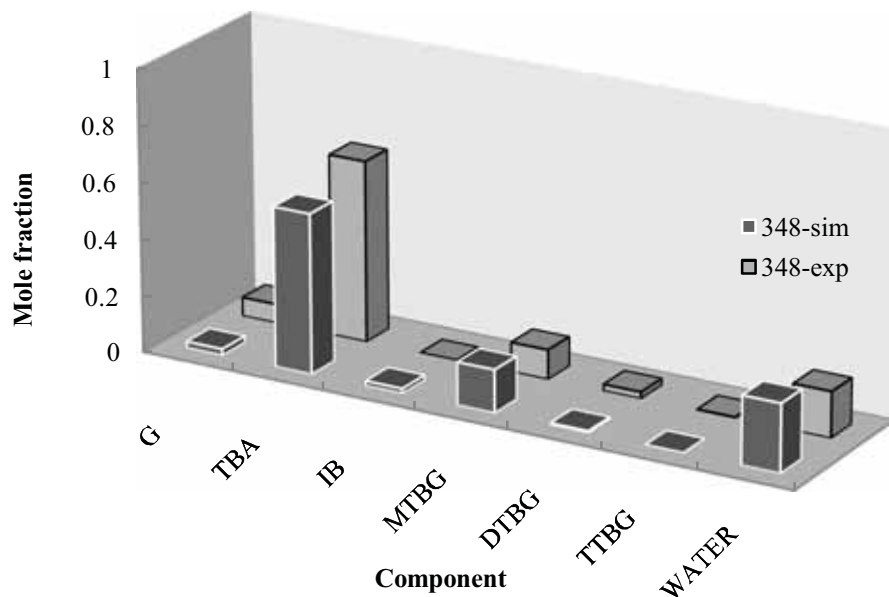


Figure 17 Equilibrium comparison from simulation and experiment (5 bar, Glycerol:TBA=1:4).

The reactions taking place in the direct etherification of Glycerol and *tert*-butyl alcohol can be summarized as follows



For the equilibrium kinetic constants were define as

$$K_i = \frac{k_i}{k_{-i}} \quad (5.4)$$

where i =forward reaction and $-i$ =backward reaction

To determine the equilibrium parameters for K_1 , K_2 and K_3 Gani's group contribution was added to Aspen Plus program. The model REquil in Aspen plus program was calculated these reaction equilibrium constants from the components at

equilibrium in term of activity. Equilibrium constants calculated from Aspen Plus program was defined as

$$K_{ia} = \frac{\prod_{j=\text{product}} a_j}{\prod_{j=\text{reactant}} a_j} \quad (5.5)$$

where i = reaction number and j = component of product and reactant

The module of REquil reactor in Aspen Plus program was used to determine equilibrium constant base on activity (abbreviated as K_{ia}) at temperature 338, 348 and 358 K. The UNIFAC method was used for mixture property estimation. Figure 18 show Arrhenius's plots for equilibrium constant base on activity estimated by Gani's group contribution and UNIFAC property.

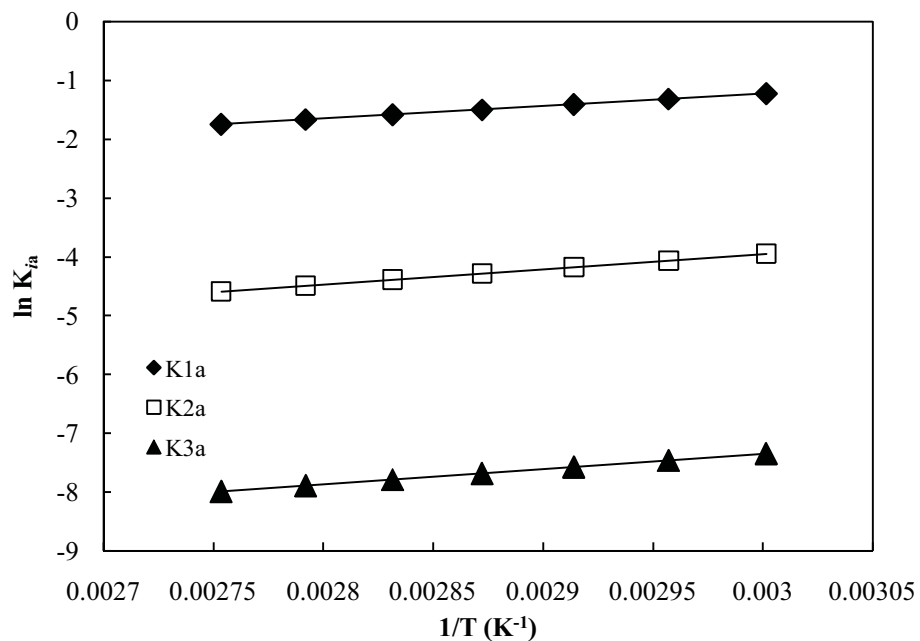


Figure 18 Arrhenius's plots for K_{1a} , K_{2a} and K_{3a} estimated by minimize Gibbs free energy.

The equilibrium constant base on concentration was calculated by the relation in equations 5.6-5.8.

$$a_i = \gamma_i x_i \quad (5.6)$$

$$K_{ia} = \frac{\prod_{j=product} a_j}{\prod_{j=reactant} a_j} = \frac{\prod_{j=product} \gamma_j x_j}{\prod_{j=reactant} \gamma_j x_j}$$

$$K_{ia} = \left[\frac{\prod_{j=product} \gamma_j}{\prod_{j=reactant} \gamma_j} \right] \left[\frac{\prod_{j=product} x_j}{\prod_{j=reactant} x_j} \right] = K_{ic} \left[\frac{\prod_{j=product} \gamma_j}{\prod_{j=reactant} \gamma_j} \right] \quad (5.7)$$

then

$$K_{ic} = \frac{K_{ia}}{\left[\frac{\prod_{j=product} \gamma_j}{\prod_{j=reactant} \gamma_j} \right]} \quad (5.8)$$

where x_i is mole fraction of species i in the liquid mixture and γ_i is the activity coefficient, can be estimated by using UNIFAC method (see detail in Appendix F).

The equilibrium constant both activity and concentration of glycerol etherification obtained from the Arrhenius' plots are summarized in Table 7.

Table 7 Equilibrium constant of etherification between glycerol and *tert*-butyl alcohol

reaction	Rate constant
r_1	$K_{1a} = \exp(-7.565+2112/T)$
	$K_{1c} = \exp(-5.155+1523/T)$
r_2	$K_{2a} = \exp(-11.71+2588/T)$
	$K_{2c} = \exp(-10.31+1857/T)$
r_3	$K_{3a} = \exp(-15.09+2588/T)$
	$K_{3c} = \exp(-17.44+3315/T)$

2 Kinetic study

2.1 The effect of external mass transfer

The effect of external mass transfer of catalyst (Amberlyst-15) was studied by varying stirring speeds. Figure 19 shows the relationship between conversion of glycerol at 8 h and the stirring speed between 200 and 700 rpm. It was found that the conversion increased with increasing speed level and, finally, it leveled off at the speed level of 600 rpm. This can be concluded that the effect of external mass transfer could be negligible with stirring speed of 600 rpm. In the subsequent studies, the speed of 600 rpm was used throughout the experiment.

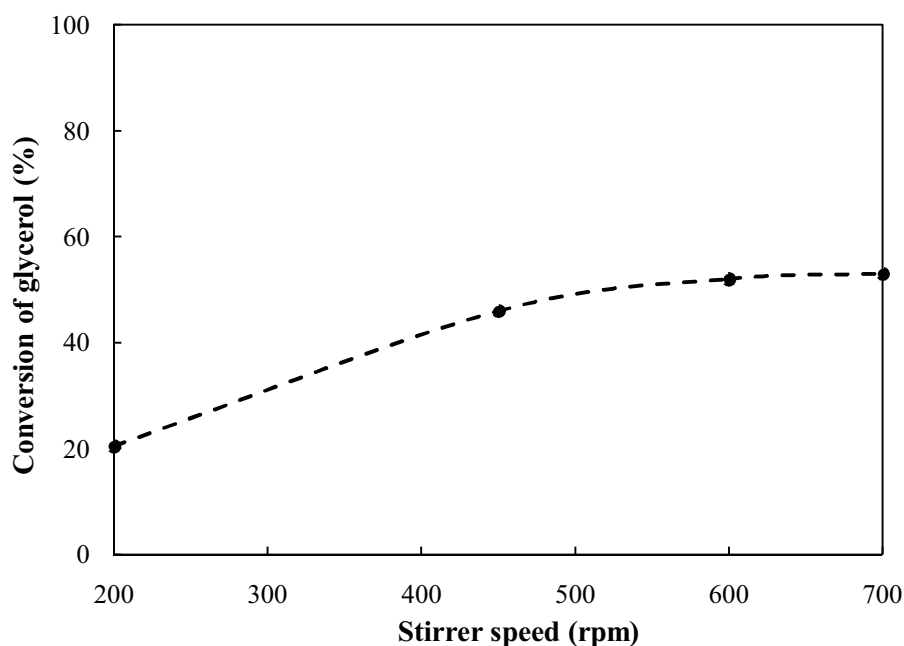
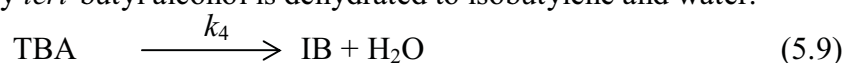


Figure 19 The effect of speed level on the glycerol conversion (Catalyst = A-15, catalys weight = 1.025 g, TBA:G = 4:1, $T = 338$ K, $P = 5$ bar and reaction time = 8 h).

2.2 Development of mathematical models

The reactions taking place in the direct etherification of Glycerol and *tert*-butyl alcohol can be summarized as shown previously in Eq. 5.1-5.3. For the indirect reaction, firstly *tert*-butyl alcohol is dehydrated to isobutylene and water.



Isobutylene from dehydration reaction is further reacted with glycerol as follows



The reverse reactions in Eq. 5.9 and the reaction in Eq. 5.10-5.12 were neglected since the operating pressure in this study was set at 5 bar. Consequently, only small amount of IB can be dissolved in the liquid solution. It was confirmed by

our experimental results that the concentration of IB in liquid mixture was negligibly small.

The results were fitting with two kinetic models; Langmuir-Hinshelwood (LH) and Power Law model (PL) based on activities (a_i) and concentration (c_i) (abbreviated as LH-A, PL-A for activity and PL-C for concentration), respectively. The LH model is based on the following assumptions; all components adsorb on the single site of the catalyst and the surface reaction is the rate determining step. To development of mathematical models for etherification of glycerol shows in Eq. 5.1 to Eq. 5.3, the consecutive reaction path way were used to describe the experimental data.

The mathematical model of consecutive reaction scheme as show in Eq. 5.1-5.3 could be written in term of activity as

$$r_{1a} = k_{1a} \left[\frac{a_G a_{TBA} - a_{MTBG} a_{water} / K_{1a}}{(1 + K_{wa} a_{water})^Z} \right] \quad (5.13)$$

$$r_{2a} = k_{2a} \left[\frac{a_{MTBG} a_{TBA} - a_{DTBG} a_{water} / K_{2a}}{(1 + K_{wa} a_{water})^Z} \right] \quad (5.14)$$

$$r_{3a} = k_{3a} \left[\frac{a_{DTBG} a_{TBA} - a_{TTBG} a_{water} / K_{3a}}{(1 + K_{wa} a_{water})^Z} \right] \quad (5.15)$$

$$r_{4a} = k_{4a} \left[\frac{a_{TBA}}{(1 + K_{wa} a_{water})^Z} \right] \quad (5.16)$$

where $Z=0$ for Power Law (PL) model and $Z=1$ for Langmuir-Hinshelwood (L-H) model. k_{jm} are reaction rate constants of reaction j ($j = 1-4$) in model reaction base on activity (a) or concentration (c). a_i and x_i are activity and concentration of species i , respectively. K_{jm} is the equilibrium constant. K_{wc} and K_{wa} are water inhibition parameters from in the concentration-based models, respectively. The mathematical model in term of concentration could be calculated from Eq. 5.6.

By performing a material balance for a semi-batch reactor, the following expressions are obtained.

$$-\frac{dm_{TBA}}{dt} = \frac{dm_{water}}{dt} = W(r_{1m} + r_{2m} + r_{3m} + r_{4m}) \quad (5.21)$$

$$-\frac{dm_{glycerol}}{dt} = \frac{dm_{MTBG}}{dt} + \frac{dm_{DTBG}}{dt} + \frac{dm_{TTBG}}{dt} = W(r_{1m} + r_{2m} + r_{3m}) \quad (5.22)$$

$$\frac{dm_{MTBG}}{dt} = W(r_{1m}) \quad (5.23)$$

$$\frac{dm_{\text{DTBG}}}{dt} = W(r_{2m}) \quad (5.24)$$

$$\frac{dm_{\text{TTBG}}}{dt} = W(r_{3m}) \quad (5.25)$$

where m_i and W represent the number of mole of species i and the catalyst weight, respectively. It is noted that the number of moles in the liquid phase at any time is constant because IB can only slightly dissolved in the liquid phase. For dehydration of TBA (Eq. 5.9), the kinetic parameter was shown below (Yang *et al.*).

$$k_{4a} = \exp(15.451 - 10325/T) \quad (5.26)$$

$$k_{4c} = \exp(15.39 - 10270/T) \quad (5.27)$$

$$K_{wa} = \exp(-36.456 + 7646/T) \quad (5.28)$$

$$K_{wc} = \exp(-35.62 + 7530/T) \quad (5.29)$$

*Note that ion-exchange capacity for A-15 = 4.4 [mol-H (kg dry resin)⁻¹]

The minimizing root mean square deviation (RMSD) method was used to estimate there kinetic parameter (k_1 , k_2 , k_3 and K_w) as show above. A MATLAB program was employed to find the best-fitted kinetic parameters which minimize the relative root mean square deviation (RMSD) values expressed by Eq. 5.30.

$$RMSD_i = \frac{1}{M} \sqrt{\sum_{k=1}^M \left[\frac{(x_{i,k} - x_{i,\text{exp},k})}{x_{i,\text{exp},k}} \right]^2} \quad (5.30)$$

where i and M represent the component and the number of experiment data point.

2.3 Kinetic parameter determination

A set of experiments was carried out at three temperature levels to investigate the kinetic parameters. The mathematical models from the previous study were used to determine the kinetic parameters. Firstly, the power law base on both activity (a_i) and concentration (c_i) were compare to find the best mathematic model for etherification of glycerol with *tert*-butyl alcohol. Figures 20, 21 and 22 show typical results of mole changes with time at $T = 348, 358$ and 368 K. The solid lines in the figures represent the simulation results from the PL-A model and the dash lines represent the PL-C model. It was found that the simulation results for both PL-A and PL-C kinetic model agree well with the experimental results.

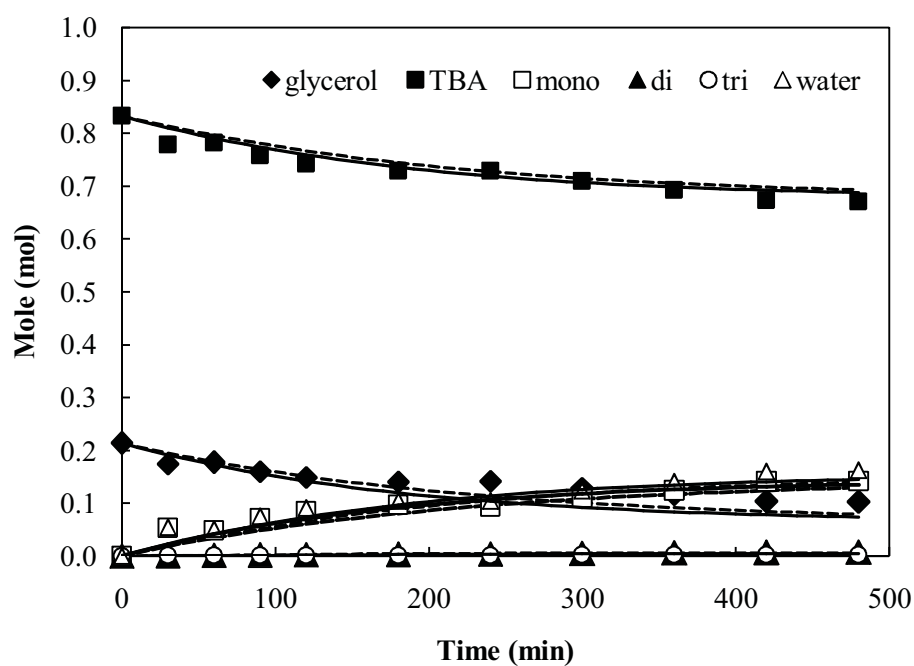


Figure 20 Mole change with time at 338 K(catalyst weight = 1.025 g, G:TBA = 1:4, 5 bar). (solid lines: PL-A model, dashed lines: PL-C model)

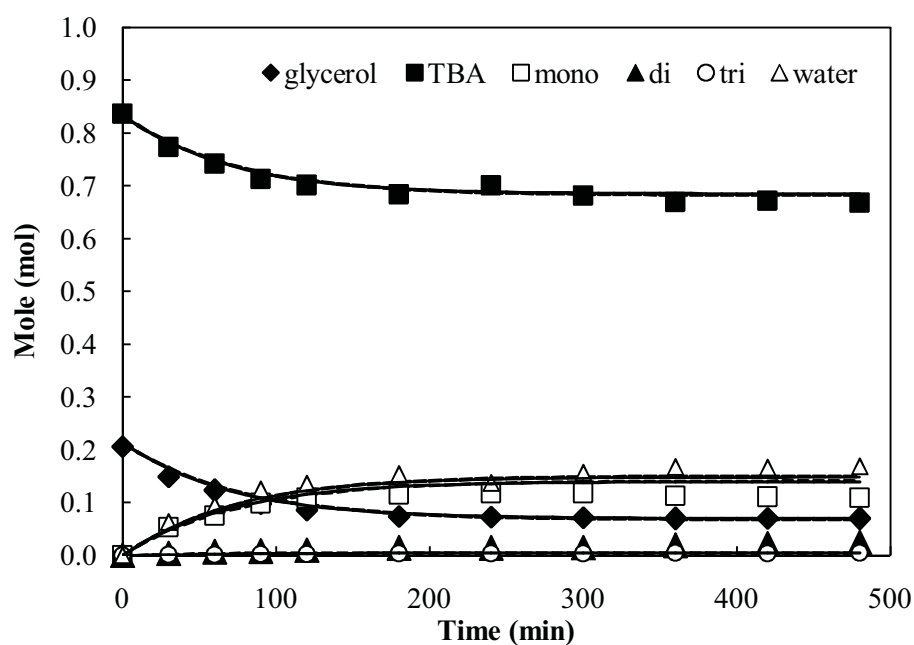


Figure 21 Mole changes with time at 348 K(catalyst weight = 1.025 g, G:TBA = 1:4, 5 bar). (solid lines: PL-A model, dashed lines: PL-C model)

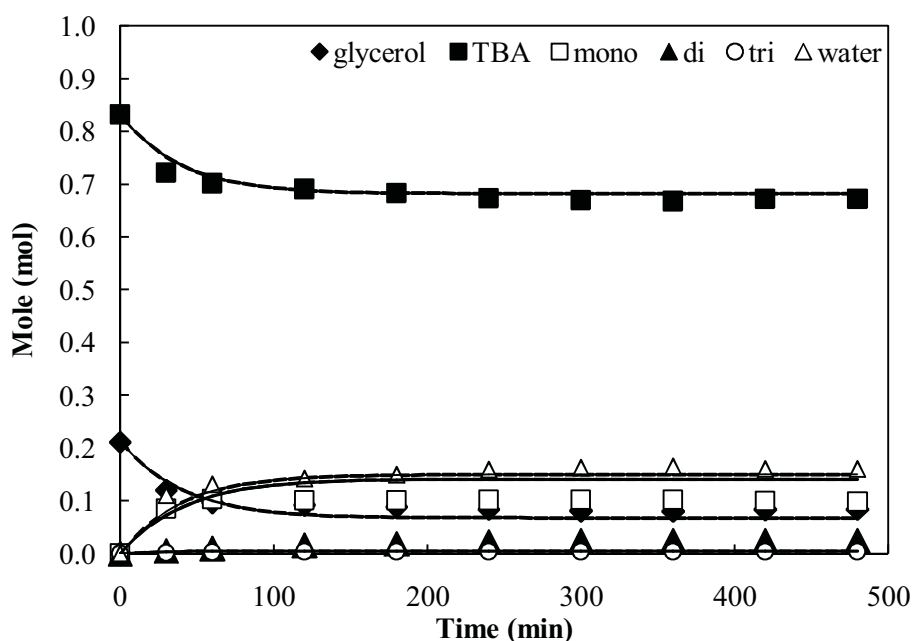


Figure 22 Mole change with time at 358 K(catalyst weight = 1.025 g, G:TBA = 1:4, 5 bar). (solid lines: PL-A model, dashed lines: PL-C model)

Furthermore, the LH model was considered to find the best kinetic model for this reaction. From the previous study, both of PL-A and PL-C were showed a good performance to describe the glycerol etherification reaction. However, the model base on activities was used instead of the model base on concentrations to account for the non-ideal behavior of liquid phase reaction system. The activity of i th component was calculated by using the equation as show in Eq. 5.21. Figures 23, 24 and 25 show the experimental results of mole profile compare with the simulation result from LH-A kinetic model of each component in the glycerol etherification with *tert*-butyl alcohol at 338, 348 and 358 K. It was found that the experimental results agree well with the simulation results of LH kinetic models for activity base model. As shown in Figure 26 summarizing the average RMSD values with different models, the LH-A model can describe the rate of glycerol etherification better than both PL model.

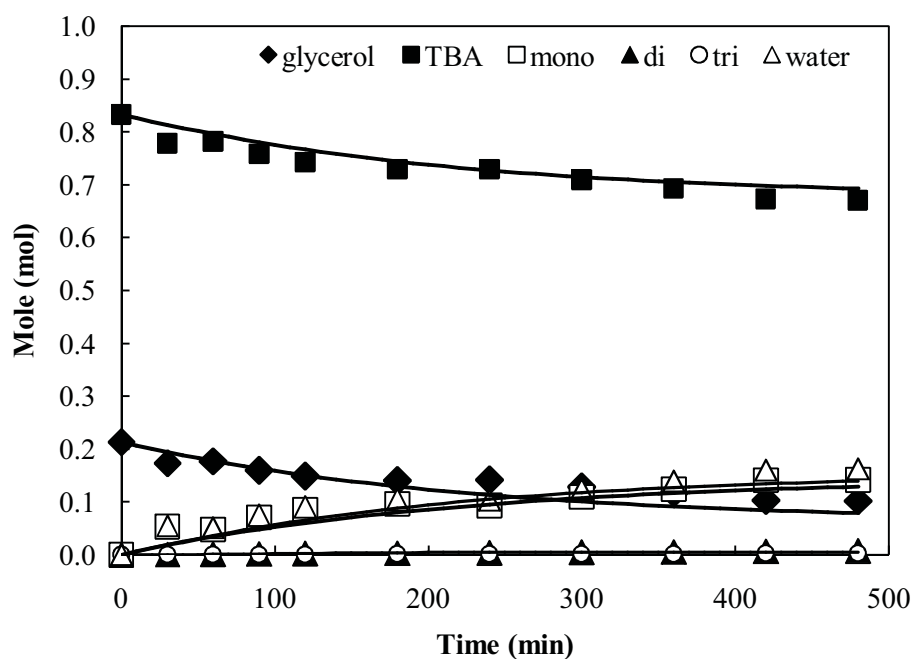


Figure 23 Mole change with time at 338 K (catalyst weight = 1.025 g, G:TBA = 1:4, 5 bar and $T = 338$ C), (symbols: experiment results, solid lines: LH-A model).

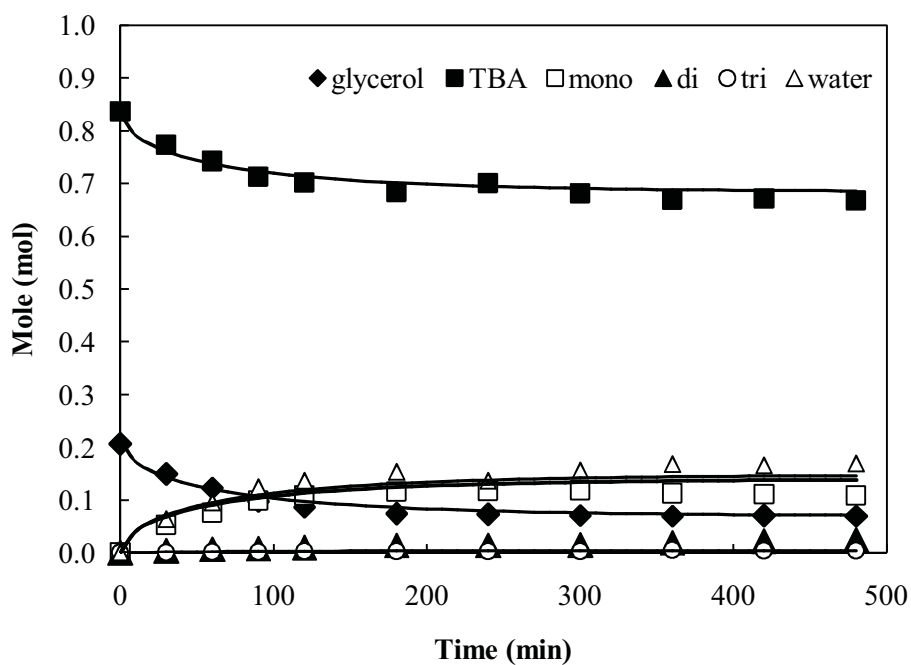


Figure 24 Mole change with time at 348 K (catalyst weight = 1.025 g, G:TBA = 1:4, 5 bar and $T = 338$ C), (symbols: experiment results, solid lines: LH-A model).

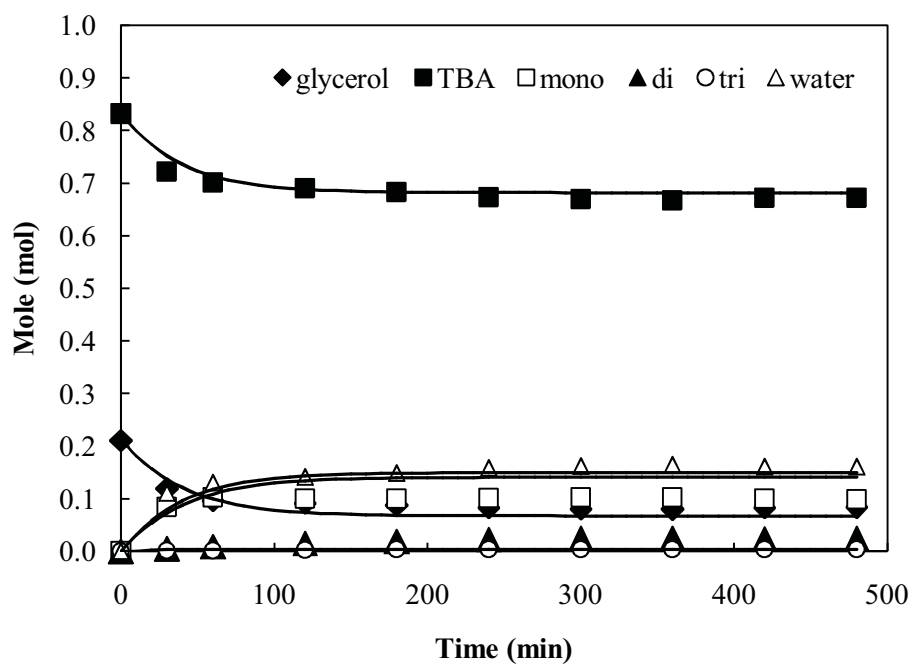


Figure 25 Mole change with time at 358 K (catalyst weight = 1.025 g, G:TBA = 1:4, 5 bar and $T = 338$ C), (symbols: experiment results, solid lines: LH-A model).

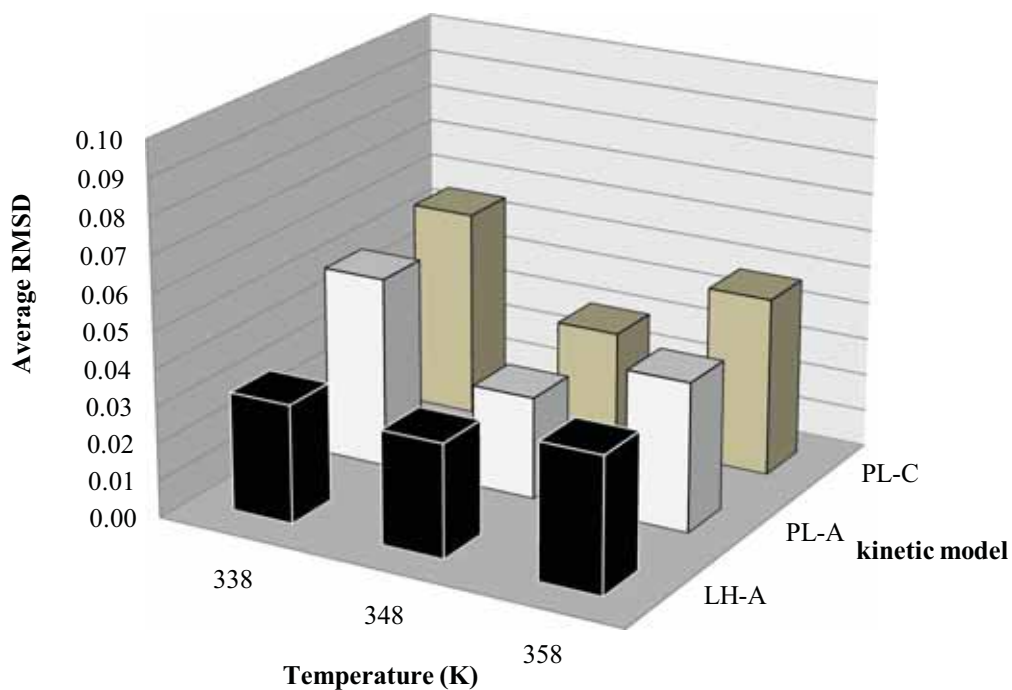


Figure 26 average RMSD values of PL and LH kinetic model for both activity and concentration in each temperature

The temperature dependent rate constants were determined by plotting the relationships according to the Arrhenius' equation for both PL-C and PL-A kinetic model (Figure 27) and for LH-A model (Figure 28). The sorption equilibrium constant of H₂O as a function of temperature can be determined by Van't Hoff plot (Figure 28). It was found that the value of sorption equilibrium of H₂O decreased with the increase of temperature. This is a conventional behavior observed in most adsorption processes. The temperature dependent rate constant and the chemical equilibrium constant of both models can be expressed by the Arrhenius's equation (Eq. 5.33). The sorption equilibrium constant and values of the adsorption enthalpies and adsorption entropies of H₂O for LH-A kinetic model can be expressed by the Van't Hoff equation (Eq. 5.34). The expressions of the rate constants, activation energy and sorption equilibrium constants for are summarized in Table 10 and Table 11.

$$k_i = A_0 \exp \left[\frac{-E_a}{RT} \right] \quad (5.33)$$

$$K_{wa} = \exp \left[\frac{-\Delta G}{RT} \right] = \exp \left[\frac{\Delta S}{R} - \frac{\Delta H}{RT} \right] \quad (5.34)$$

where E_a is the activation energy (kJ/mole), ΔH is the standard enthalpy change of the reaction, ΔS is standard entropy change of the reaction and R is the gas constant.

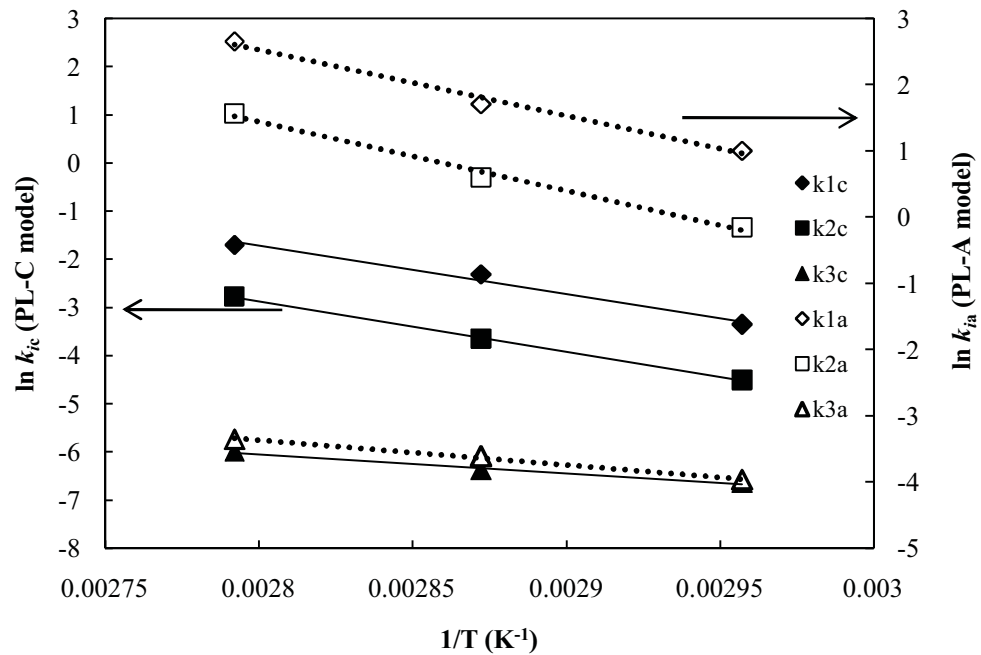


Figure 27 Arrhenius's plots for PL-A (dashed lines) and PL-C (solid lines)

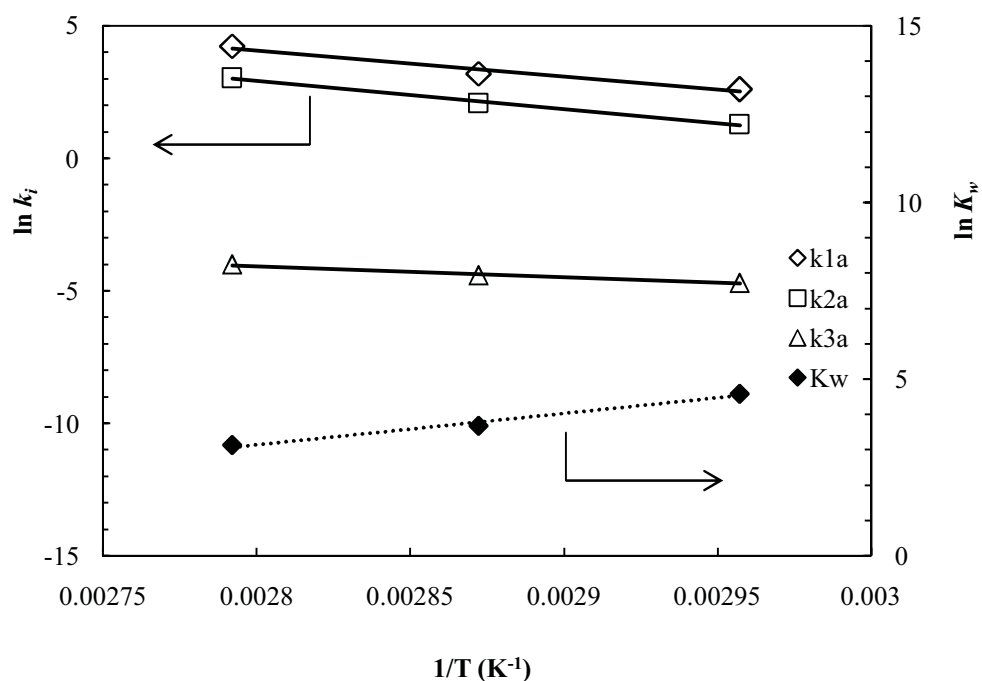


Figure 28 Arrhenius's (solid line) and Van't Hoff plots (dashed line) of LH-A model.

Table 8 Reaction rate constants and activation energy

Model	rate constant (kg mol s ⁻¹)	activation energy, Ea (kJ mole ⁻¹)
PL-C	$k_1 = \exp(26.299-10006/T)$	81.77
	$k_2 = \exp(26.437-10468/T)$	88.09
	$k_3 = \exp(5.0194-3952/T)$	32.85
PL-A	$k_1 = \exp(30.499-9988/T)$	83.04
	$k_2 = \exp(30.629-10425/T)$	86.67
	$K_3 = \exp(7.0013-3704/T)$	30.79
LH-A	$k_1 = \exp(31.872-8690/T)$	82.15
	$k_2 = \exp(32.659-10624/T)$	88.33
	$k_3 = \exp(7.6561-4189/T)$	34.83

Table 9 Sorption equilibrium constant and values of the adsorption enthalpies and adsorption entropies of H₂O for LH-A kinetic model

Model	Sorption equilibrium constant
LH-A	$K_w = \exp(-21.51+8806/T)$
	adsorption enthalpies ΔH (kJ mol⁻¹)
LH-A	-73.21
	adsorption entropies ΔS (J mol⁻¹ K⁻¹)
LH-A	-178.78

3. Reactive distillation: Experiment and simulation

Both experiment and simulation by using Aspen plus program were carried out to investigate the ethers synthesis from glycerol and *tert*-butyl alcohol in the reactive distillation. Various operating parameters; i.e. reflux ratio, location of feed stage and reaction section, catalyst weight and heat duty were investigated. The rate expressions obtained from the previous study were important input data for the program. The performance of reactive distillation at standard operating condition was described and then the influence of each operating parameter was discussed.

3.1 Performance of reactive distillation at standard condition

Simulation of the etherification of glycerol and *tert*-butyl alcohol in a Reactive Distillation (RD) is carried out using the Aspen Engineering suit. The RADFRAC model, which a rigorous equilibrium-stage distillation model to describe a multistage vapor-liquid separation in the distillation column in Aspen Plus simulation package is use to simulation etherification of glycerol and *tert*-butyl alcohol. The property option was set UNIFAC. A typical configuration of reactive distillation column used in the simulation studies is shown in Figure 29. The column contains a total of 20 stage counted down from the top (includes condenser and reboiler as respectively shown as stage 1 and 20). The reactive distillation column is divided into three sections: 6 stages of rectifying section, 6 stages of reaction section and 6 stages of stripping section. The chemical reactions are assumed to occur in the liquid phase in the reaction section represented by 6 reactive stages (stage 8-13). It is noted here that such a column configuration is determined as a preliminary simulation study. However, it can be adjust to meet optimal performance of the RD column. Table 10 summarizes the column parameters and feed conditions under the standard operation. The simulation input to Aspen Plus was mainly based on experimental operating condition. However, there laboratory scale values are too small for Aspen Plus program, which was suitable for industrial scale simulation. Then, the flowrate and the weight of catalyst were multiplied by one thousand.

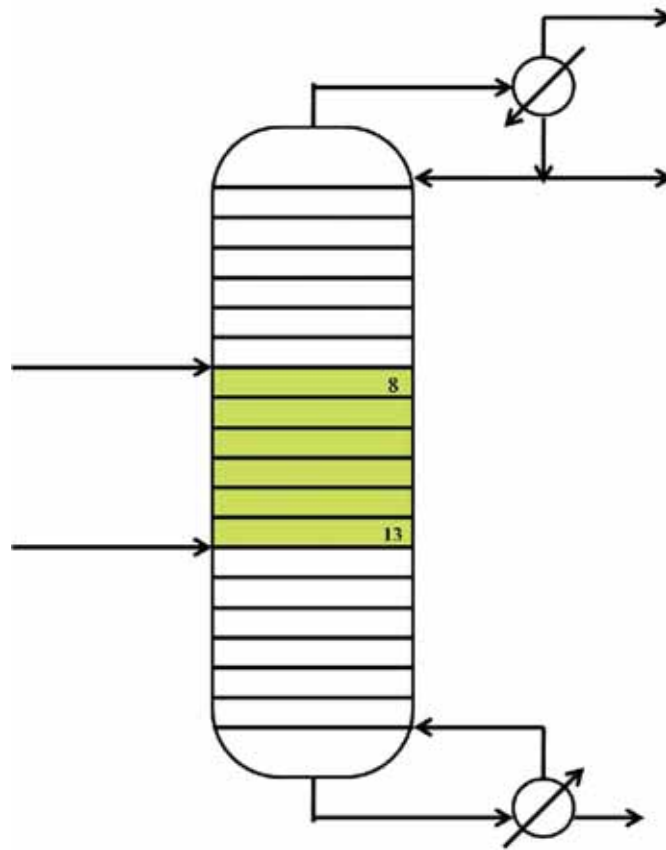


Figure 29 The configuration of standard model Reactive distillation column.

Table 10 Feed conditions and specification of Reactive Distillation column under the standard condition for Aspen Plus simulator

Condition of feed		Column specification	
Temperature (K)	298	Rectifying stage	6
Feed flow rate (Liter/min)		Reaction stage	6
glycerol	2	Stripping stage	6
<i>tert</i> -butyl alcohol	8	Heat duty(kW)	80
Pressure (bar)	1	Catalyst weight (kg)	2
Feed stage		Reflux ratio	2
glycerol	8		
<i>tert</i> -butyl alcohol	13		

The conversion of glycerol and selectivity defined below are considered to compare the performance of the reactive distillation.

$$\text{Conversion of glycerol} = \frac{\text{difference in molar flowrate of inlet and outlet of glycerol}}{\text{feed molar flowrate of glycerol}} \times 100$$

$$\text{Selectivity} = \frac{\text{molar flowrate of DTBG and TTBG}}{\text{difference in molar flowrate of inlet and outlet of glycerol}} \times 100$$

The simulation with Aspen Plus program was carried out at the standard operating condition (shown in Table 12) in reactive distillation at standard model (as show in Figure 29). From simulation results, the distillate product consists of main composition of TBA (62 mole%), water (36 mole%) and small amount of IB (2 mole%) while the bottom product consists of the main composition of TBA (59 mole%), glycerol (13 mole%), MTBG (17 mole%), and water (13 mole%). Figures 30 show the typical composition profile and temperature profile in the reactive distillation with the standard configuration.

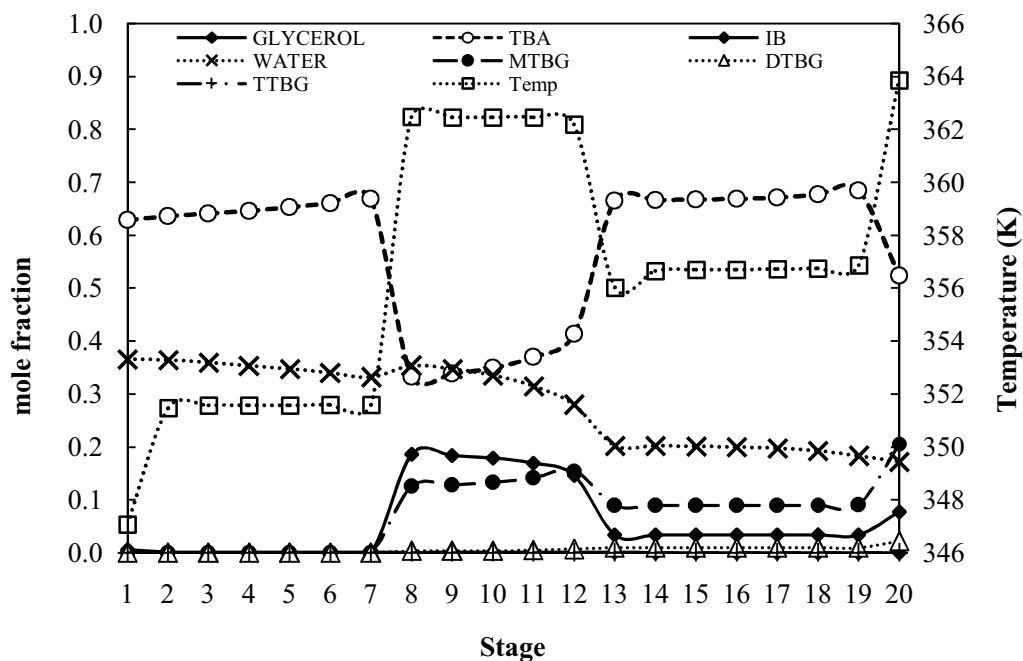


Figure 30 Mole fraction and temperature profile inside the column at standard operating condition.

3.2 Effect of design variables

As stated earlier, the specification of RD give in Table 12 is a preliminary configuration. To find optimal design variables for operation of the RD, simulation are carried out to study the effect of these variable on the RD performance. The important design variables considered here include the number of rectifying, reaction and stage.

3.2.1 Number of stripping stage

Firstly, the impact of a number of the stripping stages on the performance of reactive distillation is investigated. With the specified number of the rectifying stages (= 6 stages) as in the standard condition, the number of the stripping stages are varied from 1 to 9 and the results are presented in Figure 31. When the number of stages in the stripping section is increased (with fix heat duty of reboiler), more glycerol unreacted cannot separated from the bottom product stream and doesn't returned to the reactive section. This results in a decrease in the conversion of glycerol and selectivity of ethers product. Figure 31 also show the influence of the number of stages in the reactive section. It can be seen that the performance of the reactive distillation increased with the increase of the number of reactive stages. This is expected as more reactive stages pronounce the etherification of glycerol and *tert*-butyl alcohol. According to the simulation results, the suitable number of stages in the reaction and stripping section is 1 and 6 stages, respectively.

3.2.2 Number of rectifying stage

The purposes of a rectifying section are to remove light component from the reaction zone and to recycle the unreacted reactants back to the reaction section in the RD column. The effect of the number of the rectifying stages on the conversion of glycerol and selectivity is shown in Figure 32. It is found that even though the glycerol conversion and selectivity increase when increase the number of rectifying stage. This can be explained by the fact that with increase the number of rectifying stage, water and IB, the light component, is more remove from the reaction section. This causes the equilibrium of reaction shifting in the forward reaction and thus, the conversion of glycerol becomes higher.

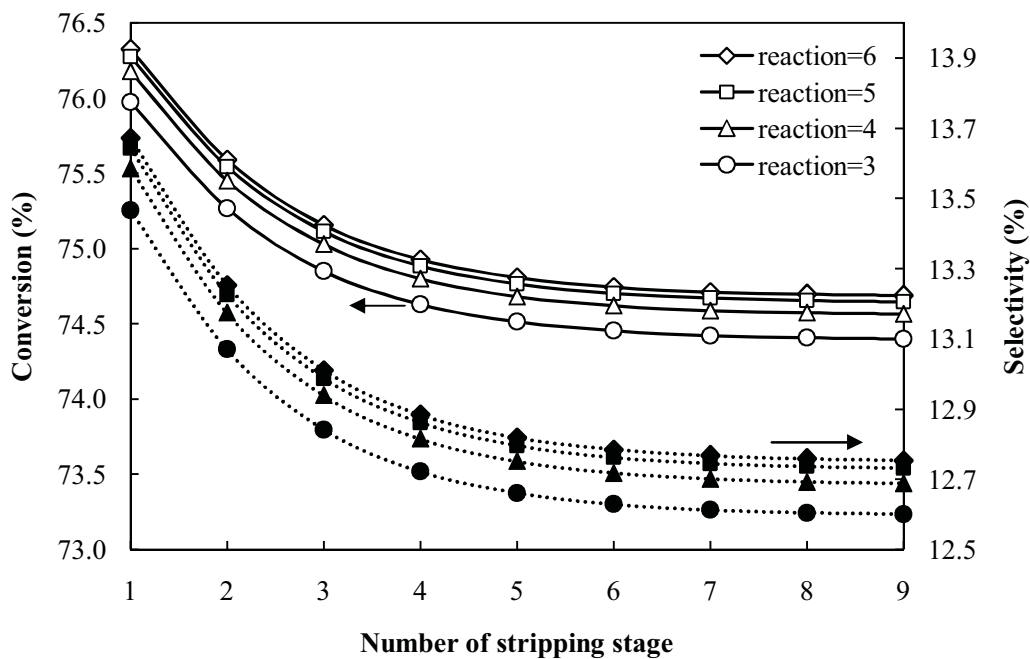


Figure 31 Effect of the number of stripping stages on the conversion and selectivity for various reaction stages (rectifying stages = 6).

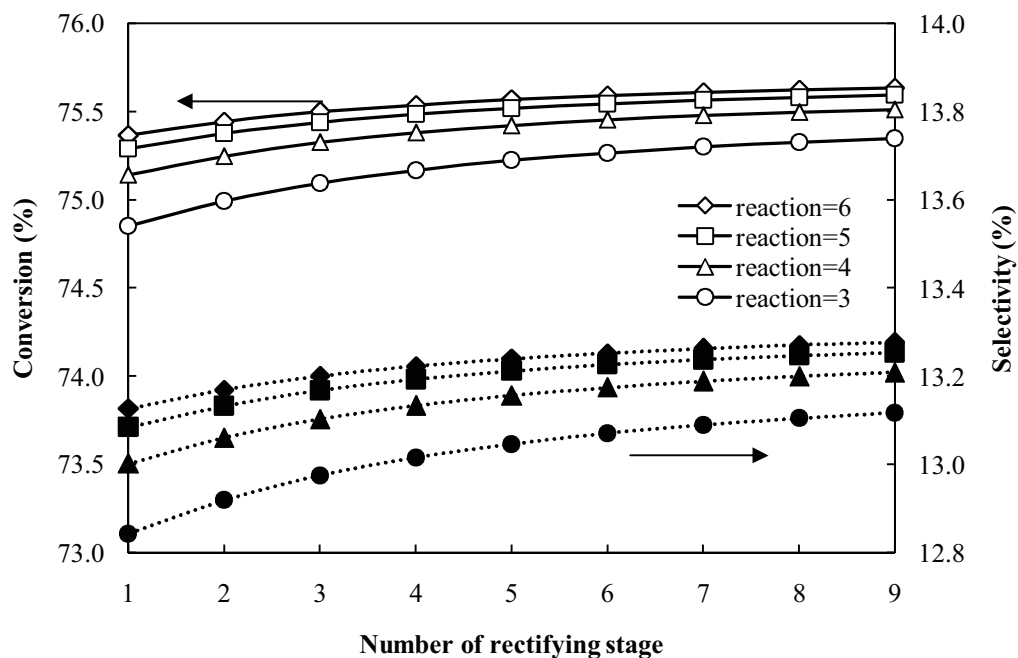


Figure 32 Effect of the number of rectifying stages on the conversion and selectivity for various reaction stages (stripping stages = 1).

For the reaction section within the RD column, the function is to provide a location where the reactions occur. According to Figure 31-32, it is noted that all other design and operating variables such as number of rectifying and stripping stages, reflux ratio, reboiler duty and feed condition are kept at the values of the standard condition. The glycerol feed is still introduced in the top of reaction section and TBA feed in the bottom of reaction section. The performance of the reactive distillation increased with the increase of the number of reactive stages (3-6 stages and fixed the total catalyst load). This is expected as, when increases the height of the column, the products generated by the reaction are too great to be separated from the system; chemical equilibrium will force reaction in the wrong direction. According to the simulation results, the suitable number of stages in the reaction is 6 stages, respectively.

At this stage, the optimal design for reactive distillation is 6 rectifying, 6 reaction and 1 stripping stage. It should be note that the location of glycerol feed stream is still fixed at the top of tray for reaction section and TBA feed is still fixed at the bottom of reaction section. This suitable configuration will be further used in order to examine the effect of operating variable: reflux ratio, feed stage location heat duty of reboiler and feed flow rate of glycerol and TBA stream. An experiment was carried out at the standard operating condition and the modified configuration (6 rectifying, 6 reaction and 1 stripping stage). An experiment was carried out at the standard condition show in Table 11. The concentration profile of residue from the experiment compare with the simulation was show in Figure 33. Figure 34 show liquid mole fraction at any stage in reactive distillation and the temperature profile from the simulation comparison with the experiment. The dashed lines showed the simulation results from the program and the symbols represent the data from experiment. From experimental results, it took around 12 hours to achieve the steady state condition. In the bottom stream, the concentration of glycerol, TBA and MTBG were 1.13 (0.99), 7.10 (6.94) and 2.4 (2.77), respectively. The values in the parenthesis are those from the simulation.

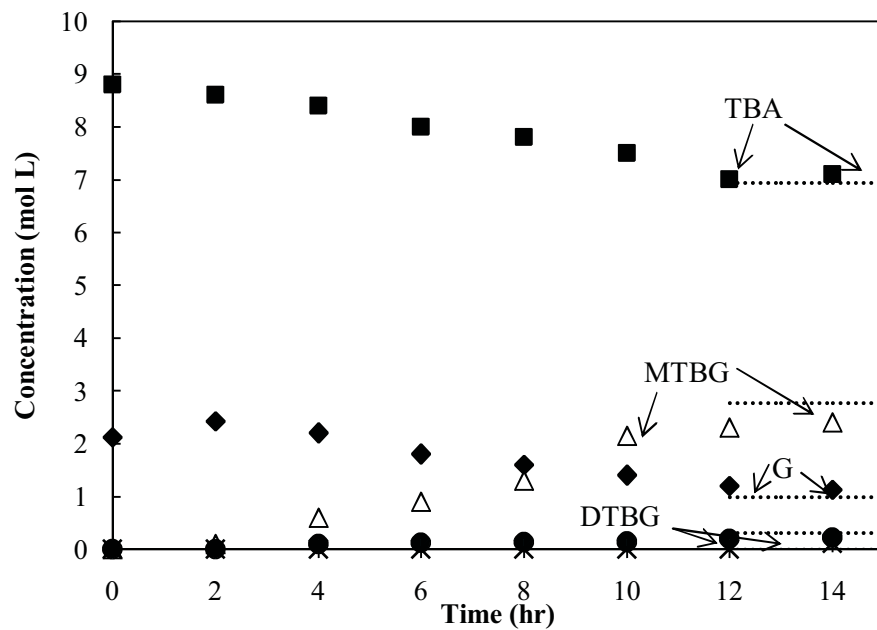


Figure 33 Concentration profiles of bottom at standard operating condition.

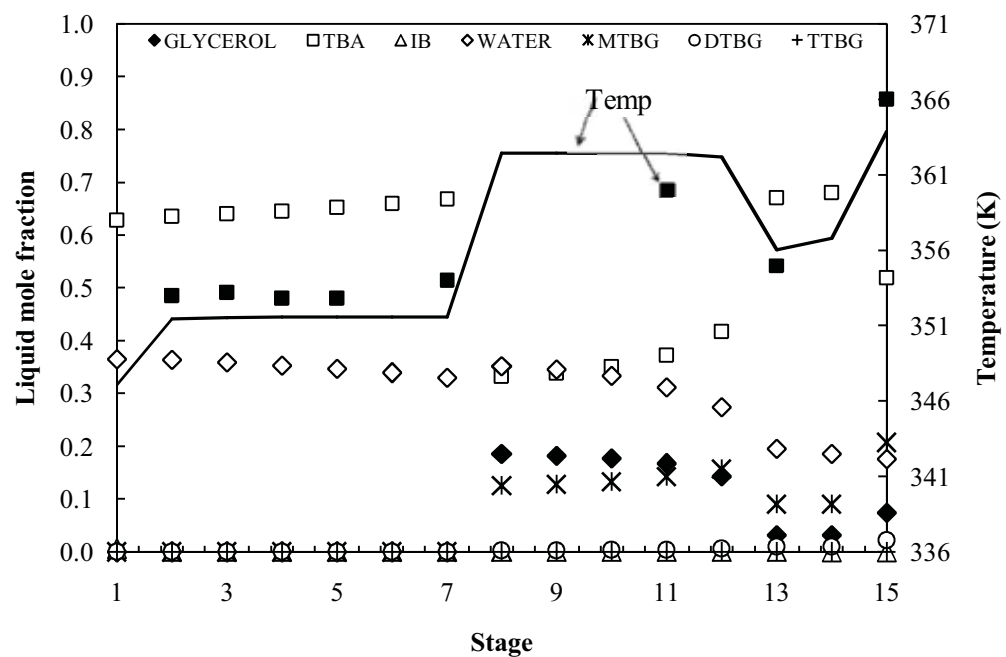


Figure 34 Mole fraction and temperature profiles at standard operating condition change with stages.

3.3 Effect of operating parameters

Aspen Plus program was employed as a main tool to simulate the performance of reactive distillation at various operating parameters. The effects of the reflux ratio, location of feed stage and reaction section, heat duty and feed flowrate were investigated. Due to limitation of the equipment, only some experiments were performed and their results were provided for the main purpose of validation of the simulation results.

3.2.1 Effect of reflux ratio

Figure 35 shows the effect of reflux ratio on the performance of the reactive distillation. The ratio was varied between 1 and 20 while the other operating parameters remained the same as the standard condition. It was found that when the reflux ratio is increased from 1 to 20. The conversion of glycerol and selectivity are optimum when used the reflux ratio at 2. This because the increase of reflux ratio increases the concentration of water and IB in reaction section then the equilibrium cannot shift forward. However, it should be note that some extents of the reflux IB can react with water (reverse reaction) generating more TBA. This is a probably a reason for a slight decrease of glycerol conversion at height reflux ratio.

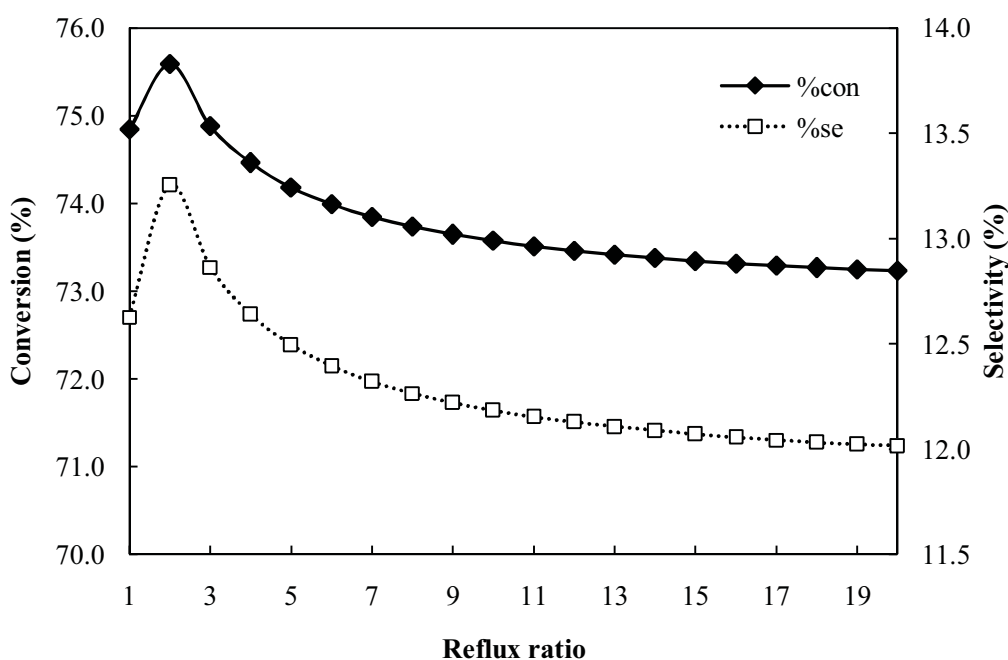


Figure 35 Effect of reflux ratio on reactive distillation performance.

3.2.2 Effect of heat duty

Figure 36 shows the effect of heat duty on the performance of reactive distillation. The heat duty show more significant effect on the conversion of glycerol within the range of study (65-230 W). As the heat duty increases, more glycerol can travel up in to the reactive section and then reacted with TBA. At highest heat duty, the column is operated at higher vapor-liquid load and temperature. When the reflux ratio is kept unchanged, more reactant especially TBA is lost from the column as the distillate, leading to the decrease of the conversion and selectivity of glycerol. The change in the conversion is mainly governed by the temperature and the liquid concentration in the reaction section which are influenced by the change of heat duty.

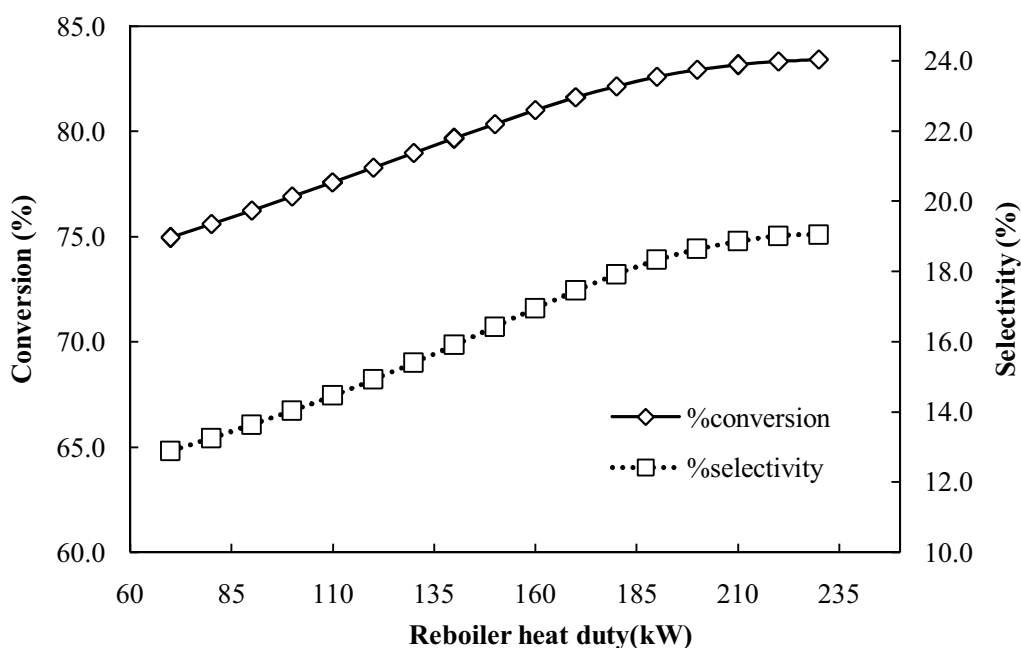


Figure 36 Effect of heat duty on reactive distillation performance.

3.2.3 Effect of feed stage location

Since the location of the feed can be adjusted to make the best separation and the most favorable reaction condition, simulation are performed to investigate the effect of the feed location of glycerol stream and TBA stream. Figure 37 and 38 show the effect of feed location of glycerol stream and TBA stream on the performance of reactive distillation. It was found that feeding glycerol at the top of the reaction section and TBA at the bottom section gives the best reactive distillation

performance in terms of the glycerol conversion and selectivity. This may be caused of the height normal boiling point reactant can be reacted with the lower normal boiling point component and decreased residence time of the reactants as the location of feed is far away from the reaction section.

3.2.4 Effect of feed flow rate

Figure 39 and 40 show the effect of glycerol and TBA feed flow rate on reactive distillation performance. The conversion of glycerol and selectivity were decrease when increase reactant feed flow rate of TBA stream. It was found that, height feed flow rate of glycerol and TBA cause reduce the reaction time in reaction section and glycerol will travel down to the bottom part of the column without being reacted.

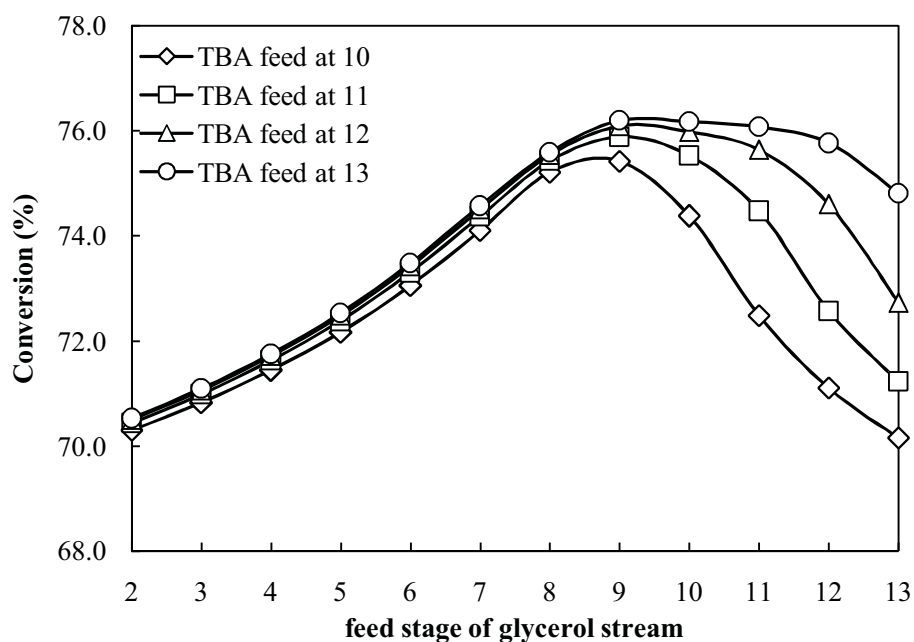


Figure 37 Effect of glycerol feed stage location on glycerol conversion for various TBA feed stage location.

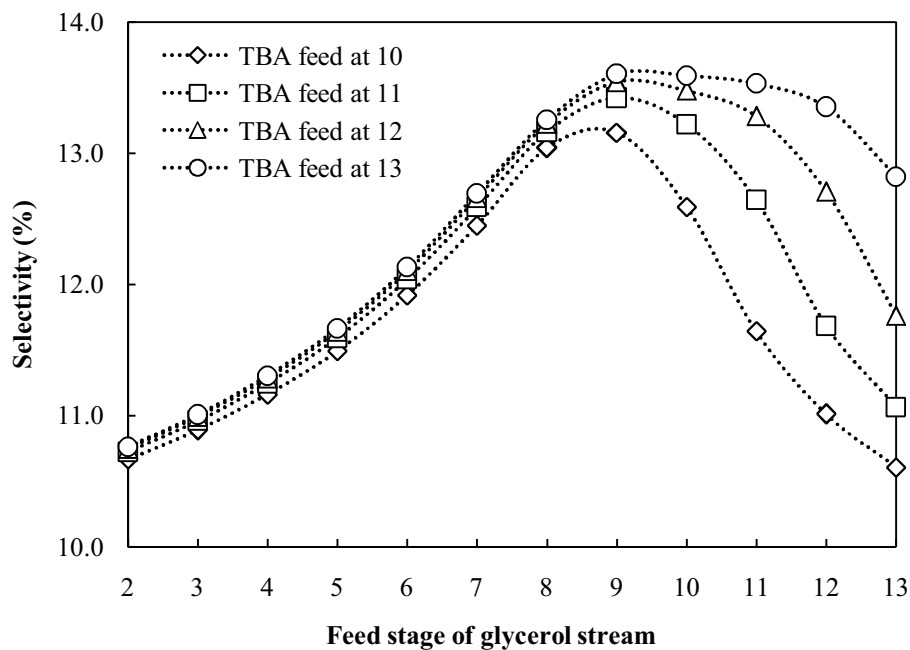


Figure 38 Effect of glycerol feed stage location on glycerol conversion for various TBA feed stage location.

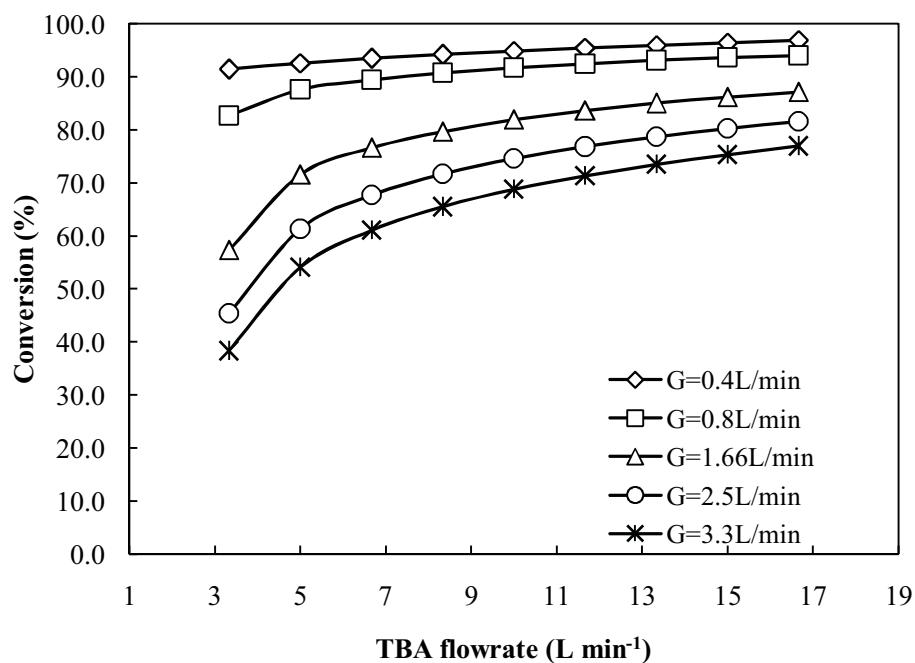


Figure 39 Effect of TBA feed flow rate on glycerol conversion for various glycerol feed flow rate.

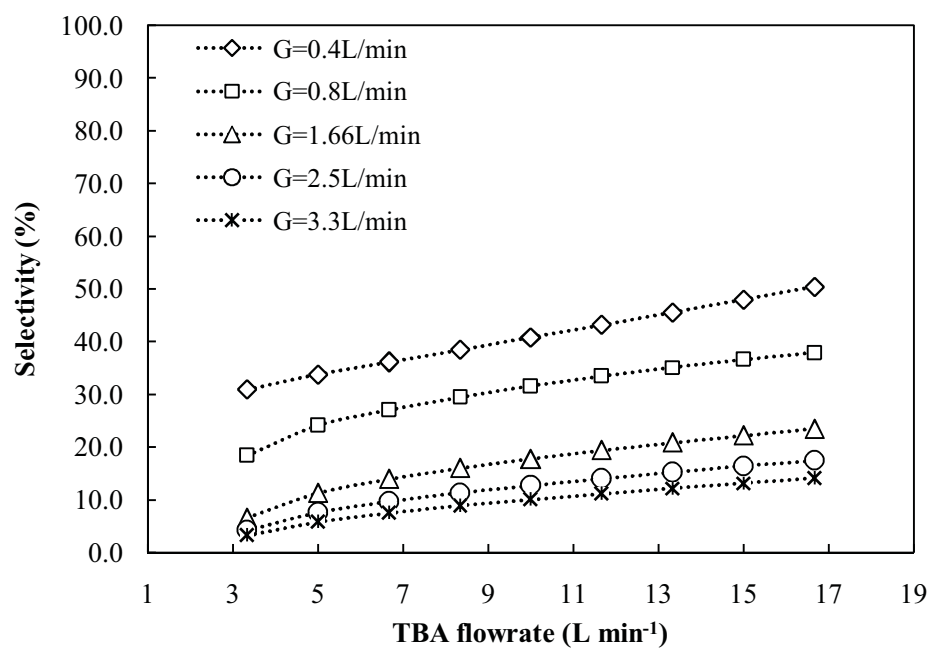


Figure 40 Effect of TBA feed flow rate on selectivity for various glycerol feed flow rate.

CHAPTER 6

CONCLUSIONS AND RECOMMENDATIONS

This chapter contained the result conclusion of group contribution method. The optimum operating condition such as temperature and ethanol volume will be concluded.

1. Thermodynamic study

Among there group contribution methods i.e. Joback, Benson and Gani group contribution method, Gani's group contribution method estimated the nearest Gibbs free energy comparing to available database. The estimated equilibrium conversion and product distribution at reaction temperature in a range of 338, 348 and 358 K showed good agreement with that obtained by experimental results from this study and reported in the literature. So, the recommendation for estimate standard Gibb's free energy for *tert*-butyl of glycerol was Gani's method. Gani's method can be used to determine the equilibrium kinetic constant for ethers production from glycerol and *tert*-butyl alcohol. The equilibrium kinetic constant

2. Kinetic study

Form kinetics study of glycerol etherification with *tert*-butyl alcohol in the semi-batch reactor at 5 bar. Three temperature levels of 338, 348, and 358 K were used in the study to obtain the parameters in the Arrhenius's equation of the reaction rate constant and the Van't Hoff equation of water sorption equilibrium. The reactor was operated at the maximum agitation speed (600 rpm) to avoid the external mass transfer. The experimental results were fitted with two kinetics models on both Activity and concentration base model of Langmuir-Hinshelwood (LH) and Power-

Law (PL). The Gani's group contribution method was used to estimate the equilibrium kinetic constant for all etherification reaction. The consecutive reaction schemes of PL and LH models were compared through the values of RMSD. The experimental results agree well with the simulation results for both PL and LH kinetic model. However, the LH-A model which takes into account the effect of water adsorption is the best kinetic model to fit the experimental results.

3. Reactive distillation study

The liquid phase synthesis of *tert*-butyl ether of glycerol from glycerol and TBA in reactive distillation column has been studied in this thesis. The simulation of this process using a rate-based kinetic expression and an equilibrium stage model are performed via Aspen Plus program. The influences of design variables on the performance of the reactive distillation are investigated. Various operating parameters; i.e. reflux ratio, location of feed stage of glycerol and TBA streams, heat duty and feed flow rate were investigated. The suitable reactive distillation configuration consists of 7 rectifying stage, 6 reaction stages and 1 stripping stage. The simulation results agree well with the experimental results. For the effect of operating parameter, feed flow rate and reflux ratio have significant effect on the performance of reactive distillation. From this study, when the feed flow rate and reflux ratio are increased, the selectivity and conversion was decrease.

4 Recommendations

As seen from the simulation studies using the Aspen Plus program; the equilibrium conversion for Gani group contribution does not perfect to explain the conversion from the experiment. Furthermore, the addition of a modified group contribution or subprogram to estimate should be alternative route to increase the performance of estimated equilibrium. From reactive distillation study, the complete conversion of glycerol to ethers product could not be obtained. To improve the ethers production it is recommended as follows:

1. A membrane should be combined inside the reactive distillation column to help the remove of water from reaction section.

2. Another reactive distillation column should be included in the process to further react glycerol to form ethers product.
3. Used reactor combine with membrane to remove water outside the system.

Bibliography

- Assabumrungrat, Suttichai et al. "Kinetics of Liquid Phase Synthesis of Ethyl *tert*-Butyl Ether from *tert*-Butyl Alcohol and Ethanol Catalyzed by Supported β -Zeolite." International Journal of Chemical Kinetics 34, 5 (2002) : 292-299.
- Assabumrungrat, Suttichai et al. "Production of Ethyl *tert*-Butyl Ether from *tert*-Butyl Alcohol and Ethanol Catalyzed by β -Zeolite in Reactive Distillation." Korean Journal of Chemical Engineering 21, 6 (December 2004) : 1139-1146.
- Benson, Sidney William. Thermochemical Kinetics 2nd ed. New York: John Wiley and Sons, 1996.
- Bouchez, M., D. Blanchet, and JP. Vandecasteele. "Degradation of polycyclic aromatic hydrocarbons by pure strains and by defined strain associations: inhibition phenomena and cometabolism." Applied Microbiology and Biotechnology 43, 1 (April 1995) : 156–164.
- Clothier, P. Q. E., S. M. Heck, and H. O. Pritchard. "Retardation of Spontaneous Hydrocarbon Ignition in Diesel Engines by Di-*tert*-butyl Peroxide." Combustion and Flame 121, 4 (June 2000) : 689–694.
- Collinon, F. et al. "Liquid phase synthesis of MTBE from methanol and isobutylene over acid zeolites and amberlyst-15." Journal of Catalysis 182, 2 (March 1999) : 302-312.
- Leonidas, Constantinou, and Gani Rafiqul. "New group contribution method for estimating properties of pure compounds." AIChE Journal 40, 10 (October 1994) : 1697-1701
- Cunill, Fider et al. "Effect of water-presence on methyl *tert*-butyl ether and ethyl *tert*-butyl ether liquid phase synthesis." Industrial & Engineering Chemistry Research 32, 3 (March 1993) : 564-569.
- Dalmazzone, Didier, Anna Salmon, and Sofiane Guella. "A second order group contribution method for the prediction of critical temperatures and

- enthalpies of vaporization of organic compounds.” Fluid Phase Equilibria 242, 2 (April 2006) : 29-42.
- Delgado, Patricia, Maria Teresa Sanz, and Sagrario Beltran. “Kinetic study for esterification of lactic acid with ethanol and hydrolysis of ethyl lactate using an ion-exchange resin catalyst.” Chemical Engineering Journal 126, 2 (February 2007), 111–118.
- Demirbas, Ayhan. “Biodiesel production from vegetable oils via catalytic and non-catalytic supercritical methanol transesterification methods.” Progress in Energy and Combustion Science 31, 5-6 (2005) : 466–487.
- Dorado, M. Pilar. “Kinetic parameters affecting the alkali-catalyzed transesterification process of used olive oil.” Energy & Fuels 18, 5 (September 2004) : 1457-1462.
- Fuchigami, Yoshio. “Hydrolysis of methyl acetate in distillation column packed with reactive packing of ion exchange resin.” Journal of Chemical Engineering of Japan 23, 3 (1989) : 354-359.
- Fukuda, Hideki, Akihiko Kondo, and Hideo Noda. “Review Biodiesel fuel production by transesterification of oils.” Journal of Bioscience and Bioengineering 92, 5 (2001) : 405-416.
- George, Boyd et al. “Computation of Multicomponent, Multiphase Equilibrium.” Industrial and Engineering Chemistry Process Design and Development 15, 3 (July 1976) : 372-377.
- Hoydonckx, Hans E. et al. “Esterification of renewable chemicals.” Topics in Catalysis 27, 1 (February 2004) : 83-96.
- Hatchings, G. J., C. P. Nicolaidis, and M. S. Scurrall. “Developments in the production of methyl *tert*-butyl ether.” Catalysis Today 15, 1 (May 1992) : 15-23.
- Iwai, Yoshio, Shin Yamanaga, and Yasuhiko Arai. “Calculation of normal boiling points for alkane isomers by a second order group contribution method.” Fluid Phase Equilibria 163, 1 (September 1999) : 1-8.

- Jamróz, Malgorzata E. et al. "Mono-, di-, and tri-tert-butyl ethers of glycerol A molecular spectroscopic study." Spectrochimica Acta Part A: Molecular and Biomolecular Spectroscopy 67, 3-4 (July 2007) : 980–988.
- Jang, Jinyoung, and Choongsik Bae. "Effects of valve events on the engine efficiency in a homogeneous charge compression ignition engine fueled by dimethyl ether." Fuel 88, 7 (2009) : 1228–1234.
- Jimenez, Laureano, Alfonso Garvín, and Joe Costa-López. "The Production of Butyl Acetate and Methanol via Reactive and Extractive Distillation. I. Chemical Equilibrium, Kinetics and Mass-Transfer Issues." Industrial & Engineering Chemistry Research 41, 26 (December 2002) : 6663–6669.
- Gerpen, Jon Van. "Biodiesel processing and production." Fuel Processing Technology 86, 10 (June 2005) : 1097-1107.
- Karinen, R. S., and A.O.I. Krause. "New biocomponents from glycerol." Applied Catalysis A-General 306 (June 2006) : 128–133.
- Klepáčová, Katarína, Dusan Mravec, and Martin Bajus. "*tert*-Butylation of glycerol catalysed by ion-exchange resins." Applied Catalysis A-General 294, 2 (2005) : 141–147.
- _____. "Etherification of glycerol with tert-butyl alcohol catalysed by ion-exchange resin." Chemical Paper 60, 3 (June 2006) : 224-230.
- _____. "Etherification of glycerol and ethylene glycol by isobutylene." Applied Catalysis A-General 328, 1 (August 2007): 1–13.
- Knothe, G., M.O. Bagby, and T.W. Ryan. "Precombustion of fatty acids and esters of biodiesel. A possible explanation for differing cetane numbers." JAOCS. 5 (1998) : 1007–1013.
- Lai, I. K. et al. "Design and control of reactive distillation for ethyl and isopropyl acetates production with azeotropic feeds." Chemical Engineering Science 62, 3 (February 2007) : 878 – 898.
- Lotero, Edgar et al. "Synthesis of Biodiesel via Acid Catalysis." Industrial & Engineering Chemistry Research 44, 14 (July 2005) : 5353-5363.

- Mavrovouniotis, L. M. "Group contributions for estimating standard gibbs energies of formation of biochemical compounds in aqueous solution." Biotechnology and Bioengineering 36, 10 (February 2004) : 1070 – 1082.
- Mao, R. Lee Van et al. "synthesis of methyl tertiary butyl ether (MTBE) over Triflic Acid Loaded ZSM-5 and Y Zeolites." Catalysis Letter 6, 3 (May 1990) : 321-330.
- Matouq, M. et al. "Reactive distillation for synthesizing ethyl *tert*-butyl ether from low grade alcohol catalyst by potassium hydrogen sulfate." Industrial & Engineering Chemistry Research 35, 3 (March 1996), 982-984
- Matouq Mohammed, T. Tagawa, and Shigeo Goto, "Combine process for production methyl *tert*-butyl ether from *tert*-butyl alcohol and methanol." Journal of Chemical Engineering of Japan 27 (1993) : 302-306.
- Mao, Wei et al. "Thermodynamic and kinetic study of *tert*-amyl methyl ether (TAME) synthesis." Chemical Engineering and Processing 47, 5 (May 2008) : 761-769.
- Sanz, M. T. et al. "Kinetic Study for the Reactive System of Lactic Acid Esterification with Methanol: Methyl Lactate Hydrolysis Reaction." Industrial & Engineering Chemistry Research 43, 9 (April 2004) : 2049–2053.
- Noureddini, Hossein, W. R. Dailey, and B. A. Hunt. "Production of ethers of glycerol from crude glycerol – the byproduct of biodiesel production." Chemical and Biochemical Engineering Research 20, 2 (May 1998) : 10-16.
- Quitain, Amando, Hatoshi Itoh, and Shigeo Goto. "Reactive Distillation for Synthesizing Ethyl *tert*-Butyl Ether from Bioethanol." Journal of Chemical Engineering of Japan 32, 4 (June 1999) : 280-287.
- _____. "Industrial-Scale Simulation of Proposed Process for Synthesizing Ethyl *tert*-Butyl Ether from Bioethanol." Journal of Chemical Engineering of Japan 32, 4 (1999) : 539-543.
- Krishnaswamy, Rajagopal, Ruiz Ahon Victor, and Moreno Esteban. "Estimating thermochemical properties of hydroprocessing reactions by molecular simulation and group contribution methods." Catalysis Today 109 (2005) : 195-204.

- Ramadhas, A. S., S. Jayaraj, and C. Muraleedharan. "Biodiesel production from high FFA rubber seed oil." Fuel 84, 4 (March 2005) : 335-340.
- Romas, M. J. et al. "Influence of fatty acid composition of raw materials on biodiesel properties." Bioresource Technology 100, 2 (2009) : 261–268.
- Karinen, R. S., and A. Outi I. Krause. "Kinetic Model for the Etherification of 2,4,4-Trimethyl-1-pentene and 2,4,4-Trimethyl-2-pentene with Methanol." Industrial & Engineering Chemistry Research 40 (2001) : 6073-6080.
- Rihko, L. K., and A. O. Krause. "Etherification of FCC light gasoline with methanol." Industrial & Engineering Chemistry Research 35 (1996) : 2500-2507.
- Sneesby, M. G. et al. "ETBE synthesis via reactive distillation. 2. Dynamic simulation and control aspects." Industrial & Engineering Chemistry Research 36 (1997) : 1870-1881.
- Steinigeweg, S., and J. Gmehling "Transesterification processes by combination of reactive distillation and pervaporation." Chemical Engineering and Processing 43 (2004) : 447–456.
- Venkataraman, S., W.K. Chan, and J.F. Boston. "Reactive distillation using Aspen plus." Chemical Engineering and Processing 86 (1990) : 45-54.
- Yang, Bo-Lun, San-Ba Yang, and Rui-qinq Yao. "Synthesis of ethyl tert-butyl ether from *tert*-butyl alcohol and ethanol on strong acid cation-exchange resins." Reactive & Functional Polymers 44, 2 (July 2000) : 167- 175.
- Yang ,B-L, S-B Yang, and H-J Wang. "Simulation for reactive distillation process to synthesize ethyl *tert*-butyl ether." Journal of Chemical Engineering of Japan 33, 9 (2001) : 1165-1170.
- Yin, Xiaodong, Bolun Yang, and Shigeo Goto. "Kinetics of liquid-phase synthesis of ethyl *tert*-butyl ether form *tert*-butyl alcohol and ethanol catalyzed by ion-exchange resin and heteropoly acid." International Journal of Chemical Kinetics 27, 1 (Sep 2004) : 1065-1074.
- Zhang, Yang, Li Ma, and Jichu Yang. "Kinetics of esterification of lactic acid with ethanol catalyzed by cation-exchange resins." Reactive & Functional Polymers 61, 1 (August 2004) : 101–114.

Zheng, Ming et al. "Biodiesel engine performance and emissions in low temperature combustion." Fuel 87, 6 (May 2008) : 714-722.

APPENDIX

APPENDIX A

NOMENCLATURE

a_i	activity of component i	[-]
c_i	concentration of component i	[mol L ⁻¹]
E_a	activation energy	[J mol ⁻¹]
G_b	Gibbs free energy	[kJ s ⁻¹]
H_f	standard enthalpy change of the reaction	[kJ s ⁻¹]
$k_{j,a}$	kinetic constant based on activity	[mol (s mol-H ⁺) ⁻¹]
$k_{j,c}$	kinetic constant based on concentration	[mol (s mol-H ⁺) ⁻¹]
$K_{eq,j}$	chemical equilibrium constant	[-]
K_i	partition equilibrium constant	[-]
LD	liquid distillate flow rate	[mol s ⁻¹]
L	liquid flow rate returning from stage 1 to stage 2	[mol s ⁻¹]
m_i	mole of species I	[mol]
M	number of components	[-]
M_i	molecular weight of species i	[kg mol ⁻¹]
n_i	number of mole of species i in the reactor	[mol]
P_c	critical pressure	[bar]
Q_r	ion-exchange capacity (= 5.0)	[meq-H ⁺ kg-cat. ⁻¹]
Q	reboiler duty	[W]
r_j	reaction rate	[mole (s meq -H ⁺) ⁻¹]
R	residue flow rate	[mol s ⁻¹]
R_g	gas constant (=8.314)	[J mol ⁻¹ K ⁻¹]
T	operating temperature	[K]
T_b	normal boiling point	[K]
T_c	critical temperature	[K]
$RMSD_i$	Relative Root Mean Square Deviation	[-]
W	catalyst weight	[kg]
$X_{glycerol}$	conversion of TAA	[-]

Greeks letters

γ_i activity coefficients of species i [-]

Subscripts

a activity
 Exp experimental result
 i species i
 j reaction step
 x mole fraction
 Sim simulation result
 z order of reaction

Abbreviations

CO carbon monoxide
 DME dimethyl ether
 DEE diethyl ether
 DTBG di *tert*-butyl of glycerol
 ETBE ethyl tertiary butyl ether
 EtOH ethyl alcohol
 G glycerol
 H₂O water
 IB isobutylene
 KHSO₄ potassium hydrogen sulfate
 LH Langmuir-Hinshelwood
 MeOH methanol
 MTBE methyl *tert*-butyl ether
 MTBG methyl *tert*-butyl of glycerol
 NO_x oxides of nitrogen
 PL Power Law
 TBA *tert*-butyl alcohol
 TTBG tri *tert*-butyl of glycerol

APPENDIX B

JOBACK'S GROUP CONTRIBUTION METHOD

The functional groups of components in olefins are listed below with the number of subgroup in each component. Joback's group contribution method will be used to estimate the property of olefin components. This method can be used to estimate critical properties such as critical temperature and critical pressure or normal boiling point or estimated the thermodynamic properties such as Gibbs of formation.

Table 11 Joback's subgroup.

component	formula	Number of subgroup							
		CH ₃	CH ₂	CH	C	OH	O	=CH ₂	=C-
MTBG	C ₇ H ₁₆ O ₃	3	2	1	1	2	1	0	0
DTBG	C ₁₁ H ₂₄ O ₃	6	2	1	2	1	2	0	0
TTBG	C ₁₅ H ₃₂ O ₃	9	2	1	3		3	0	0
TBA	C ₄ H ₁₀ O	3	0	0	1	1	0	0	0
IB	C ₄ H ₈	2	0	0	0	0	0	1	1
Glycerol	C ₃ H ₈ O ₃	0	2	1	0	3	0	0	0
Ethanol	C ₂ H ₆ O	1	1	0	0	1	0	0	0
Methanol	CH ₄ O	1	0	0	0	1	0	0	0
ETBE	C ₆ H ₁₄ O	4	1	0	1	0	1	0	0
MTBE	C ₅ H ₁₂ O	4	0	0	1	0	1	0	0

Equation to estimated properties by Joback group contribution method

$$T_c(\text{K}) = T_b [0.5084 + 0.965 \{ \sum_k N_k (tck) \} - \{ \sum_k N_k (tck) \}^2]^{-1}$$

$$P_c(\text{bar}) = [0.113 + 0.0032 N_{\text{atom}} - \sum_k N_k (pck)]^{-2}$$

$$T_b(\text{K}) = 198 + \sum_k N_k (tbk)$$

$$G_f^0(\text{kJ mol}^{-1}) = 53.88 + \sum_k N_k (gfk)$$

Table 12 Joback constant for any subgroup

variable	Joback's subgroup							
	CH3	CH2	CH	C	OH	O	=CH2	=C-
<i>tbk</i>	23.58	22.88	21.74	18.25	92.88	22.42	18.18	24.14
<i>tck</i>	0.0141	0.0189	0.0164	0.0067	0.0741	0.0168	0.0113	0.0117
<i>pck</i>	-0.0012	0	0.002	0.0043	0.0112	0.0015	-0.0028	0.0011
<i>gfk</i>	-43.96	8.42	58.36	116.02	-189.2	-105	3.77	92.36
<i>hfk</i>	-76.45	-20.64	29.89	82.23	-208.04	-132.22	-9.63	83.99

APPENDIX C

GANI'S GROUP CONTRIBUTION METHOD

The functional groups of components in this study are listed below with the number of subgroup in each component. Gani's group contribution method will be used to estimate the property of all components in this. This method can be used to estimate critical properties such as critical temperature and critical pressure or normal boiling point or estimated the thermodynamic properties such as Gibbs of formation.

Table 13 Gani's 1st order subgroup

name	Number of 1 st order subgroup (N_k)									
	CH ₃	CH ₂	CH	C	CH ₂ O	OH	CH-O	CH ₂ =C	CH ₃ OH	CH ₃ O
MTBG	3	1	1	1	1	2	0	0	0	0
DTBG	6	0	0	2	2	1	0	0	0	0
TTBG	9	0	0	3	2	0	1	0	0	0
TBA	3	0	0	1	0	1	0	0	0	0
IB	2	0	0	0	0	0	0	1	0	0
Glycerol	0	2	1	0	0	3	0	0	0	0
Ethanol	1	1	0	0	0	1	0	0	0	0
Methanol	1	0	0	0	0	1	0	0	0	0
ETBE	4	0	0	1	1	0	0	0	0	0
MTBE	3	0	0	1	0	0	0	0	0	0

Table 14 Gani's 2nd order subgroup

name	Number of 2 nd order subgroup (N_k)				
	(CH ₃) ₃ C	CHOH	COH	CH _m (OH)C _n (OH) m,n (0,2)	CH ₃ -CH _m =CH _n m,n (0,2)
MTBG	1	0	0	1	0
DTBG	2	1	0	0	0
TTBG	3	0	0	0	0
TBA	1	0	1	0	0
IB	0	0	0	0	2
Glycerol	0	0	0	2	0
Methanol		0	0	0	0
ETBE	1	0	0	0	0
MTBE	1	0	0	0	0

Equation to estimated properties by Gani group contribution method

$$F = f[\sum_k N_k (F_{1k}) + W \sum_j M_j (F_{2j})]$$

$$T_b(K) = 204.359 \ln [\sum_k N_k (tb1k) + W \sum_j M_j (tb2j)]$$

$$T_c(K) = 181.128 \ln [\sum_k N_k (tc1k) + W \sum_j M_j (tc2j)]$$

$$P_c(\text{bar}) = [\sum_k N_k (pc1k) + \sum_j M_j (pc2j) + 0.10022]^{-2} + 1.3705$$

$$G_f^0(\text{kJ mol}^{-1}) = -14.83 + [\sum_k N_k (gf1k) + W \sum_j M_j (gf2j)]$$

for this study $M_j=0$ then

$$F = f[\sum_k N_k (F_{1k})]$$

$$T_b(K) = 204.359 \ln [\sum_k N_k (tb1k)]$$

$$T_c(K) = 181.128 \ln [\sum_k N_k (tc1k)]$$

$$P_c(\text{bar}) = [\sum_k N_k (pc1k) + 0.10022]^{-2} + 1.3705$$

$$G_f^0(\text{kJ mol}^{-1}) = -14.83 + [\sum_k N_k (gf1k)]$$

APPENDIX D

BENSON'S GROUP CONTRIBUTION METHOD

The functional groups of components in this study are listed below with the number of subgroup in each component. Benson's group contribution method is used to estimate the property of all components in this study. This method will be used to estimate thermodynamic properties and Gibbs of formation.

Equation to estimated properties by Benson group contribution method

$$\Delta H_{f(298.15K)}^0 = \sum_k N_k (\Delta H_{fk}^0)$$

$$S_{f(298.15K)}^0 = \sum_k N_k (S_k^0 + S_s^0) + S_s^0$$

$$S_{el(298.15K)}^0 = \sum_e v_e (S_e^0)$$

$$\Delta G_{f(298.15K)}^0 = \Delta H_{f(298.15K)}^0 - 298.15 [S_{f(298.15K)}^0 - S_{el(298.15K)}^0]$$

The sample entropy, S_s^s is independent of T and given by

$$S_s^0 = R \ln(N_{oi}) - R \ln(N_{ts})$$

Table 15 Benson's subgroup

name	Number order subgroup (N_k)								
	CH ₃ -(C)	CH ₂ -(C)(O)	CH-(2C)(O)	C-(3C)(O)	OH-(C)	O-(2C)	=CH ₂ (C)	=C(3C)	CH ₃ -(O)
MTBG	3	2	1	1	2	1	0	0	0
DTBG	6	2	1	2	1	2	0	0	0
TTBG	9	2	1	3	0	3	0	0	0
TBA	3	0	0	1	1	0	0	0	0
IB	2	0	0	0	0	0	1	1	0
Glycerol	0	2	1	0	3	0	0	0	0
Ethanol	1	1	0	0	1	0	0	0	0
Methanol	1	0	0	0	1	0	0	0	0
ETBE	4	1	0	1	0	1	0	0	0
MTBE	3	0	0	1	0	1	0	0	1

Table 16 ΔH_{fk}^0 and S_k^0 constant for Benson's method calculation

Variable	Benson's subgroup								
	CH ₃ -(C)	CH ₂ -(C)(O)	CH-(2C)(O)	C-(3C)(O)	OH-(C)	O-(2C)	=CH ₂ (C)	=C(3C)	CH ₃ -(O)
ΔH_{fk}^0	-42.19	-33.91	-30.14	-27.63	-158.56	-97.11	26.2	43.28	-42.19
S_k^0	127.29	41.02	-46.04	-140.48	121.68	36.33	0	0	127.29

Table 17 N_e , S_e , N_{oi} and N_{ts} constant for Benson's method calculation

name	formular	N_e			S_e			N_{oi}	N_{ts}
		C	H	O	C	H	O		
MTBG	C ₇ H ₁₆ O ₃	7	16	3	6	75	102.5	2	3
DTBG	C ₁₁ H ₂₄ O ₃	11	24	3	6	75	102.5	1	9
TTBG	C ₁₅ H ₃₂ O ₃	15	32	3	6	75	102.5	1	27
TBA	C ₄ H ₁₀ O	4	10	1	6	75	102.5	1	3
IB	C ₄ H ₈	4	8	0	6	75	102.5	1	2
Glycerol	C ₃ H ₈ O ₃	3	8	3	6	75	102.5	1	1
Ethanol	C ₂ H ₆ O	2	6	1	6	75	102.5	1	1
Methanol	CH ₄ O	1	4	1	6	75	102.5	1	1
ETBE	C ₆ H ₁₄ O	6	14	1	6	75	102.5	1	3
MTBE	C ₅ H ₁₂ O	5	12	1	6	75	102.5	1	3

APPENDIX E

ASPENPLUS PROGRAM

This chapter will be described the Simulation procedure for study of the etherification reaction of reactive glycerol with tert-butyl alcohol using the Gibbs reactor. It is explained the step detail for added the components that not exist in data bank in Aspen plus program. The detail as follow

1. Start Aspen Plus program by click Start and then select Programs. Select Aspen Tech | Aspen Engineering Suite | Aspen Plus 2006.5 | Aspen Plus User Interface. The Aspen Plus Startup dialog box appears. Aspen Plus displays a dialog box whenever you must enter information or make a selection before proceeding. In this simulation, use an Aspen Plus template.

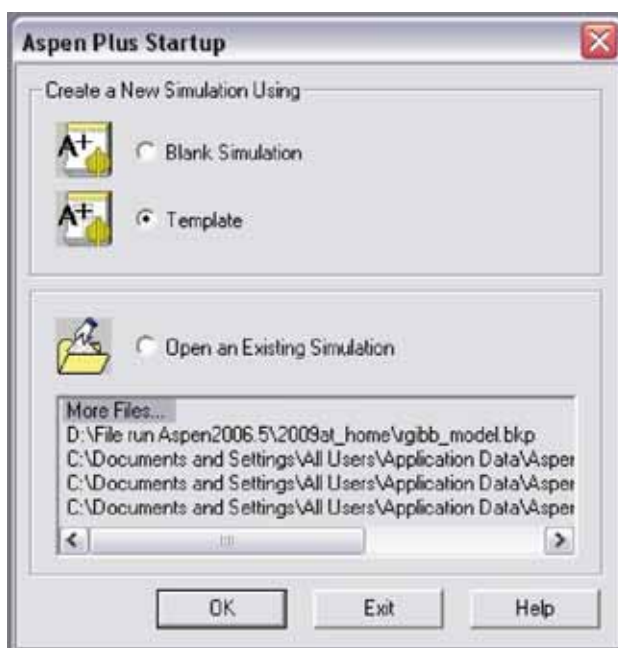


Figure 41 Aspen Plus startup

2. Select Template and click OK to apply this option.

3. Select the General with Metric Units template and Click OK to apply these options.

4. From the Model Library, select the Reactor tab and select Rgibbs model.



Figure 42 Aspen Plus program

5. Create one input stream name FEED and one product streams name PRODUCT.

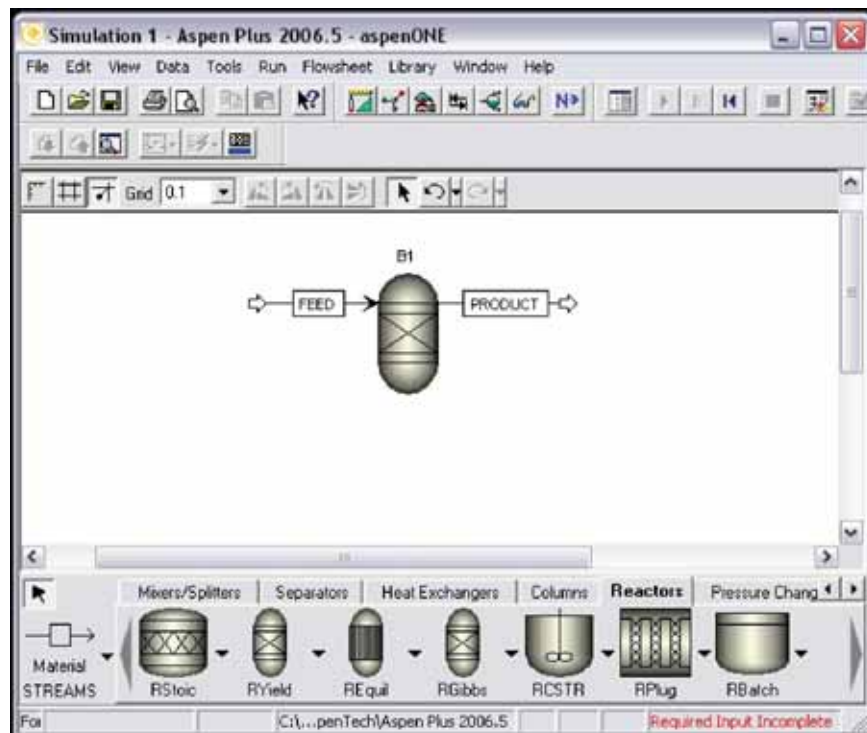


Figure 43 Rgibbs flowsheet in Aspen Plus program

6. Press F8 to open the Data Browser.
7. Go to the Components | Specifications | Selection sheet. In the Component ID field, type WATER and press Enter on the keyboard. Do the same thing by adding component Glycerol, MTBG, DTBG and TTBG.

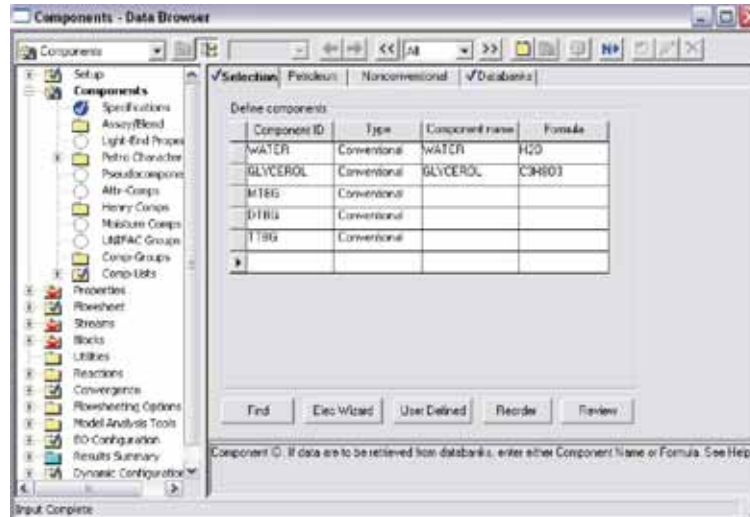


Figure 44 component data browser

8. For the component tert-butyl alcohol, click icon Find. Enter “tert” in component name and formula area and press Enter.

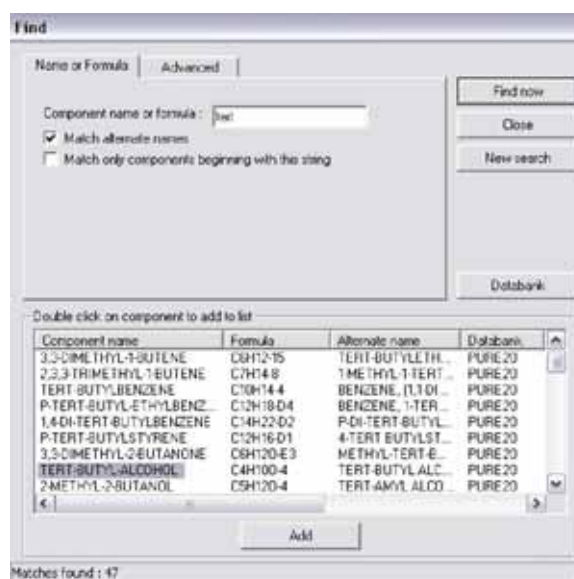


Figure 45 Find components in Aspen Plus program

9. Click on component name “TERT-BUTYL-ALCOHOL” and click icon ADD. Do same way to find component isobutylene.

10. Go to the Properties | Specifications | Global sheet and select the UNIFAC model in the Base method field.

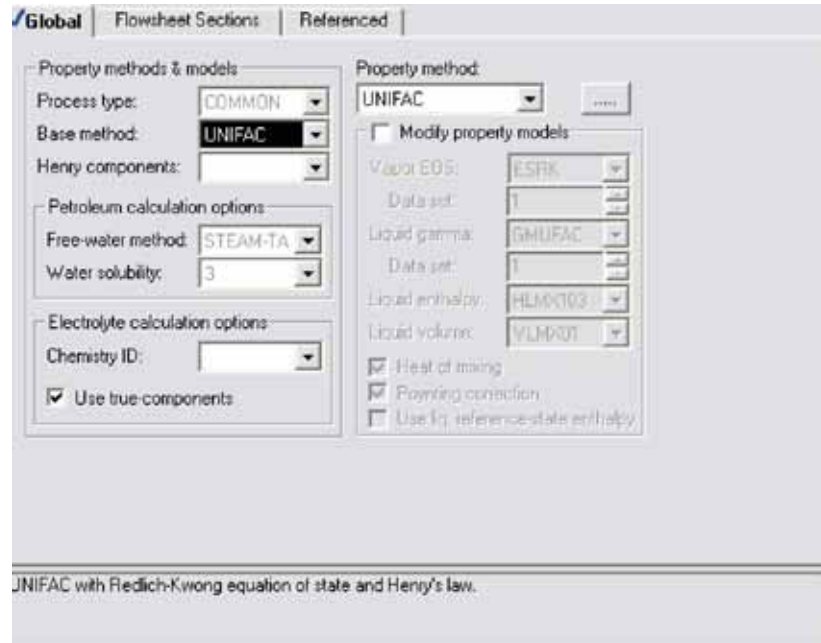


Figure 46 Property method and model

11. Go to the Properties | Estimation | Setup and select Estimate all missing parameters in Estimation options field.

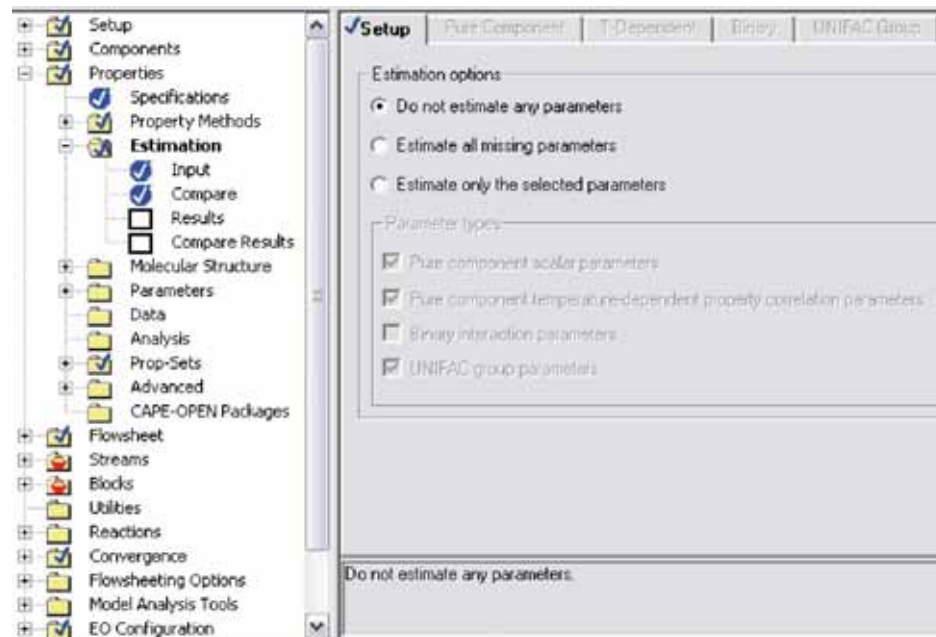


Figure 47 Estimation field in Aspen Plus program

12. Go to the Properties | Estimation | Pure component and select parameter to estimate in parameter field.

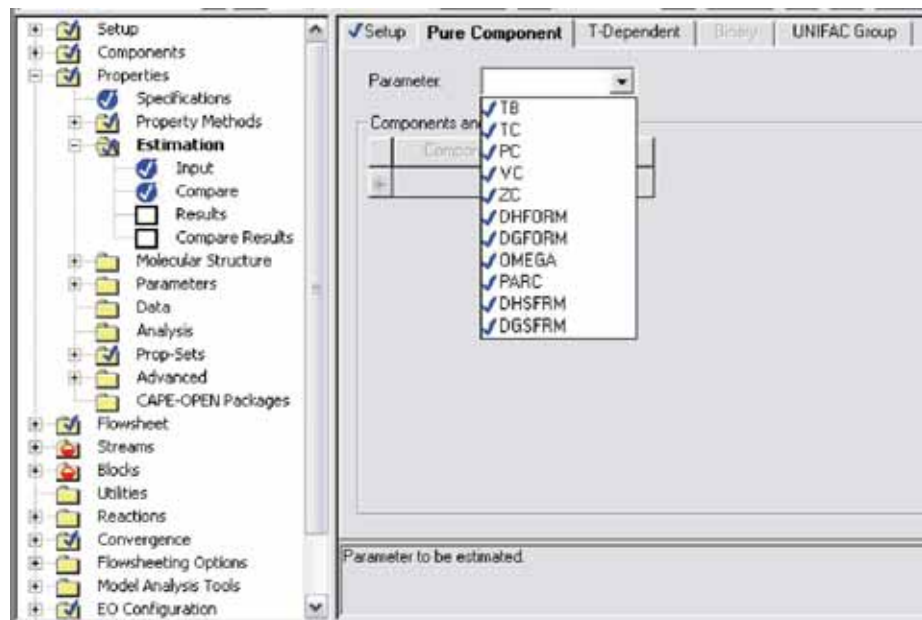


Figure 48 Selection parameter to estimate

13. Choose the properties that want to estimate and select group contribution method to estimate.

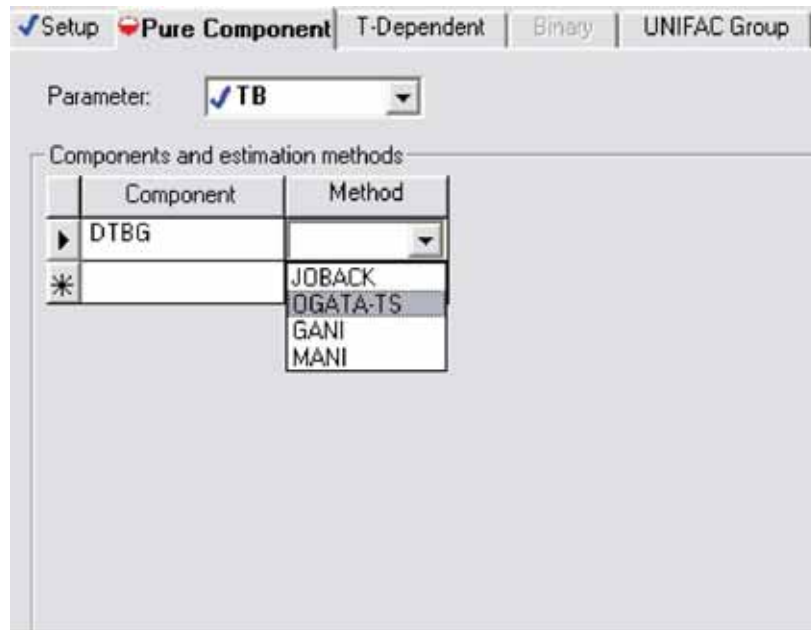


Figure 49 Select method to estimate properties

14. Go to the Properties | Molecular Structure | DTBG | General and click on Structure tab to imports molecular structure (.mol file). Click on Import Structure and brows to find structure file.

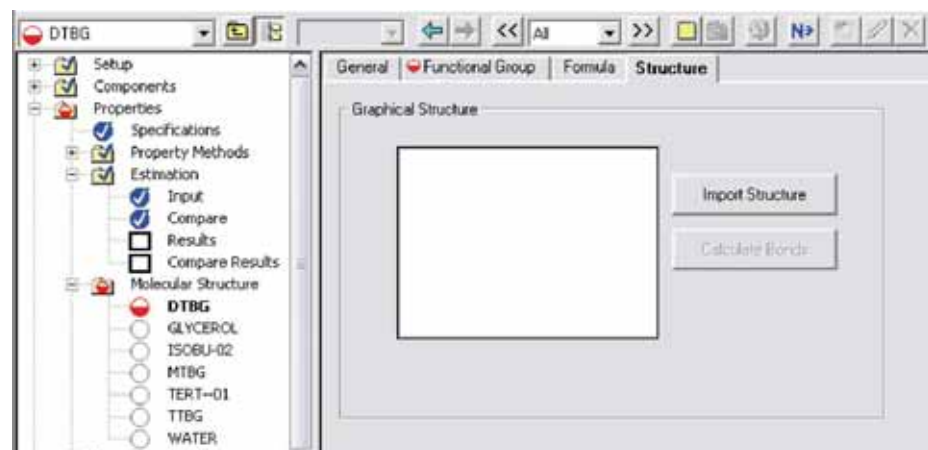


Figure 50 Import molecular structure

15. Click on icon Calculate bonds. In the molecular structure detail click OK.

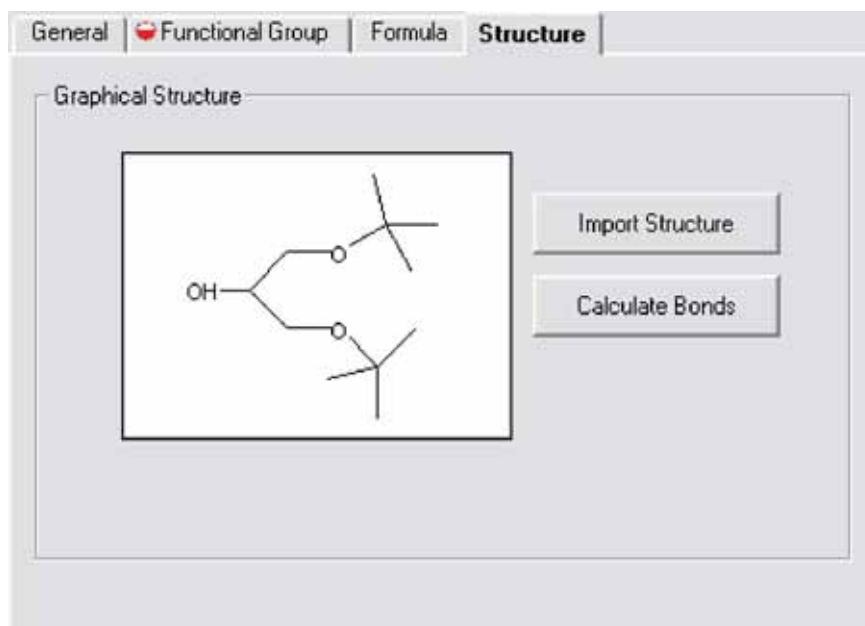


Figure 51 Calculate bonds of the component

16. Go to the Streams | FEED | Input | Specifications sheet. In the Total flow section of the State variables area, change the type of composition to Stdvol-Flow and change unit to l/sec. In the experiment, 16 ml of glycerol was reacted with 83 ml of *tert*-butyl alcohol in batch reactor. In the simulation, input glycerol 0.016 l/sec and *tert*-butyl alcohol 0.083 l/sec.

The screenshot shows the 'Specifications' sheet for a substream named 'MIXED'. The 'State variables' section includes Temperature (25 C) and Pressure (1 bar). The 'Composition' section is set to 'Stdvol-Flow' with a unit of 'l/sec'. A table lists the components and their values:

Component	Value
WATER	
GLYCEROL	0.016
MTBG	
DTBG	
TTBG	
ISDBU-02	
TERT-01	0.083

The total flow is 0.099. A note at the bottom states: 'Lets you type the component flow, fraction or concentration. See Help.'

Figure 52 Stream detail

17. On the Blocks | B1 | Setup | Specification sheet, specify the operating condition. In the calculation option select “Restrict chemical equilibrium – specify temperature approach or reaction”.

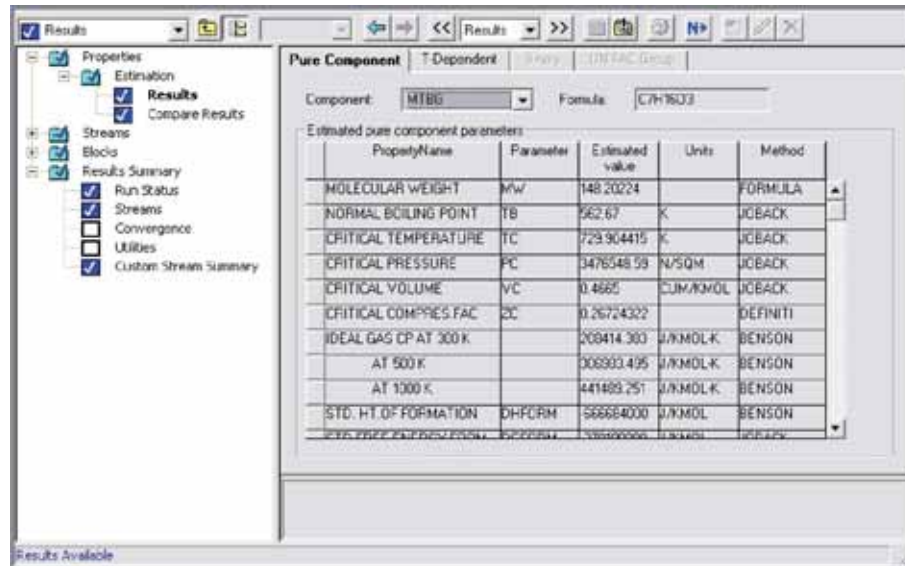
Figure 53 Block setup

18. Click on Restricted Equilibrium tap, in the Restricted Chemical Equilibrium field chose Individual reaction and click on “New...” icon. Choose reactants, products and coefficient of the reaction.

Rxn No.	Specification type	Stoichiometry
1	Temp. approach	MTBG + TERT-01 -> DTBG + WATER

Figure 54 Define reactions in the reactor

19. Run the simulation and the result will show the component in each stream.



Results Available

Property Name	Parameter	Estimated value	Units	Method
MOLECULAR WEIGHT	MW	148.20224		FORMULA
NORMAL BOILING POINT	TB	562.67	K	JOBACK
CRITICAL TEMPERATURE	TC	729.904415	K	JOBACK
CRITICAL PRESSURE	PC	3476548.59	N/SQM	JOBACK
CRITICAL VOLUME	VC	0.4665	CUM/KMOL	JOBACK
CRITICAL COMPRES FAC	ZC	0.26724322		DEFINITI
IDEAL GAS CP AT 300 K		208414.303	J/KMOL.K	BENSON
AT 500 K		308993.495	J/KMOL.K	BENSON
AT 1000 K		441489.251	J/KMOL.K	BENSON
STD. HT. OF FORMATION	DHFORM	566684000	J/KMOL	BENSON

Figure 55 The result form Aspen Plus program

APPENDIX F

UNIFAC METHOD

Basic Background

The UNIFAC (UNIQUAC Functional-group Activity Coefficients) method for estimation of liquid-phase activity coefficient is based on the concept that a liquid mixture may be considered as a solution of the structural units from which the molecules are formed rather than a solution of the molecules themselves. These structural units are called subgroups, and some of them are listed in the second column of Table C.1. A number, designated k , identifies each subgroup. The relative volume R_k and relative surface area Q_k are properties of the subgroups, and values are listed in column 4 and 5 of Table C.1. When it is possible to construct a molecule from more than one set of subgroups, the set containing the least member of different subgroups is the correct set. The great advantages of the UNIFAC method are;

1. Theory is based on the UNIQUAC method.
2. Parameters are essentially independent of temperature.
3. Size and binary interaction parameters are available for wide range of types of functional groups.
4. Prediction can be made over a temperature range of 275 to 425 K and for pressure up to a few atmospheres.
5. Extensive comparisons with experimental data are available.

Activity coefficients depend not only on the subgroup properties R_k and Q_k , but also on interactions between subgroups. Here, similar subgroups are assigned to a main group, as shown in the first two columns of Table C.1. The designations of main groups, such as “CH₂”, “ACH”, etc., are descriptive only. All subgroups belonging to the same main group are considered identical with respect to group interactions. Therefore parameters characterizing group interactions are identified with pairs of main groups.

The UNIFAC method is based on the UNIQUAC equation which treats $g \equiv G^E / RT$ as comprised of two additive parts, a *combinatorial* term g^C to account for molecular size and shape differences, and a *residual* term g^R to account for molecular interactions:

$$g = g^C + g^R \quad (\text{F-1})$$

The function g^C contains pure-species parameters only, whereas the function g^R incorporates two binary parameters for each pair of molecules. For a multi-component system,

$$g^C = \sum x_i \ln \frac{\phi_i}{x_i} + 5 \sum q_i x_i \ln \frac{\theta_i}{\phi_i} \quad (\text{F-2})$$

and

$$g^R = -\sum q_i x_i \ln(\sum \theta_j \tau_{ji}) \quad (\text{F-3})$$

where

$$\phi_i = \frac{x_i r_i}{x_j r_{j i}} \quad (\text{F-4})$$

and

$$\theta_i = \frac{x_i q_i}{x_j q_{j i}} \quad (\text{F-5})$$

Subscript i identifies species, and j is a dummy index; all summations are over all species. Note that $\tau_{ji} \neq \tau_{ii}$; however, when $i = j$, then $\tau_{jj} = \tau_{ii} = 1$. In these equations, r_i (a relative molecular volume) and q_i (a relative molecular surface area) are pure-species parameters. The influence of temperature on g enters through the interaction parameters τ_{ji} of Eq. (C-3), which are temperature dependent:

$$\tau_{ji} = \exp \frac{-(u_{ji} - u_{ii})}{RT} \quad (\text{F-6})$$

Parameters for the UNIQUAC equation are therefore values of $(u_{ji} - u_{ii})$.

Calculation of Activity Coefficient

An expression for $\ln \gamma_i$ is applied to the UNIQUAC equation for g [Eqs. (F-1) through (F-3)]. The result is given by the following equations:

$$\ln \gamma_i = \ln \gamma_i^C + \ln \gamma_i^R \quad (\text{F-7})$$

$$\ln \gamma_i^C = 1 - J_i + \ln J_i - 5q_i \left(1 - \frac{J_i}{L_i} + \ln \frac{J_i}{L_i}\right) \quad (\text{F-8})$$

and

$$\ln \gamma_i^R = q_i(1 - \ln s_i - \sum \theta_j \frac{\tau_{ij}}{s_j}) \quad (\text{F-9})$$

where

$$J_i = \frac{r_i}{\sum x_j r_j} S \quad (\text{F-10})$$

$$L_i = \frac{q_i}{\sum x_j q_j} S \quad (\text{F-11})$$

$$s_i = \sum \theta_l \tau_{li} \quad (\text{F-12})$$

Again, subscript i identifies species, and j and l are dummy indices. All summations are over all species, and $\tau_{ij}=1$ for $i=j$. Values for the parameters ($u_{ij} - u_{jj}$) are found by regression of binary VLE data.

When applied to a solution of groups, the activity coefficients are calculated by:

$$\ln \gamma_i = \ln \gamma_i^C + \ln \gamma_i^R \quad (\text{F-13})$$

when

$$\ln \gamma_i^C = 1 - J_i + \ln J_i - 5q_i(1 - \frac{J_i}{L_i} + \ln \frac{J_i}{L_i}) \quad (\text{F-14})$$

and

$$\ln \gamma_i^R = q_i[1 - (\theta_k \frac{\beta_{ik}}{s_k} - e_{ki} \ln \frac{\beta_{ik}}{s_k})] \quad (\text{F-15})$$

The quantities J_i and L_i are given by:

$$J_i = \frac{r_i}{x_j r_j} \quad (\text{F-16})$$

$$L_i = \frac{q_i}{x_j q_j} \quad (\text{F-17})$$

In addition, the following definitions of parameters in Eqs. F-14 and F-15 are applied:

$$r_i = v_k^{(i)} R_k \quad (\text{F-18})$$

$$q_i = v_k^{(i)} Q_k \quad (\text{F-19})$$

$$e_{ki} = \frac{v_k^{(i)} Q_k}{q_i} \quad (\text{F-20})$$

$$\beta_{ik} = e_{mi} \tau_{mk} \quad (\text{F-21})$$

$$\theta_{ik} = \frac{x_i q_i e_{ki}}{x_j q_j} \quad (\text{F-22})$$

$$s_k = \theta_m \tau_{mk} \quad (\text{F-23})$$

$$\tau_{mk} = \exp\left(\frac{-a_{mk}}{T}\right) \quad (\text{F-24})$$

Subscript i identifies species, and j is a dummy index running over all species. Subscript k identifies subgroups, and m is a dummy index running over all subgroups. The quantity $v_k^{(i)}$ is the number of subgroups of type k in a molecule of species i . Values of the subgroup parameters R_k and Q_k and of the group interaction parameters, a_{mk} come from tabulation in the literature.

Table 18 UNIFAC-VLE group interaction parameters, a_{mk} , in Kelvins[†]

a_{mk}	k	1	2	3	4	5	6	7	8	9	10	11	12	13	14	15	16	17	18	19	20
m	Name	CH ₂	C=C	ACH	ACCH ₂	OH	CH ₃ OH	H ₂ O	ACOH	CH ₂ CO	CHO	CCOO	HCOO	CH ₂ O	CNH ₂	CNH ₂	(C) ₃ N	ACNH ₂	PYRIDINE	CCN	COOH
1	CH ₂	0	86.02	61.13	76.5	986.5	697.2	1318	1333	476.4	677	232.1	741.4	251.5	391.5	225.7	206.6	920.7	287.7	597	663.5
2	C=C	-35.36	0	38.81	74.15	524.1	787.6	270.6	526.1	182.6	448.8	37.85	449.1	214.5	240.9	163.9	61.11	749.3	0	336.9	318.9
3	ACH	-11.12	3.446	0	167	636.1	637.3	903.8	1329	25.77	347.3	5.994	-92.55	32.14	161.7	122.8	90.49	648.2	-4.449	212.5	537.4
4	ACCH ₂	-69.7	-113.6	-146.8	0	803.2	603.2	5695	884.9	-52.1	586.6	5688	115.2	213.1	0	-49.29	23.5	664.2	52.8	6096	603.8
5	OH	156.4	457	89.6	25.82	0	-137.1	353.5	-259.7	84	441.8	101.1	193.1	28.06	83.02	42.7	-323	-52.39	170	6.712	199
6	CH ₃ OH	16.51	-12.52	-50	-44.5	249.1	0	-181	-101.7	23.39	306.4	-10.72	193.4	-128.6	359.3	266	53.9	489.7	580.5	36.23	-289.5
7	H ₂ O	300	496.1	362.3	377.6	-229.1	289.6	0	324.5	-195.4	-257.3	72.87	0	540.5	48.89	168	304	-52.29	459	112.6	-14.09
8	ACOH	275.8	217.5	25.34	244.2	-451.6	-265.2	-601.8	0	-356.1	0	-449.4	0	0	0	0	0	119.9	-305.5	0	0
9	CH ₂ CO	26.76	42.92	140.1	365.8	164.5	108.7	472.5	-133.1	0	-37.36	-213.7	-38.47	-103.6	0	0	-169	6201	165.1	481.7	669.4
10	CHO	505.7	56.3	23.39	106	-404.8	-340.2	232.7	0	128	0	-110.3	11.31	304.1	0	0	0	0	0	0	0
11	CCOO	114.8	132.1	85.84	-170	245.4	249.6	200.8	-36.72	372.2	185.1	0	372.9	-235.7	0	-73.5	0	475.5	0	494.6	660.2
12	HCOO	90.49	-62.55	1967	2347	191.2	155.7	0	0	70.42	35.35	-261.1	0	0	0	0	0	0	0	0	-356.3
13	CH ₂ O	83.36	26.51	52.13	65.69	237.7	238.4	-314.7	0	191.1	-7.838	461.3	0	0	0	141.7	0	0	0	-18.51	664.6
14	CNH ₂	-30.48	1.163	-44.85	0	-164	-481.7	-330.4	0	0	0	0	0	0	0	63.72	-41.11	-200.7	0	0	0
15	CNH ₂	65.33	-28.7	-22.31	223	-150	-500.4	-448.2	0	0	0	136	0	-49.3	108.8	0	-189.2	0	0	0	0
16	(C) ₃ N	-83.98	-25.38	-223.9	109.9	28.6	-406.8	-598.8	0	225.3	0	0	0	0	38.89	865.9	0	0	0	0	0
17	ACNH ₂	1139	2000	247.5	762.8	-17.4	-118.1	-367.8	-253.1	-450.3	0	-294.8	0	0	-15.07	0	0	0	0	-281.6	0
18	PYRIDINE	-101.6	0	31.87	49.8	-132.3	-378.2	-332.9	-341.6	-51.54	0	0	0	0	0	0	0	0	0	-169.7	-153.7
19	CCN	24.82	-40.62	-22.97	-138.4	-185.4	157.8	242.8	0	-287.5	0	-266.6	0	38.81	0	0	0	777.4	134.3	0	0
20	COOH	315.3	1264	62.32	268.2	-151	1020	-66.17	0	-297.8	0	-256.3	312.5	-338.5	0	0	0	0	-313.5	0	0

† Adapted from xlUNIFAC Version 1.0

APPENDIX G

International Proceeding

Parinya Intaracharoen, Worapon Kiatkittipong, Piyasan Prasertthdam and Suttichai Assabumrungrat, "Ether from glycerol: Development of equilibrium thermodynamic model", A Regional Conference on Chemical & Biomolecular Engineering, National University of Singapore, Singapore, 19-20 Dec, 2008 (oral presentation)

Parinya Intaracharoen, Worapon Kiatkittipong, Piyasan Prasertthdam and Suttichai Assabumrungrat, "Equilibrium thermodynamic analysis of ethers production from glycerol", 15th Regional Symposium on Chemical Engineering (RSCE) in conjunction with 22th Symposium of Malaysian Chemical Engineers (SOMChE) Kuala Lumpur, Malaysia, 2-3 Dec, 2008 (oral presentation)

National Proceeding

ปริญญา อินทเรเจริญ, วรพล เกียรติกิตติพงษ์, นวพล เหล่าศิริพจน์, ปิยะสาร ประเสริฐธรรม, สุทธิชัย อัสสะบำรุงรัตน์, “การผลิตสารเพิ่มค่าซีเทนจากกลีเซอรอล : การศึกษาจลนพลศาสตร์ ด้วยตัวเร่งปฏิกิริยา Amberlyst 15”, การประชุมวิชาการวิศวกรรมเคมีและเคมีประยุกต์ แห่งประเทศไทย ครั้งที่ 19 “Research cooperation between academies and industries in Thailand” กาญจนบุรี, 26-27 ตุลาคม 2552 (ประเภทบรรยาย)

ปริญญา อินทเรเจริญ, วรพล เกียรติกิตติพงษ์, นวพล เหล่าศิริพจน์, ปิยะสาร ประเสริฐธรรม, สุทธิชัย อัสสะบำรุงรัตน์, “การผลิตสารเพิ่มค่าซีเทนจากกลีเซอรอล : การประยุกต์ใช้หอกลับแบบมีปฏิกิริยา”, การประชุมวิชาการวิศวกรรมเคมีและเคมีประยุกต์แห่งประเทศไทย ครั้งที่ 19 “Research cooperation between academies and industries in Thailand” กาญจนบุรี, 26-27 ตุลาคม 2552 (ประเภทโปสเตอร์)

Biography

Name-Family name	Mr.Parinya Intaracharoen
Birth	2 nd February 1984 in Ubonratchathani, Thailand.
Address	152 Suriyat road, Nai Muang Muang District, Ubonratchathani, Thailand, 34000. Tel. 045-243130
Education	
2009	further studied in the degree of the master of Chemical Engineering at graduate school, Faculty of Engineering and Industrial Technology, Graduate School, Silpakorn University, Thailand.
2007	received the degree of the Bachelor of Petrochemicals and Polymeric materials Engineering, Faculty of Engineering and Industrial Technology, Silpakorn University, Nakhon Phathom, Thailand.
2002	High school certificate from Princess Chulabhorn's college Mukdahan.
Special Interest	Simulation/ Aspen Plus program/ MATLAB program/ renewable energy